Technische Universität München

Zentrum Mathematik

Radii of Convex Bodies

René Brandenberg

Deutschsprachige Übersicht über die Dissertation

1. Einführung in den wissenschaftlichen Kontext

Geometrische Ungleichungen spielen eine herausragende Rolle in der Konvexgeometrie, wie etwa die Auswahl der Beiträge zu 'Part I' im 'Handbook of Convex Geometry' [44] erkennen lässt. Viele dieser Ungleichungen beziehen sich auf die fundamentalen Maßzahlen wie Volumen oder Oberfläche und deren Verallgemeinerungen (z.B. die inneren und äußeren Quermaße oder die Quermaßintegrale).

Die Geschichte der Erforschung solcher Ungleichungen ist eng verknüpft mit derjenigen der zugehörigen Extremalkörper. Im Laufe der Zeit hat sich dabei herausgestellt, dass diese Körper grob in zwei Klassen eingeteilt werden können: Die eine Klasse enthält Körper, die gewisse Regularitätsbedingungen erfüllen, wie zum Beispiel die Kugel, reguläre Polytope oder zentralsymmetrische Körper. In der anderen Klasse befinden sich Körper, deren pure Existenz, zumindest auf den ersten Blick, dem 'gesunden Menschenverstand' widerspricht. Hier sind besonders die Körper konstanter Breite (oftmals auch Körper konstanter Dicke oder Gleichdicke genannt) zu erwähnen.

Wir beschäftigen uns in dieser Arbeit mit den Radien konvexer Körper, insbesondere im Hinblick auf gültige geometrische Ungleichungen bezüglich der Radien. Wie sich später herausstellen wird, sind die beiden oben erwähnten Klassen möglicher Extremalkörper dabei wieder von exponierter Bedeutung.

Die wohl ältesten nicht-trivialen Ungleichungen, die sich auf Radien beziehen, sind Jung und Steinhagen zuzuschreiben. In seinem 1901 veröffentlichten Artikel [54] bestimmt Jung eine scharfe obere Schranke für das Verhältnis von Umkugelradius und Durchmesser konvexer Körper im d-dimensionalen Euklidischen Raum. Die zugehörigen Extremalkörper sind (u.a.) reguläre Simplexe (man beachte die Zugehörigkeit zur ersten der beiden oben erwähnten Klassen). Steinhagens 1921 erschienene Arbeit [72] korrespondiert in gewisser Weise mit derjenigen

von Jung. Dort wird eine obere Schranke für das Verhältnis von Dicke und In-
kugelradius konvexer Körper des d-dimensionalen Euklidischen Raums bewiesen,
die wiederum durch reguläre Simplexe erreicht wird. Die Dicke eine Körpers C
ist dabei definiert als der minimale Abstand zweier paralleler Stützhyperebenen
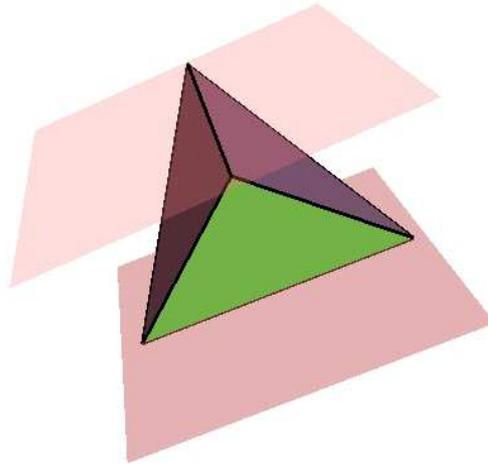an C (siehe Abbildung 1).

ABBILDUNG 1. Ein Tetraeder und ein Paar paralleler Stützhyper-
ebenen minimalen Abstands.

In der Folge dieser Resultate wurden die vier grundlegenden Radien (Dicke,
Durchmesser, In- und Umkugelradius) in einer Vielzahl von Arbeiten behandelt.
In den Literaturverzeichnissen findet man u.a. Artikel zu speziellen geometrischen
Ungleichungen für planare Mengen [**63, 11, 66, 67, 69, 50, 3, 19, 20, 70, 21**]
oder Verallgemeinerungen von Jung und Steinhagens Theoremen für allgemeine
Minkowski-Räume [**9, 57, 26**]. Wie bereits erwähnt, sind die Extremalkörper
bei der Analyse der Ungleichungen von großer Bedeutung. Allgemeine Veröffent-
lichungen über Extremalkörper sind z.B. [**42, 41, 43**], speziell mit Simplexen
beschäftigen sich [**2, 76**] und mit Körpern konstanter Breite [**10, 15, 32, 17,
65, 8**]. Diese Literaturangaben streben keine Vollständigkeit an, sondern sind
mit Bezug zu den nachfolgend behandelten Themen ausgewählt.

Es gibt verschiedene Verallgemeinerungen der vier grundlegenden Radien für
d-dimensionale Räume (einen Überblick gibt [**49**]). Wir wählen jedoch diejeni-
ge die den engsten Bezug zu den inneren und äußeren Quermaßen aufweist, es

uns also ermöglicht, einige analoge Betrachtungen zu den bekannten Fragen im Bereich der Volumina durchzuführen.

Wir definieren daher den inneren j-Radius $r_j(C)$, $1 \leq j \leq d$ eines d-dimensionalen Körpers C als den Radius einer größten in C enthaltenen j-Kugel (das vorangestellte j wird hier und im folgenden als Kurzform für j-dimensional verwendet). Der innere 2-Radius eines Körpers C gibt zum Beispiel den Radius einer größten in C enthaltenen Kreisscheibe an (siehe Abbildung 2).
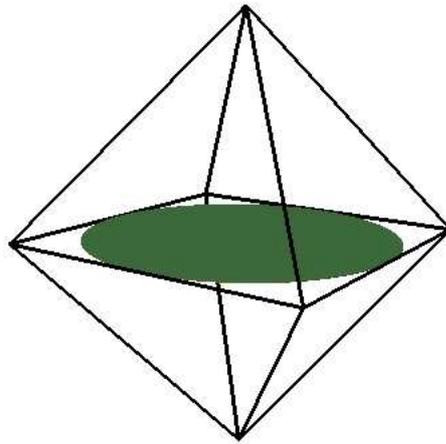

ABBILDUNG 2.   Der innere 2-Radius eines Oktaeders. Der zugehörige Optimalitätsbeweis kann in Kapitel 2.3 nachgelesen werden.

Für $j = d$ erhält man offensichtlich den üblichen Inkugelradius und für $j = 1$ den halben Durchmesser, da eine eindimensionale Kugel einem Liniensegment entspricht.

Der äußere j-Radius $R_j(C)$, $1 \leq j \leq d$ eines Körpers C misst, wie gut C durch eine $(d-j)$-Ebene approximiert werden kann (siehe Abbildung 3).

Ist $j = d$ und wird daher C durch einen Punkt approximiert, so erhält man natürlich den vertrauten Umkugelradius. Ferner ist es nicht schwer zu erkennen, dass sich für $j = 1$ die halbe Dicke ergibt.

Im Euklidischen Raum können die äußeren Radien auch als Umradien minimaler (Orthogonal-) Projektionen verstanden werden, d.h. für einen Körper C
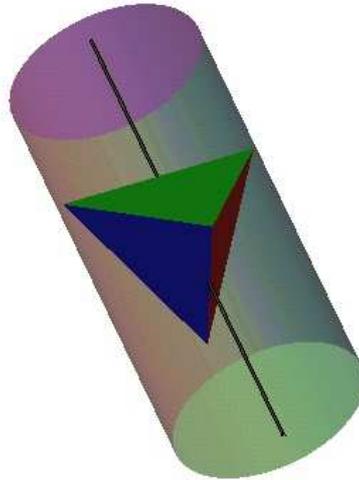
ABBILDUNG 3. Der äußere 2-Radius eines Tetraeders. Die Achse
des abgebildeten Zylinders stellt dabei die 1-Ebene da, durch die
das Tetraeder approximiert wird.

gibt $R_j(C)$ gerade den minimalen Umkugelradius aller Projektionen von C in
j-dimensionale Unterräume an.

Wie die korrespondierenden inneren und äußeren Quermaße verhalten sich
auch die inneren und äußeren Radien dual zueinander, d.h. bezeichnet man mit
C° den polaren Körper von C, dann gilt $r_j(C)R_j(C^\circ) = 1$ für alle zentralsymme-
trischen Körper C. Gerade die Dualität der inneren und äußeren Radien zueinan-
der zeigt, dass sich die beiden Klassen nicht nur als Verallgemeinerung, sondern
auch als Vereinheitlichung der grundlegenden Radien auffassen lassen.

Im Gegensatz zu den Resultaten über die vier grundlegenden Radien, sind
Publikationen zu den allgemeinen j-Radien überwiegend in den letzten zehn bis
fünfzehn Jahren erschienen. Das älteste Ergebnis, das sich diesem Bereich zu-
ordnen lässt, ist wahrscheinlich die Arbeit von Shklarsky, Chentzov und Yaglom
[71, russisch]. Dort wird der maximale Radius einer Kreisscheibe berechnet, die
in einen Würfel passt, also $r_2(B^3)$, wenn man den Würfel mit B^3 bezeichnet.

Geometrische Ungleichungen bezüglich der Nicht-Standardradien gibt es fast
überhaupt nicht. Eine Ausnahme bildet die Arbeit von Perel'man [58]. Unglei-
chungen in Bezug auf die oben angesprochenen anderen Klassen verallgemeinerter

Radien können in [**5, 49**] gefunden werden. Eine ausführliche Zusammenfassung bekannter Resultate, speziell im Hinblick auf algorithmische Fragestellungen, zu den beiden hier betrachteten Radienklassen findet man in [**39, 40**].

Die Radien und die mit ihnen zusammenhängenden geometrischen Ungleichungen sind zwar in erster Linie innerhalb der Konvexgeometrie von großer Bedeutung. Es gibt aber auch eine ganze Reihe von Anwendungen, die in andere Gebiete der Mathematik oder über deren Grenzen hinaus reichen. Z.B. besitzen einige Fragestellungen in der Optimierung einen direkten Bezug zu den Radien, wie etwa Fragen aus dem Bereich der Globalen Optimierung oder der Sensitivitätsanalyse in der Linearen Programmierung. Für die Statistik sind besonders die allgemeinen äußeren Radien in Bezug auf die Orthogonale Minimax-Regression von Bedeutung. Weitere Anwendungsgebiete sind Computer-Grafik, Robotersteuerung, Chromosomen-Klassifikation oder die Messtechnik (siehe [**40, 1**] und die dortigen Literaturangaben). Die zahlreichen Anwendungen sind wohl auch einer der Gründe dafür, dass es mittlerweile eine ganze Reihe von Veröffentlichungen gibt, die sich mit der Berechnung bzw. der Approximation, und den zugehörigen Komplexitätsaussagen, der Radien befassen [**52, 40, 1, 18, 14, 31**].

Gerade aber die engen theoretischen Zusammenhänge zu den Volumina und den dazugehörigen Quermaßen sind es, die uns hier veranlassen einige grundlegende Fragestellungen bezüglich der Radien konvexer Körper anzugehen.

Im folgenden werden die wichtigsten Ergebnisse dieser Arbeit zusammengefasst. Hierbei halten wir uns nicht nur an die durch die Arbeit vorgegebene Kapitelaufteilung, sondern geben die zitierten Resultate auch mit ihrer Originalnummerierung wieder. Dadurch treten in der Zusammenfassung natürlich Lücken in der Nummerierung auf und auch die Reihenfolge der Ergebniswiedergabe stimmt nicht durchgängig mit der der eigentlichen Arbeit überein.

2. Radien regulärer Polytope

Nach den beiden einführenden Kapiteln ("Introduction" und "Preliminaries") hat das erste inhaltliche Hauptkapitel die Radien der regulären Polytope (und der mit diesen eng verwandten Polytopklassen) zum Thema.

Wie bereits angesprochen besitzen reguläre Polytope, und unter diesen in erster Linie die regulären Simplexe, für eine Vielzahl geometrischer Ungleichung

die Extremaleigenschaft. Auch in den bereits erwähnten Ungleichungen von Jung und Steinhagen wird durch die regulären Simplexe die jeweils gegebene Schranke scharf erreicht.

Sichtet man die vorhandene Literatur so stellt man fest, dass alle inneren Radien der Simplexe bekannt sind [4]. An Ergebnisse zu den äußeren Radien mangelt es dagegen. Hier können nur die Fälle $j = d$ und $j = 1$ aus den Arbeiten von Jung und Steinhagen gewonnen werden und die Lösung für $j = d - 1$ gibt Weissbach [74, 75]. Zu allen anderen äußeren Simplexradien fehlten bisher die Resultate.

Die Bestimmung möglichst vieler offener Simplexradien ist daher ein erstes Ziel dieser Arbeit, dass im ersten Abschnitt von Kapitel 3 behandelt wird. Das erste Resultat gibt eine allgemeingültige untere Schranke an (T^d bezeichnet das reguläre Simplex).

SATZ 3.4. Für alle $d \geq 2$ und $j \in \{1, \ldots, d\}$ ist

$$R_j(T^d) \geq \sqrt{\frac{j}{d+1}}.$$

Eine weiteres interessantes und später hilfreiches Resultat wird in Korollar 3.5 erzielt. Dieses korrespondiert sehr stark mit Resultaten von Filliman über die Quermaße regulärer Simplexe [33, 34].

FOLGERUNG 3.5. Für alle $d \geq 2$ und $j \in \{1, \ldots, d\}$ ist

$$R_j(T^d) = \sqrt{\frac{j}{d+1}} \Leftrightarrow R_{d-j}(T^d) = \sqrt{\frac{d-j}{d+1}}.$$

Außerdem liegen die zugehörigen optimalen Projektionen in zueinander orthogonalen Teilräumen.

Der entscheidende Schritt in Richtung der Bestimmung möglichst vieler äußerer Simplexradien gelingt durch Anwendung des Satzes von John [53], die zur Definition der *(quasi-) isotropischen Polytope* führt (siehe Definition 3.7).

LEMMA 3.9. Es gilt genau dann $R_j(T^d) = \sqrt{\frac{j}{d+1}}$, wenn es ein quasi isotropisches j-dimensionales Polytop C mit $d + 1$ nicht notwendig verschiedenen Ecken

gibt. Außerdem ist in diesem Fall die zu $R_j(T^d)$ gehörende optimale Projektion ähnlich zu C.

Dabei bezeichnen wir zwei Polytope als *ähnlich*, falls sie durch Translation, Rotation und Dilatation auseinander hervorgehen. Dieser Zusammenhang zwischen den Simplexradien und der Existenz der quasi isotropischen Polytope ist der Kern dieses Abschnitts. Im weiteren Verlauf werden nun Techniken entwickelt um die Existenz solcher Polytope in möglichst allgemeiner Dimension zu verifizieren. Wir gelangen schließlich zu folgendem Hauptsatz des Abschnitts:

SATZ 3.14. Es ist $R_j(T^d) = \sqrt{\frac{j}{d+1}}$, falls

(i) d ungerade oder

(ii) j gerade und $d \neq 2j$.

Die Bedingungen in Satz 3.14 sind hinreichend aber nicht notwendig. In einem nachfolgenden Lemma gelingt es sogar in einigen der Fälle mit $d = 2j$ und geradem j quasi isotropische Polytope zu konstruieren. Die in diesem Abschnitt erzielten Ergebnisse fasst Tabelle 1 zusammen.

Der zweite Abschnitt des Kapitels widmet sich den allgemeinen Simplexen. Hier gelingt es für den Fall, dass $d+1$ und $d-j+1$ einen gemeinsamen Teiler besitzen, den äußeren j-Radius eines Simplexes durch minimale äußere Radien niedrig dimensionalerer Seiten des Simplexes nach oben abzuschätzen. Interessanter als dieses Ergebnis selbst ist aber die daraus abgeleitete geometrische Ungleichung:

SATZ 3.17. Es sei S^d ein allgemeines d-dimensionales Simplex. Erfüllt $j \in \{1, \ldots, d\}$ eine der beiden Bedingungen

(i) $d - j + 1$ teilt $d + 1$ oder

(ii) $j = 1$,

dann gilt

$$\frac{R_j(S^d)}{r_1(S^d)} \leq \sqrt{\frac{2j}{d+1}},$$

und Gleichheit wird durch das reguläre d-Simplex erreicht.

j,d	1	2	3	4	5	6	7	8	9	10	11	12	13	14	15	16
1	+	-	+	-	+	-	+	-	+	-	+	-	+	-	+	-
2		+	+	+	+	+	+	+	+	+	+	+	+	+	+	+
3			+	-	+	(-)	+	(-)	+	(-)	+	(-)	+	(-)	+	(-)
4				+	+	+	+	+	+	+	+	+	+	+	+	+
5					+	-	+	(-)	+	(-)	+	(-)	+	(-)	+	(-)
6						+	+	+	+	+	+	?	+	+	+	+
7							+	-	+	(-)	+	(-)	+	(-)	+	(-)
8								+	+	+	+	+	+	+	+	?
9									+	-	+	(-)	+	(-)	+	(-)
10										+	+	+	+	+	+	+

TABELLE 1. Die Tabelle zeigt die Existenz der j-dimensionalen quasi isotropischen Polytope mit $d+1$ Ecken an (und folglich die Fälle in denen die untere Schranke für die Simplexradien scharf erreicht wird). Ein '+' symbolisiert dabei die Existenz, ein '-' die bewiesene Nicht-Existenz. Die '(-)' Einträge stehen für noch offene Fälle, für die es aber 'gute' Gründe gibt anzunehmen, dass keine quasi-isotropischen Polytope der entsprechenden Dimensionen existieren. Die '?' markieren dagegen die 'wirklich' offenen Fälle.

Nach den allgemeinen Simplexen folgt ein Abschnitt über d-dimensionale Quader und (allgemeine) Kreuzpolytope. Während die inneren Radien der Quader in [30] vollständig bestimmt wurden, fehlt das entsprechende Resultat zu den äußeren Radien. Dies wird in Satz 3.20 nachgeholt. Dabei zeigt sich, dass, wie nicht anders zu erwarten, der äußere j-Radius gerade durch Projektion auf eine minimale j-Seite des Quaders erreicht wird. Die Radien der Kreuzpolytope erhält man durch Polarisation.

Interessant in diesem Zusammenhang ist aber auch, dass sich die speziellen Radien des Würfels und des regulären Kreuzpolytopes in fast allen Dimension auch schon aus den Ergebnissen über die äußeren Radien der regulären Simplexe herleiten lassen. Dies ist möglich, da beide nicht nur selbst isotropisch sind, sondern sich auch auf isotropische Polytope in fast allen niedrigeren Dimensionen

projizieren lassen. Dieser Zusammenhang zwischen den drei Klassen regulärer Polytope in allgemeiner Dimension führt die Ergebnisse des Kapitels zusammen und rundet es somit ab.

3. Total nicht-sphärische Körper konstanter Breite

Das vierte Kapitel dieser Arbeit ist aus einer gemeinsamen Arbeit mit David Larman hervorgegangen [13].

Schon die Existenz von Körpern konstanter Breite ungleich der d-Kugel ist zunächst recht unerwartet. Ihr Vorhandensein in der Ebene war allerdings schon Euler bekannt [29] und die berühmteste konvexe Menge konstanter Breite ist wohl das Reuleaux-Dreieck, benannt nach Reuleaux, der es in seiner Arbeit von 1875 beschrieben hat [60]. Reuleaux-Dreiecke und etwas allgemeiner Reuleaux-n-Ecke, wobei n ungerade sein muss, werden in vielen Artikeln untersucht und finden darüber hinaus auch im alltäglichen Leben ihre Nutzung, z.B. als Münzen (siehe Abbildung 4).

ABBILDUNG 4.   Da sich die Ausmaße einer Scheibe konstanter Breite leicht in jeglicher Art von Münzautomaten bestimmen lassen, können sie als Alternative zu den üblicherweise runden Geldstücken verwendet werden, wie hier das Reuleaux-Siebeneck als britische 20 und 50 Pence Münzen.

Wir gehen allerdings in diesem Kapitel noch einen Schritt weiter und zeigen die Existenz einer Klasse spezieller Körper konstanter Breite, deren sämtliche Projektionen auf die Ebene keine Kreisscheibe ergeben. Körper mit dieser Eigenschaft bezeichnen wir als total nicht-sphärische Körper konstanter Breite. Das

Ziel dieses Kapitels ist daher der Beweis des folgenden Satzes:

SATZ 4.8. Für alle $d \geq 2$ existiert ein d-dimensionaler total nicht-sphärischer Körper.

Für $d = 2$ sind natürlich alle konvexen Mengen konstanter Breite, außer der Kreisscheibe selber, bereits total nicht-sphärisch. Schon für $d = 3$ ist die Existenz solcher Körper aber nicht mehr offensichtlich. Die bekanntesten 3-dimensionalen Körper konstanter Breite dürften wohl die beiden Meißner-Körper sein (siehe Abbildung 5), gefolgt von Rotationskörpern, die aus einer planaren Menge konstanter Breite mit Symmetrieachse entstehen.

ABBILDUNG 5. Ein Foto eines Meißner-Körpers. Man kann gut die beiden Kantentypen erkennen; nämlich jene, die direkt aus dem Schnitt zweier Sphären entstehen und jene die nachträglich etwas abgerundet werden, damit der Körper zwischen den gegenüberliegenden Kanten nicht einen zu großen Durchmesser besitzt.

Die Rotationskörper können offensichtlich entlang ihrer Rotationsachse auf eine Kreisscheibe projiziert werden. Aber auch die Meißner-Körper gehören nicht zu den total nicht-sphärischen Körpern. Projiziert man sie orthogonal zu einem Paar sich gegenüberliegender Kanten, erhält man wieder eine Kreisscheibe.

Eggleston [27] und Weissbach [74] beschreiben in ihren Arbeiten Körper der Dimension $d \geq 3$, deren $(d-1)$-dimensionale Projektionen alle nicht-sphärisch

sind. Für $d = 3$ genügt diese zu betrachtende Tatsache als Existenzbeweis total nicht-sphärischer Körper. Für $d \geq 4$ bleibt das Problem zunächst jedoch offen.

Um nun obigen Satz zu beweisen, führen wir zunächst den Begriff der Dunkelwolken ein, ein Konzept das auf einer Arbeit von Erdős und Rogers [**28**] basiert und von Danzer in [**24**] ausführlich behandelt wird. Wir verwenden hier nur das für unsere Zwecke notwendige, transferieren dazu zusätzlich aber die Idee der Dunkelwolken auch auf die Kugeloberfläche. Der zweite Abschnitt dient dann der Herleitung des obigen Satzes, ein Ergebnis, das uns schließlich ermöglicht ein Diagramm anzugeben, in dem alle generellen kleiner-größer Beziehungen zwischen den Radien eingezeichnet sind (siehe Abbildung 6).
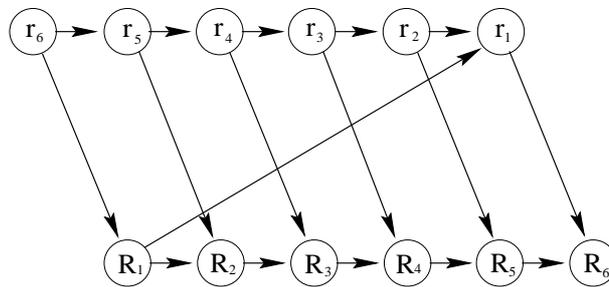

ABBILDUNG 6. Die Pfeile zwischen den Radien zeigen eine kleinergleich Beziehung an, also z.B. $r_6 \leq r_5$. Gibt es keinen gerichteten Pfad zwischen einem Paar von Radien, so gibt es Körper, für die in die eine oder die andere Richtung '<' gilt.

4. Total isoradiale Körper

Die besondere Bedeutung der Körper konstanter Breite in Hinblick auf geometrische Ungleichungen wurde bereits herausgestellt und mit dem vorherigen Kapitel nochmals unterlegt. Nun möchten wir im Kapitel über total isoradiale Körper, das auf gemeinsamen Forschungsergebnissen mit Abhi Dattasharma und Peter Gritzmann beruht [**12**], eine vielleicht noch überraschendere Teilklasse der Körper konstanter Breite vorstellen.

Aufgrund seiner großen Bedeutung wird in der Literatur natürlich versucht das Konzept der konstanten Breite auf andere Maßzahlen zu übertragen. Eine solche Erweiterung definiert sich über die Quermaße. Dabei sagt man ein Körper habe ein konstantes in inneres bzw. äußeres j-Quermaß ($1 \leq j \leq d - 1$), falls

das jeweilige Quermaß nicht von der Richtung der möglichen Schnitte bzw. der Projektionen abhängt. Die Körper mit konstantem 1-Quermaß sind gerade wieder die Körper konstanter Breite, und anstelle von konstantem $(d-1)$-Quermaß wird auch der Begriff der konstanten Helligkeit verwendet. Während nun die Existenz von Körpern mit konstantem äußerem j-Quermaß abgesehen von der Kugel für jede Wahl von j durch Firey [**35**] gesichert wurde, ist eine der wichtigen offenen Fragen der Konvexgeometrie, diejenige nach der Existenz von Körpern konstanter Breite und konstanter Helligkeit. Es wird vermutet, dass die Kugel der einzige Körper mit dieser Eigenschaft ist.

Die enge Verbindung zwischen den Quermaßen und den Radien haben wir bereits im ersten Abschnitt dieses Kapitels angesprochen. Diesen Zusammenhang nutzen wir nun um einen Begriff entsprechend dem der konstanten Quermaße für die Radien zu definieren. Wir bezeichnen daher einen Körper als inner- bzw. außer-j-isoradial, falls der jeweilige j-Radius nicht von der Richtung der j-Ebene mit der geschnitten bzw. auf die projiziert wird abhängt (siehe Definition 5.1).

Auch in diesem Fall sind die 1-isoradialen Körper gerade wieder die Körper konstanter Breite, der Begriff der Isoradialität stellt also eine Verallgemeinerung in Bezug auf die j-Radien dar. Bezeichnen wir nun aber die Klasse der Körper, die für alle j inner- und außer-j-isoradial sind als total isoradial, so haben wir gleichzeitig auch eine neue sehr spezielle Teilklasse der Körper konstanter Breite beschrieben.

Für $d = 3$ bildet die Frage nach total isoradialen nicht-sphärischen Körpern gerade das Pendant für Radien zu der oben angesprochenen Frage nach Körpern konstanter Breite und konstanter Helligkeit, die nicht die Kugel sind. Im Gegensatz zur nicht gelösten zweiten Frage gelingt es uns die erste Frage in dieser Arbeit zu beantworten.

SATZ 5.5. Es gibt neben der Kugel weitere total isoradiale 3-dimensionale Körper.

Die Existenz eines solchen Körpers ist nicht nur recht überraschend sondern auch schlecht zu visualisieren. Ein Grund hierfür ist die enorme Ähnlichkeit zur

Kugel selber. Darstellen lässt sich aber einer der im Beweis des Satzes 5.5 er-
zeugten außer-2-isoradialen Körper, dessen Vervollständigung innerhalb seiner
Umkugel (existiert nach Scott, siehe [**68**] und vergleiche auch Proposition 2.5)
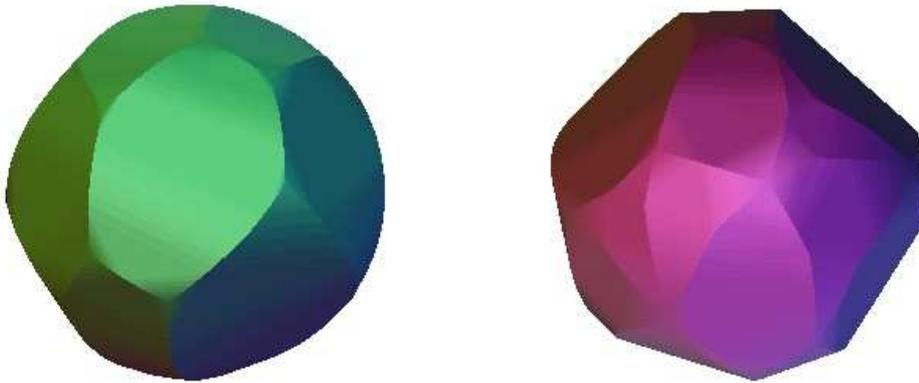den gewünschten total isoradialen Körper ergibt (siehe Abbildung 7).

ABBILDUNG 7.   Zwei Ansichten eines außer-2-isoradialen Körpers,
dessen umkugelerhaltende Vervollständigung total isoradial ist, sich
aber von der Kugel unterscheidet.

5. Blaschke-Santaló Diagramme

In seiner berühmten Arbeit "Eine Frage über konvexe Körper" [**7**] schlug
Blaschke 1916 die Abbildung 3-dimensionaler Körper in ein ebenes Diagramm
vor. Die Koordinaten dieses Diagramms werden dabei durch

$$x = \frac{4\pi F(C)}{M(C)^2}, \, y = \frac{48\pi^2 V(C)}{M(C)^3}$$

definiert, wobei $F(C)$ die Oberfläche, $V(C)$ das Volumen und $M(C)$ das Integral
der mittleren Krümmung des abzubildenden Körpers C bezeichnen. Hadwiger
[**47**] betitelt diese Werte zusammen mit der Gesamtkrümmung 4π als "die fun-
damentalen Maßzahlen" und widmet sich in einem kompletten Abschnitt seines
Buches dem Blaschke Diagramm. Viele Wissenschaftler haben seither versucht
eine vollständige Beschreibung des Diagramms zu erstellen, bis heute konnten

xvi DEUTSCHSPRACHIGE ÜBERSICHT ÜBER DIE DISSERTATION

jedoch für die letzte Begrenzung nur approximative Ergebnisse bewiesen werden [**61, 22**].

Vollständige Systeme beschreibender Ungleichungen sind auch das Ziel der Diagramme für planare Mengen [**63**], die Santaló 1961 vorgeschlagen hat. In ihnen werden je drei der Größen Fläche, Umkugelradius, Inkugelradius, Durchmesser, Umfang und Dicke berücksichtigt (siehe Abschnitt 6.2 für Details). Für 6 der 20 möglichen Tripel gibt Santaló in seiner Originalarbeit bereits eine Lösung an, darunter auch eine von vier möglichen Auswahlen die nur Radien umfasst. Vollständige Systeme für die drei verbleibenden reinen Radiendiagramme werden in [**19, 20**] bestimmt.

Diese so genannten Blaschke-Santaló-Diagramme bilden die beste bekannte Möglichkeit zu bestimmen, welche geometrischen Ungleichungen wirklich essentiell sind und welche durch andere Ungleichungen dominiert werden. Allerdings bedingt die Auswahl von je drei der vier Radien auch entscheidende Nachteile. Zum einen können Ungleichungen zwischen allen vier Standardradien (Durchmesser, Dicke, In- und Umkugelradius) mit ihrer Hilfe nicht entdeckt werden. Zum anderen ergeben sich für die getrennt behandelten Blaschke-Santaló-Diagramme Ungleichungen, die immer wieder die gleichen Extremmengen beschreiben. Hier lässt sich vermuten, dass diese einer gemeinsamen Grundeigenschaft entstammen und nur durch die getrennte Betrachtung der einzelnen Diagramme zu jeweils anderen Ungleichungen führen.

Insbesondere das zuletzt erwähnte Phänomen wollen wir in diesem Kapitel angehen. Zuerst wird allerdings in einem technischen Abschnitt das Verhalten der Radien bezüglich der Minkowski-Summation zweier Körper untersucht. Im zweiten Abschnitt geben wir dann eine Zusammenfassung der Resultate zu den vier Blaschke-Santaló-Diagrammen bezüglich der Standardradien an. Danach folgt der Hauptteil des Kapitels. Hier verbessern wir das Konzept der Blaschke-Santaló-Diagramme. Anstelle getrennter 2-dimensionaler Diagramme betrachten wir hier erstmals ein alle vier Radien umfassendes 3-dimensionales Diagramm, dessen Projektionen entlang der Koordinatenachsen gerade wieder die herkömmlichen Blaschke-Santaló-Diagramme ergeben. Dieses neue Diagramm ermöglicht einen viel tieferen Einblick in die Zusammenhänge und dadurch nicht nur die Reduktion des Systems der wirklich essentiellen Ungleichungen, sondern auch das Aufdecken

neuer schärferer Ungleichungen, die alle vier Radien involvieren. Ferner ergeben sich bei der Beschreibung der eindimensionalen Begrenzungen des Diagramms eine Reihe von neuartigen Ungleichungen in Bezug auf die extremalen Teilmengen unter den allgemeinen konvexen Mengen der Ebene. Etwas überraschend ist auch die Aufdeckung sechs weiterer essentieller Mengen, die Extrempunkte des Diagramms beschreiben. Die Koordinatenprojektionen ließen bisher nur vier erkennen.

Aber schauen wir uns die Ergebnisse im Einzelnen an. Da das Verhältnis zwischen den vier Standardradien für ähnliche Körper übereinstimmt, betrachten wir nur die Teilklasse $\mathcal{C}_1^2$ der konvexen Mengen in der Ebene mit Umkugelradius 1. Die Funktion

$$f : \mathcal{C}_1^2 \to [0,1]^3, \ \ f(K) = (x, y, z) = (r_2(K), R_1(K), r_1(K))$$

beschreibt nun das verallgemeinerte Blaschke-Santaló-Diagramm.

Von den besagten 10 Extrempunkten können 9 als extrem bewiesen werden (siehe Abbildung 8 für Skizzen der zugehörigen Mengen), nur für das gebogene Trapez gibt es noch eine minimale Unsicherheit:

SATZ 6.17. Die Mengen $L, \mathbb{B}, T^2, RT, I_{\frac{\pi}{2}}, SR_{\frac{\pi}{6}}, SR_{\mathrm{arcsin}(\sqrt{3}-1)}, RSB_{\frac{\pi}{4}}$, und H_{τ^*} implizieren Extrempunkte von $f(\mathcal{C}_1^2)$.

Dabei bestimmt sich τ^* als Lösung einer Polynomgleichung vierten Grades:

$$\tau^* = \frac{1}{2}\sqrt{\zeta + \xi} + \sqrt{-\zeta - \xi + \frac{16}{\sqrt{\zeta + \xi}}} - 1$$

mit $\zeta = \frac{1}{3}(864 - 96\sqrt{69})^{\frac{1}{3}}$ und $\xi = 2(\frac{2}{3})^{\frac{2}{3}}(9 + \sqrt{69})^{\frac{1}{3}}$.
Von den zehn vermuteten 2-dimensionalen Seitenflächen können für acht die induzierende Ungleichungen bestimmt werden, von denen wiederum sechs als gültig für $f(\mathcal{C}_1^2)$ nachgewiesen werden können. Letztere sind

(i) $x \leq y$,

(ii) $z \leq 1$,
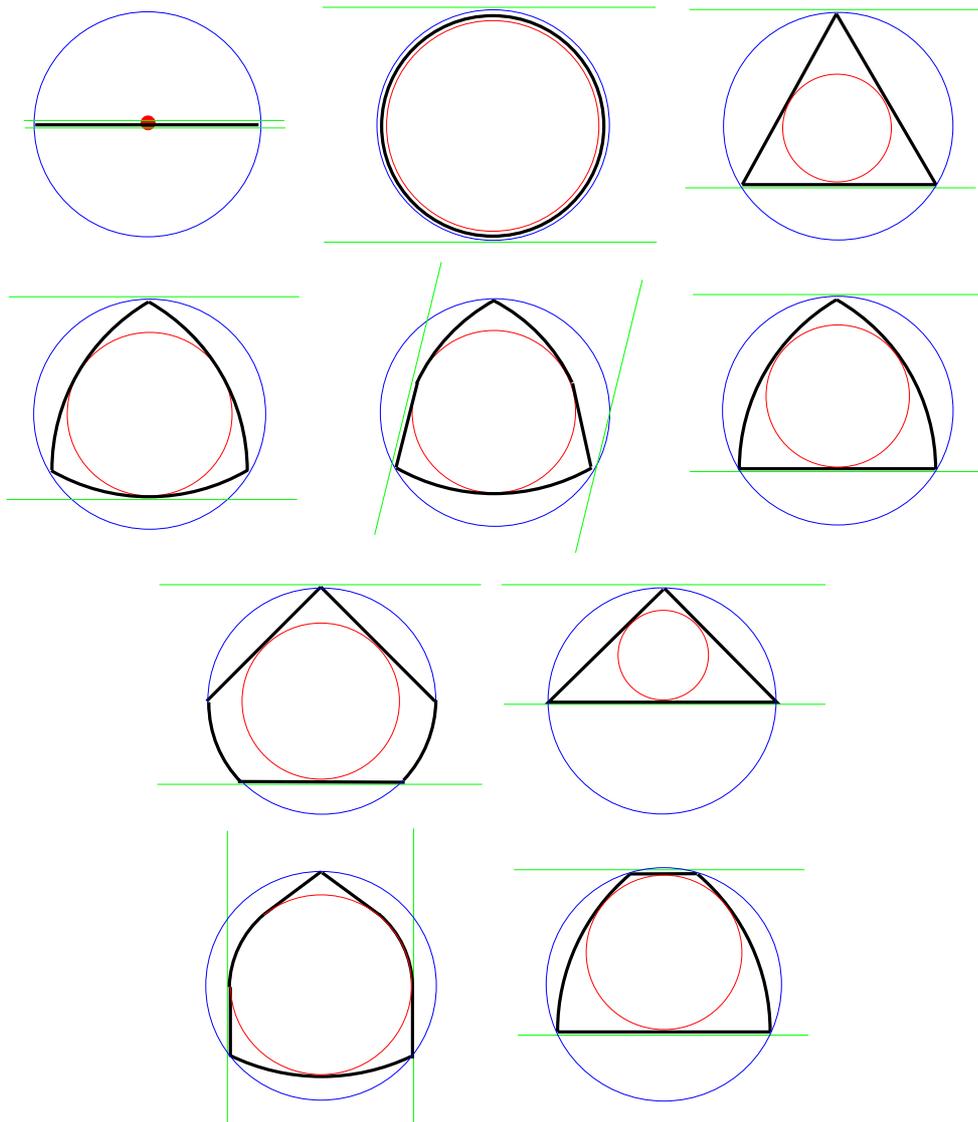
(iii) $x + 1 \geq 2y$,

(iv) $x + 1 \leq 2z$,

ABBILDUNG 8. Die Extrempunkte des 3-dimensionalen Blaschke-Santaló-Diagramms (von links nach rechts). Erste Reihe: das Liniensegment L, der Kreis $\mathbb{B}$, das gleichseitige Dreieck T^2. Zweite Reihe: das Reuleaux-Dreieck RT und die angeschnittenen Reuleaux-Dreiecke $SR_{\arcsin(\sqrt{3}-1)}$ und $SR_{\frac{\pi}{6}}$. Dritte Reihe: Das rechtwinklige Segelboot $RSB_{\frac{\pi}{4}}$ und das rechtwinklige Dreieck $I_{\frac{\pi}{2}}$. Vierte Reihe: Die Mütze H_{τ^*} und das gebogene Trapez $BT_{\arcsin(\frac{3}{4})}$.

(v) $z \geq \frac{\sqrt{3}}{2}$ und

(vi) $y^2 - 4(1 - z^2)z^4 \geq 0$.

Um die Begrenzungen der 2-dimensionalen Seitenflächen, die durch die obigen Ungleichungen induziert werden beschreiben zu können, werden außerdem eine Reihe von bereits bekannten geometrischen Ungleichungen als signifikant herausgestellt und neue bewiesen. Die neuen Ungleichungen haben wir als Sätze festgehalten:

SATZ 6.9. Für alle $K \in \mathcal{C}_1^2$ mit $r_1(K) = 1$ und $r_2(K) \leq \sqrt{12}$ gilt

$$R_1(K) \leq \begin{cases} \frac{r_2(K)}{1 - r_2(K)^2}, \text{ falls } r_2(K) \leq \sqrt{2} - 1 \\ \left(\frac{1}{2} + \sqrt{\frac{1}{2}}\right) r_2(K), \text{ falls } r_2(K) \geq \sqrt{2} - 1. \end{cases}$$

SATZ 6.10. Für alle $K \in \mathcal{C}_1^2$ mit $r_2(K) + 1 = 2R_1(K)$ und $r_2(K) \leq \sqrt{\frac{1}{2}}$ gilt:

$$r_1(K) \leq r_2(K)\sqrt{1 - r_2(K)^2}.$$

SATZ 6.11. Für alle $K \in \mathcal{C}_1^2$ mit $r_2(K) + 1 = 2r_1(K)$ und $r_2(K) \leq \tau^*$ gilt:

$$\left(\left(4(r_2(K) + 1)^2 - (r_2(K) + 1)^4 - 4R_1(K)^2\right)^{\frac{1}{2}}\right.$$
$$+ \left.\left(1 - (2R_1(K) - r_2(K))^2\right)^{\frac{1}{2}}\right)^2$$
$$\leq 1 - r_2(K)^2.$$

SATZ 6.12. Für alle $K \in \mathcal{C}_1^2$ mit $r_1(K) = \frac{\sqrt{3}}{2}$ und $r_2(K) \geq \frac{3\sqrt{3}}{8}$ gilt:

$$R_1(K) \geq \frac{\sqrt{3}}{2} \sin\left(\arccos\left(\sqrt{3 - 2\sqrt{3}r_2(K)}\right) + \frac{\pi}{6}\right).$$

SATZ 6.13 Für alle $K \in \mathcal{C}_1^2$ mit

$$R_1(K)^2 - 4r_1(K)^4(1 - r_1(K)^2) = 0$$

und $r_2(K) \geq \frac{3\sqrt{3}}{8}$ gilt:

$$R_1(K) \leq \frac{4}{3} \sin\left(2 \arccos\left(\frac{4}{3}r_2(K)\right)\right) r_2(K).$$

Im abschließenden Abschnitt dieses Kapitel befassen wir uns noch mit weiteren Erweiterungsmöglichkeiten der Blaschke-Santaló-Diagramme, in welchen zum Beispiel, wie in Blaschkes Original, 3-dimensionale Körper betrachtet werden und eventuell zusätzlich die weiteren Radien hinzukommen.

Contents

List of Figures

List of Tables

Acknowledgements

First of all, I would like to thank my advisor Peter Gritzmann, for offering me the opportunity to join him and his working group at TU München, for all his support and comments, and for the required freedom to develop myself. I really enjoyed the last four years and benefited a lot from the additional activities of our group, even though the many sideline jobs sometimes made it difficult to concentrate on research. I am especially grateful for the time in which Peter Gritzmann and I have jointly written the book "Das Geheimnis des kürzesten Weges – Ein mathematisches Abenteuer".

Next I like to thank David Larman for inviting me to University College of London and for the interesting and fruitful discussions we had together in Munich and in London.

In this context I also want to thank the European Union for their financial support of my sojourn in London through a Marie-Curie Training Grant.

I would like to thank all my friends in our working group, past and present. Each of them assisted me whenever needed. Especially, I would like to thank Franziska Berger, Abhi Dattasharma, Thorsten Theobald, and Sven de Vries for their proofreading and the valuable comments helping me to improve this thesis. Special thanks go to Sven de Vries, who always supported me with his technical knowledge.

I am grateful to Keith Ball for calling my attention to the notion of basic invariant projections and to Martin Henk for his valuable hints on useful literature.

Finally, I want to express my gratitude to my family. To Doris and Joachim, who always believed in me and backed me up with all their love; and last but by no means least, to my wife Silke. It is not possible to state my gratefulness in words for her unlimited support, so I dedicate this thesis to her.

CHAPTER 1

Introduction

1. The context

In their book about geometric inequalities [**16**], Burago and Zalgaller begin the foreword as follows: "Geometric inequalities have a wide range of applications – within geometry itself as well as beyond its limits." The importance of geometric inequalities is stressed by the huge variety of results covering several topics. Such topics typically include the minima and maxima of the fundamental measures of convex sets (e.g., the volume or the surface area); and their generalisations (e.g., the inner and outer j-measures, the quermassintegrals, mixed-volumes) in Euclidean or general Minkowski spaces. Standard references are [**10, 64, 44, 45**].

This thesis focuses on the radii of convex sets, especially on geometric inequalities among them. It is about a century since Jung [**54**] and Steinhagen [**72**] published their famous articles about the upper bounds on the circumradius-diameter ratio, and the width-inradius ratio in Euclidean space, respectively (see Proposition 2.3 for details). Since then, the four quantities (inradius, width, circumradius, and diameter) have been studied quite thoroughly, and theorems involving them are known as standard results. There are generalisations of the results of Steinhagen and Jung for general Minkowski spaces [**9, 57, 26**] and about geometric inequalities in 2-space [**63, 11, 66, 67, 69, 50, 3, 19, 20, 70, 21**]. Of particular significance for the analysis of geometric inequalities are the extremal convex sets which attain equality; simplices and bodies of constant breadth (also known as bodies of constant width) are good examples for they often do. General publications about extremal convex sets are [**42, 41, 43**], results with special focus on simplices can be found in [**2, 76**] and an (of course not complete) list of papers on bodies of constant breadth is [**10, 15, 32, 17, 65, 8**].

There are several ways to generalise the concept of radii in d-space (see [**48**] for a survey), but only one in the sense of the inner- and outer j-measures as

1

generalisations of the volume. The *outer j-radius* $R_j(C)$, $1 \leq j \leq d$, where C is a body in d-space, measures how well C can be approximated by a $(d-j)$-flat. In fact, computing the outer d-radius means approximating C by a point, thus $R_d(C)$ is the usual circumradius of C. Also, it is easy to see that $R_1(C)$ is half of the width of C. Correspondingly one can define the *inner j-radius* $r_j(C)$ of C as the radius of the largest j-dimensional ball that fits into C. We will drop the C from $r_j(C)$ and $R_j(C)$ when C is clear from the context. Observe that r_d is just the usual inradius and r_1 is half of the diameter. The inner and outer radii are dual to each other in the sense that for a symmetric (with respect to the origin) body C and its polar C°, $r_j(C)R_j(C^\circ) = 1$. In this light the two radii-classes do not only generalise, but they also unify the original four quantities.

The radii different from the four standard ones (in- and circumradius, width, and diameter) are mostly studied recently. To the best of our knowledge, the oldest is the work of Shklarsky, Chentzov, and Yaglom [**71**, in Russian]. In this paper from 1970 the authors compute the radius of a biggest disc fitting into a unit-cube in 3-space. Geometric inequalities about the non-standard radii are almost unknown, an exception being the work of Perel'man [**58**]. For inequalities about other types of generalised radii see [**5, 49**]. A very comprehensive study of the two radii classes, with a focus on the algorithmic aspect, is due to Gritzmann and Klee [**39, 40**].

Radii of convex bodies find applications in many areas, e.g., orthogonal minimax-regression, computer graphics, robotics, pattern recognition, nonlinear global optimisation, sensitivity analysis of linear programming, chromosome classification, and computational metrology (material sciences), see [**40, 1**] and the literature given there. For this reason, there exists a substantial number of publications on the computation and approximation of radii, and the complexity of these tasks [**52, 40, 1, 18, 14, 31**].

However, besides the applications, investigating these radii classes is also very interesting from the theoretical point of view, since these radii have a close relation to the outer and inner j-measures of convex bodies. In fact, if one takes the volume of the involved inball instead of the radius, computing the inner (outer) j-radii means approximating the inner (outer) j-measure of the body itself. As we will see, there are some similarities, but also important differences.

In this thesis, we will look into some of the open problems about radii; in particular, we investigate unsolved questions about the radii of special bodies (e.g., regular polytopes and constant breadth bodies), and we also establish new results on the bounds of the ratios between the radii. As they provide a deeper insight in the whole matter some new questions are raised and mostly answered. This is part of the Chapters 3 to 6, each with a different focus, but all closely related. In the following we give a short overview about the different topics in these chapters.

2. Radii of regular polytopes

"Most geometric inequalities have the property that the occurence of the equality sign characterizes geometrically significant objects, like balls, ellipsoids, or simplexes [**43**]." Because of this fact we start with a chapter about the radii of regular polytopes, with a special focus on regular simplices.

As their name suggests, the combinatorial structure of regular simplices is very simple. Hence, it might seem that geometric quantities of simplices, like their outer j-measures are easy to compute and therefore fully understood. This is not the case. The work of Filliman [**33, 34**] shows that the outer j-measures of simplices are quite hard to compute and unknown in almost all dimensions. Similarly, it follows from [**48**] and [**6**] that there are lots of dimensions where the inner and outer radii (whichever way one defines them) of regular simplices are unknown.

While Ball [**4**] showed that the inner j-radius of a regular simplex, as defined in Section 1, is just the inradius of any of its j-faces, any such nice results were previously unknown for its outer j-radii, except for $j \in \{1, d-1, d\}$ [**54, 72, 74, 75**].

The first section of Chapter 3 is its most important part. Here we give a general lower bound on the outer j-radii of regular simplices and show that this bound is attained in all odd dimensions d, and for nearly all even j in even dimensions. The proof of the latter makes strong use of John's theorem [**53**] and an isotropic position of the projections of the simplices in the sense of [**37, 38**].

In Section 2 of Chapter 3 we obtain an upper bound on the outer j-radii of general d-simplices in certain dimensions. This bound enables us to deduce

a geometric inequality about general simplices, which is given as the following theorem: *If $d - j + 1$ divides $d + 1$, then the ratio between the outer j-radius and the diameter of simplices is maximised by the regular simplex.*

In [**30**] a formula for the inner j-radii of general d-boxes is given, which, because of symmetry, can easily be transformed into a formula for the outer j-radii of general cross-polytopes. We complete this result in section 3 by stating a theorem about the outer j-radii of boxes (and therefore about the inradii of cross-polytopes) and show that in the special case of hypercubes and regular cross-polytopes, both results can be derived as corollaries of the theorem about the outer j-radii of regular simplices, which we developed in the first section. Although this corollary does not state new results anymore, it unifies the whole theory.

3. Totally non-spherical bodies

The results in the chapter about totally non-spherical bodies were obtained in collaboration with David Larman [**13**]. The main purpose of this chapter is to show the existence of constant breadth bodies of any dimension that cannot be projected orthogonally onto $\mathbb{B}^2$, the unit disc. We call such bodies totally non-spherical. This result is very important, because the proof that such totally non-spherical bodies exist, permits us to complete the diagram about the possible relations between the different inner and outer radii (see Figure 2.3 in Chapter 2).

To obtain this result we use the concept of dark clouds, which is based on the work of Erdős and Rogers [**28**] about coverings of space with convex bodies and on unpublished work of Danzer [**24**].

We give a short introduction into the matter of dark clouds in the first section of Chapter 4, and extend the concept onto spheres. The second section of this chapter settles the existence of totally non-spherical bodies in arbitrary dimensions, using spherical dark clouds in the main proof.

4. Totally isoradial bodies

In the study of geometric inequalities a class of bodies as important as the simplices are the bodies of constant breadth [**17**], especially because of their

completeness property and the fact that they always have concentric in- and circumspheres (see Chapter 2). For that reason one is interested in 'good' extensions of the concept of constant breadth. The concept of constant inner or outer j-measures, $1 \leq j \leq d-1$ is well known. Here the constant breadth bodies are exactly the bodies of constant inner or outer 1-measure and the existence of non-spherical bodies of constant outer j-measure for any $j \in \{1, \ldots, d-1\}$ is proven by [**35**]. The bodies of constant outer $(d-1)$-measure are also known as bodies of constant brightness and it is one of the challenging open tasks in the field to answer the question whether a body of constant breadth and constant brightness must always be spherical. In [**10**] it is shown that this is true under suitable smoothness assumptions on the boundary of the body.

In Chapter 5, based on joint work with Abhi Dattasharma and Peter Gritzmann [**12**], we present a quite similar generalisation of the constant breadth property in terms of the radii, which we call inner and outer j-isoradiality. Again, the notions of inner or outer 1-isoradiality coincide with the notion of constant breadth, but here, we can show that at least in 3-space, there exists a non-spherical totally isoradial body. This is an example for a convex body different from the ball, which is inner and outer j-isoradial for all possible j.

Our proof of the existence of totally-isoradial bodies in 3-space besides the ball, also shows that there exist non-spherical bodies which have equal outer 2- and outer 3-radius (circumradius). This is an interesting achievement on its own, especially with regard to the following chapter.

5. Blaschke-Santaló diagrams

It is a well known fact that every full dimensional polytope can be described by systems of valid (linear) inequalities and any such collection of inequalities is minimal if and only if every inequality induces exactly one facet of the polytope.

In the following we want to describe the boundary-structure of a non-convex set within the unit cube B^3. Certainly, we cannot do this just by linear inequalities. However, we will see that major parts of the boundary are indeed induced by a few linear inequalities or at least by polynomial inequalities.

To know minimal systems of such inequalities is of significant value to decide whether another inequality is valid and if so, by which inequalities in the system

the new one is dominated. The latter was certainly the reason why Blaschke [7] proposed to map the three fundamental geometric quantities, volume, surface area, and mean curvature, of 3-dimensional convex bodies onto a 2-dimensional diagram, the so called Blaschke-diagram. In his paper Blaschke asked for a complete system of inequalities describing the boundaries of his diagram. Two of the boundaries are described by well known geometric inequalities, but the description of the remaining part of the boundary is still an outstanding open problem [61, 22].

In 1961 Santaló [63] considered similar maps for 2-dimensional convex sets, the so called Blaschke-Santaló-diagrams. Here one chooses triples of the quantities area, perimeter, diameter, width, in- and circumradius; defines a map onto 2-space by using one of the three quantities to normalise the sets; and tries to find complete systems of inequalities describing the boundary structure of the diagram one obtains. Since four of the quantities (diameter, width, in- and circumradius) are the standard radii one gets four pure radii diagrams, each involving three out of four of the radii. A complete system of inequalities for the diagram consisting of the inradius, the diameter, and the circumradius was given already in Santalós original paper, the remaining three in [19, 20].

In Chapter 6 we start with a technical section about Minkowski-sums of convex sets and how they behave in their radii functions. The four well solved Blaschke-Santaló diagrams are given in the second section.

In the third section we step into the actual task of this chapter, which is the description of major parts of the 3-dimensional diagram one obtains from considering all four radii at once, and using the circumradius to normalise the 2-sets. In this manner, the three 2-dimensional Blaschke-Santaló diagrams, which involve the circumradius, are just the projections along the coordinate axes of the 3-dimensional diagram.

The new diagram retains a lot more structure than its projections; thereby making it possible to extract much more information. This enables us to state several new geometric inequalities. Furthermore, we will see that there are six previously unknown (essential) extreme points of the diagram. This is somewhat surprising as none of the six is extreme in any of the three coordinate projections.

We finish this chapter and the whole thesis with a short overview on other possible extensions of the Blaschke-Santaló diagrams. Here it is shown that major parts of the corresponding diagrams for 3-dimensional bodies (and even for convex sets in arbitrary dimensions) can be described by standard inequalities. On the other hand, if we consider diagrams involving radii other than the four standard ones, very little is known. However, the results of the preceding chapters enable us to determine some previously unknown boundaries even for these diagrams.

CHAPTER 2

Preliminaries

In this chapter we give a short summary of the common notations and definitions and add some propositions about well known results on radii. A standard reference for further reading is the handbook of convex geometry [**44, 45**]. A more extensive summary about radii can be found in [**39**].

1. General convexity

Let $\mathbb{E}^d = (\mathbb{R}^d, \|\cdot\|)$ denote the d-dimensional Euclidean space, $d \geq 2$, $\mathbb{B}$ and $\mathbb{S}$ the unit ball and the unit sphere in $\mathbb{E}^d$, respectively, and $\langle \cdot, \cdot \rangle$ the usual *scalar product* $\langle x, y \rangle = x^T y$. Furthermore, we use $\{e_1, \dots, e_d\}$ for the *standard basis* of $\mathbb{E}^d$, and call the subsets of $\mathbb{E}^2$ *planar*.

A *line segment* $[p, q]$ is defined as the set

$$\left\{ x \in \mathbb{E}^d : x = \lambda p + (1 - \lambda)q, \lambda \in [0, 1] \right\},$$

and a subset K of $\mathbb{E}^d$ is called *star shaped* with respect to a point $p \in K$ if for all $q \in K$ the whole line segment $[p, q]$ is in K. If K is star shaped with respect to every $p \in K$ it is *convex*. For any subset M of $\mathbb{E}^d$ the *convex hull* of M is defined as the smallest superset C of M such that C is convex. We denote the convex hull of M by $\mathrm{conv}(M)$. Analogously the *affine hull* $\mathrm{aff}(M)$ of M is the smallest affine subspace containing M. We call a set $C \subset \mathbb{E}^d$ a *body* if it is bounded, closed, and convex. Every body which contains an inner point is called *proper*. A body C is *strictly convex* if the boundary of C contains no segments.

A *face* of a body C is a convex subset F of C such that each segment in C whose relative interior meets F is entirely contained in F. If a face F is neither empty nor the body C itself it is called *proper*. Every point $x \in C$ such that x cannot be written as $\lambda y + (1 - \lambda)z$, with $y, z \in C$ and $\lambda \in (0, 1)$ is called *extreme*. A hyperplane H with $H \cap C \neq \emptyset$ and containing only boundary points of C is called a *supporting* hyperplane of C.

An important subclass of convex bodies is *polytopes*. Planar polytopes are also called *polygons*. One way to define a polytope $P \subset \mathbb{E}^d$ is by its $\mathcal{V}$-*presentation*:

$$P = \operatorname{conv}\{v_1, \ldots, v_n\}, \ v_i \in \mathbb{E}^d, \ i = 1, \ldots, n$$

Note that, if the representation is irreducible, the v_i are precisely the *vertices* (the extreme points of a polytope) of P. The $(d-1)$-dimensional faces of P are called *facets*. It is well known that every polytope P can be written either in a $\mathcal{V}$-*presentation* or as the intersection of finitely many closed halfspaces

$$P = \{x \in \mathbb{E}^d : a_i^T x \leq b_i, i = 1, \ldots, m\}, \ a_i \in \mathbb{E}^d \text{ and } b_i \in \mathbb{R}, \ i = 1, \ldots, m$$

the $\mathcal{H}$-*presentation* of P. Note that, if the $\mathcal{H}$-presentation is irreducible, the sets $\{x \in \mathbb{E}^d : a_i^T x = b_i\}$ are precisely the affine hulls of the facets of P. A *vertex figure* of a vertex v consists of all faces adjacent to v.

Regular polytopes are defined inductively: A planar polygon is called *regular* if all its edges and angles are congruent. A d-polytope is called regular if all its facets are regular and congruent and all its vertex figures are congruent. It is well known that there exist infinitely many regular polygons (the *regular m-gons*, where m denotes the number of edges), five regular polytopes in 3-space (the five *platonics*), and six in four space [**46**]. However, there exist exactly three regular polytopes in d-space if $d \geq 5$, which are the *regular d-simplex* T^d, the *d-cube* B^d, and the *regular d-cross-polytope* X^d (which are sometimes also denoted as d-octahedron).

By $\mathcal{L}_{j,d}$ and $\mathcal{A}_{j,d}$ we denote the set of all j-dimensional linear subspaces and all j-dimensional affine subspaces of $\mathbb{E}^d$, respectively. For any $F \in \mathcal{L}_{j,d}$ let $F^\perp \in \mathcal{L}_{d-j,d}$ be the space orthogonal to F. Furthermore, we use the expression *great 2-circle* to denote any set $\mathbb{S} \cap F$ with $F \in \mathcal{L}_{2,d}$.

Let $\operatorname{span}\{s_1, \ldots, s_j\}$ denote the *linear span*

$$\left\{x \in \mathbb{E}^d : x = \sum_{k=1}^{j} \lambda_k s_k, \lambda_k \in \mathbb{R}\right\}$$

of $s_1, \ldots, s_j \in \mathbb{S}$. For any set $A \subseteq \mathbb{E}^d$, $A|F$ denotes the *(orthogonal) projection* of A onto $F \in \mathcal{L}_{j,d}$. If $s_1, \ldots, s_j$ is an orthonormal basis of F we also use $A_{s_1,\ldots,s_j}$ instead of $A|F$ and $A^{s_1,\ldots,s_j}$ instead of $A|F^\perp$.

For any $x \in \mathbb{E}^{d_1}$ and $y \in \mathbb{E}^{d_2}$ let

$$x \otimes y = \begin{pmatrix} x_1 y_1 & \cdots & x_1 y_{d_2} \\ \vdots & & \vdots \\ x_{d_1} y_1 & \cdots & x_{d_1} y_{d_2} \end{pmatrix}$$

denote the matrix with elements $x_i y_j$, $i = 1, \ldots, d_1$ and $j = 1, \ldots, d_2$. Note that for any set of orthonormal vectors $\{s_1, \ldots, s_j\}$, $1 \le j \le d$ the projection

$$P : \mathbb{E}^d \to \operatorname{span}\{s_1, \ldots, s_j\}$$

can be represented by the matrix

$$\sum_{l=1}^{j} s_l \otimes s_l.$$

For any two sets $A, B \subseteq \mathbb{E}^d$ the *Minkowski sum* $A + B$ is defined as

$$A + B = \{a + b \in \mathbb{E}^d : a \in A, b \in B\}$$

and for any $\lambda \ge 0$ we write

$$\lambda A = \{\lambda a : a \in A\}.$$

A *lattice* $\mathbb{L}$ (of full rank d) in $\mathbb{E}^d$ is the set of all integer linear combinations of d linearly independent vectors $b_1, \ldots, b_d \in \mathbb{E}^d$. The set $\{b_1, \ldots, b_d\}$ is called the *basis* of $\mathbb{L}$. For $b_k = e_k$, $k = 1, \ldots, d$ we call $\mathbb{L}$ the *unit lattice*. Let C be a body and $\mathbb{L}$ a lattice. $C + \mathbb{L}$ is called a *packing* of $\mathbb{E}^d$, if every two distinct translates of C have disjoint interior; and $C + \mathbb{L}$ is called a *covering* of $\mathbb{E}^d$, if $E^d \subseteq C + \mathbb{L}$.

2. The two radii classes

For any $j \in \{1, \ldots, d\}$ the *inner j-radius* $r_j(C)$ of a convex set C is defined by

$$r_j(C) = \max\left\{\rho \ge 0 : (q + \rho\mathbb{B}) \cap F \subseteq C, q \in F \in \mathcal{A}_{j,d}\right\}$$

and the *outer j-radius* $R_j(C)$ by

$$R_j(C) = \min\left\{\rho \ge 0 : E + \rho\mathbb{B} \supseteq C, E \in \mathcal{A}_{d-j,d}\right\}.$$

For $s \in \mathbb{S}$ the *s-length* of C is defined as

$$l_s(C) = \max\{\lambda \ge 0 : c, c' \in C, \text{ such that } c' = c + \lambda s\}$$
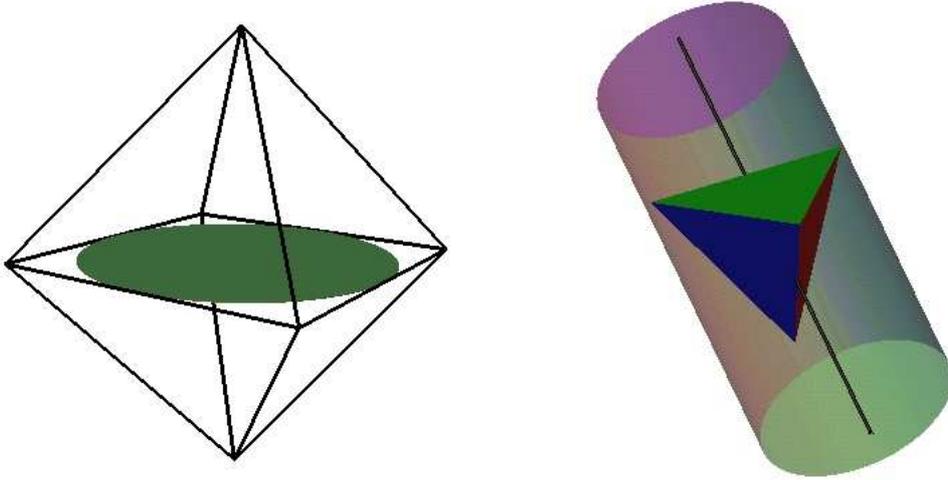
FIGURE 2.1. The inner 2-radius of an octahedron and the outer
2-radius of a tetrahedron. See Chapter 2.3 for proofs.

and the *s-breadth* $b_s(C)$ is defined as

$$b_s(C) = \max_{c \in C}\langle c, s\rangle - \min_{c \in C}\langle c, s\rangle.$$

Now the *diameter* of C is defined as $\mathrm{diam}(C) = \max_{s \in \mathbb{S}} l_s(C)$ and the *width*
as $\mathrm{width}(C) = \min_{s \in \mathbb{S}} b_s(C)$, i.e. the diameter measures the maximum distance
between two points within C, whereas the width is the minimum distance of two
parallel hyperplanes which support C.

Proofs of the following Proposition can be found in [**39**] and [**48**].

PROPOSITION 2.1. *For any d-dimensional body C the following hold*

(i) $R_1(C) \leq \cdots \leq R_d(C)$,

(ii) $r_d(C) \leq \cdots \leq r_1(C)$,

(iii) $R_1(C) = \frac{1}{2}\mathrm{width}(C) = \frac{1}{2}\min_{s \in \mathbb{S}} l_s(C)$
$\leq r_1(C) = \frac{1}{2}\mathrm{diam}(C) = \frac{1}{2}\max_{s \in \mathbb{S}} b_s(C)$, *and*

(iv) $r_j(C) \leq R_{d+1-j}(C)$, $j \in \{1, \ldots, d\}$.

The result of Proposition 2.1 is also displayed in Figure 2.3. In Chapter 4 we
will see that ths diagram is complete in the sense that for any two radii which
are not connected by a directed path there exist bodies C_1, C_2 such that the
relationship between the two radii is 'less than' for C_1 and 'greater than' for C_2.
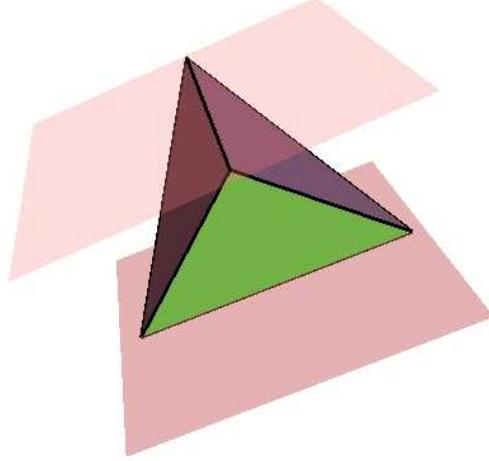
FIGURE 2.2. The width defining hyperplanes of a tetrahedron. See Chapter 2.3 for proofs.
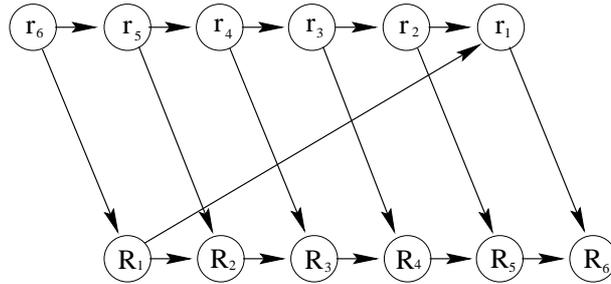
FIGURE 2.3. The arcs imply a less than or equal relationship (from their origin to their sink) between the two corresponding radii, which holds for all d-dimensional bodies.

For every body $C \subset \mathbb{E}^d$ let

$$C^\circ = \{y \in \mathbb{E}^d : \langle c, y \rangle \leq 1 \text{ for all } c \in C\}$$

denote the *polar* of C. Note that we call a body C *symmetric* if it is symmetric with respect to the origin. A proof of the following proposition can be found in [**39**]:

PROPOSITION 2.2. *If C is a proper d-dimensional symmetric body then*

$$r_j(C)R_j(C^\circ) = 1 \text{ and } R_j(C)r_j(C^\circ) = 1$$

for all $1 \leq j \leq d$.

A superscript k for the radii (e.g., R_j^{d-1}, that is $k = d - 1$) denotes the radius relative to a k-dimensional affine space, which is explicitly given or known from the context (e.g., $R_j^{d-1}(C^s)$, $s \in \mathbb{S}$ is the outer j-radius of the projection C^s of C along s, relative to the $(d-1)$-space orthogonal to s). To denote a k-ball (a k-dimensional ball) we will use the notation $\mathbb{B}^k$.

If a body C_1 arises from C_2 by rotation, translation and dilatation, we say C_1 is *similar* to C_2. Note that the radii of a body do not change if the body is translated or rotated; neither are the relationships of the radii affected by scaling the body. For this reason, we will often use the word 'ball' to signify any similar copy of $\mathbb{B}$, and the same we do for simplices, cross-polytopes and cubes (or other well described classes of similar bodies).

If we are free to choose the actual position, we take $T^d = \text{conv}\{e_1, \ldots, e_{d+1}\}$ (embedded in $\mathbb{E}^{d+1}$) and $X^d = \text{conv}\{\pm e_1, \ldots, \pm e_d\}$, where e_k denotes the k-th unit vector (of the appropriate space). By $B_{a_1,\ldots,a_d}$ we denote a d-dimensional *box* of the form $\left\{x \in \mathbb{E}^d : -a_i \leq x_i \leq a_i, i \in \{1, \ldots, d\}\right\}$ such that $B^d = B_{1,\ldots,1}$. Finally, it is well known that a *general cross-polytope* $X_{a_1,\ldots,a_d} = \text{conv}\{\pm a_1, \ldots, \pm a_d\}$ is just the polar of $B_{\frac{1}{a_1},\ldots,\frac{1}{a_d}}$.

The following proposition states the famous geometric inequalities about the circumradius-diameter-ratio and the width-inradius-ratio due to Jung [**54**] and Steinhagen [**72**], respectively. Additionally a result of Alexander [**2**] about the width-circumradius-ratio of simplices is given.

PROPOSITION 2.3. *Let C be a d-dimensional body. Then*

(i) $\dfrac{R_d(C)}{r_1(C)} \leq \sqrt{\dfrac{2d}{d+1}}$,

(ii) $\dfrac{R_1(C)}{r_d(C)} \leq \begin{cases} \sqrt{d}, & \text{if } d \text{ odd} \\ \dfrac{d+1}{\sqrt{d+2}}, & \text{if } d \text{ even} \end{cases}$, *and*

(iii) $\dfrac{R_1(C)}{R_d(C)} \leq \begin{cases} \sqrt{\dfrac{1}{d}}, & \text{if } d \text{ odd} \\ \dfrac{d+1}{d\sqrt{d+2}}, & \text{if } d \text{ even} \end{cases}$, *and if C is a simplex.*

In all cases equality is attained if C is a regular simplex, but the 'only if' direction holds only in case of (iii), as we will see in the remark after Proposition 2.5.

If $E \in \mathcal{A}_{d-j,d}$, $j \in \{1, \ldots, d\}$, we call $E + \rho\mathbb{B}$ a *j-cylinder*. In this notation a usual 3-dimensional cylinder of infinite length is a 2-cylinder. In Euclidean space we can understand the outer-radii in terms of projections onto *j*-spaces instead of smallest circumscribing *j*-cylinders as shown in the following lemma:
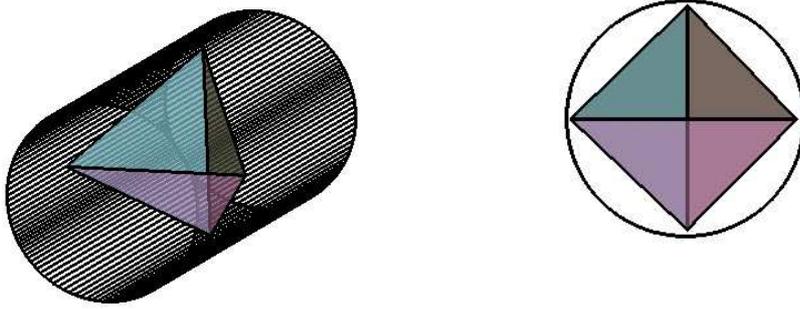
FIGURE 2.4. The tetrahedron and its minimal enclosing cylinder from a slightly skewed view and from the view along the cylinder axes, the latter showing that one can understand the outer radii also in terms of projections.

LEMMA 2.4. *Suppose C is a body, $j \in \{1, \ldots, d\}$ and $k \in \{j, \ldots, d\}$. Then*

$$R_j(C) = \min\{R_j^k(C|F) : F \in \mathcal{L}_{k,d}\}$$

PROOF. We start with the '$\geq$'-direction. Let $\rho^* = R_j(C)$. From the definition of the outer radii it follows that there exists an $E \in \mathcal{A}_{d-j,d}$ such that $E + \rho^*\mathbb{B} \supset C$, which implies that if we project both sets ($E + \rho^*\mathbb{B}$ and C) onto any linear subspace $F \in \mathcal{L}_{k,d}$ then

$$E|F + \rho^*\mathbb{B}^k = (E + \rho^*\mathbb{B})|F \supset C|F.$$

Hence $R_j^k(C|F) \leq \rho^*$ for all $F \in \mathcal{L}_{k,d}$ and therefore

$$\rho^* \geq \min\{R_j^k(C|F) : F \in \mathcal{L}_{k,d}\}.$$

Now we turn to the '$\leq$'-direction. Let $F^* \in \mathcal{L}_{k,d}$ and $\rho^* \geq 0$ such that

$$\min\{R_j^k(C|F) : F \in \mathcal{L}_{k,d}\} = R_j^k(C|F^*) = \rho^*.$$

Hence there exists $E \in \mathcal{A}_{k-j,d}, E \subseteq F^*$ such that $E + \rho^* \mathbb{B}^k \supset C|F^*$. But because

$$\left((E + (F^*)^{\perp}) + \rho^* \mathbb{B}\right) |F^* = E + \rho^* \mathbb{B}^k$$

we obtain that $E + (F^*)^{\perp} + \rho^* \mathbb{B} \supset C$ and because $E + (F^*)^{\perp} \in \mathcal{A}_{d-j,d}$ that

$$R_j(C) \leq \rho^*.$$

$\square$

Note that this lemma does NOT imply that

$$R_j(C) = R_j^k(C|F_2), \ F_2 \in \mathcal{L}_{k,d}, \ j < k < d,$$

where $C|F_2$ is a minimal projection of C for $R_k(C)$.

It is easy to see that $r_1(C) = \max\{r_1^k(C|F) : F \in \mathcal{L}_{k,d}\}$ also holds, but this cannot be extended to $j > 1$ (see the statement after Proposition 3.1).

3. Constant breadth

From Proposition 2.1 (iii) one can easily see that a body C possesses the property $R_1(C) = r_1(C)$ iff the values of its s-length and s-breadth do not depend on $s \in \mathbb{S}$. In this case C is called a *body of constant breadth*.

A body C is called *complete* if $r_1(D) > r_1(C)$ for all $D \supset C$, and for an arbitrary body C, a body $C_\Gamma \supseteq C$ is called a *completion* of C, if C_Γ is complete and $r_1(C_\Gamma) = r_1(C)$. Analogously, a body C is called *reduced* if $R_1(D) < R_1(C)$ for all $D \subset C$, and a body $C_\rho \subseteq C$ is called a *reduction* of C, if C_ρ is reduced and $R_1(C_\rho) = R_1(C)$.

The following proposition gives some known facts about bodies of constant breadth and completions which we will use in the following chapters. Proofs for the different parts can be found in [**10, 68, 25**].

PROPOSITION 2.5. *Let C be a body in $\mathbb{E}^d$.*
(a) The following statements are equivalent:
    (i) C is of constant breadth,
    (ii) for all $s \in \mathbb{S}$ the projection C^s is a body of constant breadth,

(iii) C is complete.

(b) If C is a planar body, then C is of constant breadth iff C is strictly convex and reduced.

(c) There exists a completion of C within C's circumsphere.

(d) If C is a body of constant breadth, then the incentre coincides with the circumcentre and $r_d(C) + R_d(C) = 2r_1(C)$.

Note that every body of constant breadth is reduced but, e.g., the equilateral triangle T^2 is reduced but not of constant breadth. In higher dimensions it is not even known whether Proposition 2.5 (b) holds, and also, in non-Euclidean spaces, the completeness- and the constant-breadth-property are not equivalent.

We make strong use of Proposition 2.5 (c) in Chapter 5, but there is an immediate relation with Jung's inequality (see Proposition 2.3 (i)). Let T_Γ^d denote a completion of T^d within the circumsphere of T^d (which exists because of Proposition 2.5 (c)). Now it is easy to see that all C with $T^d \subseteq C \subseteq T_\Gamma^d$, fulfill Jung's inequality with equality.

We cannot state such a rigorous result for Steinhagen's inequality (see Proposition 2.3 (ii)) as there is no such general result like Proposition 2.5 (c) about a reduction keeping the same inball. Even more, T^2 is a reduced planar set and the unique set fulfilling Steinhagen's-inequality with equality. Nevertheless, if the dimension is at least 3, the width defining hyperplanes are touching T^d not in a single vertex. Hence it is possible to cut of a bit around the vertices of T^d without changing the width or the inradius of T^d and therefore the new set will still fulfill the inequality with equality.

Finally, we give a result that will be important for development of Chapter 6. The constant breadth bodies are of course the only bodies fulfilling

$$2R_1(C) = r_d(C) + R_d(C) = 2r_1(C),$$

but even in Euclidean spaces there exist bodies which are not of constant breadth and fulfill one of the two equations. However, these bodies must at least have concentric in- and circumsphere as the following Lemma shows:

LEMMA 2.6. *Every body C in $\mathbb{E}^d$ which fulfills $2R_1(C) = r_d(C) + R_d(C)$ or $2r_1(C) = r_d(C) + R_d(C)$ has concentric in- and circumspheres.*

PROOF. Suppose non of the possible incentres of C coincides with the circumcentre of C. Then we can define a line l_1 through the circumcentre and one of its closest incentres; and a hyperplane F_1 orthogonal to l_1 containing the circumcentre. Now there must be a point $p \in C$ on its circumsphere which is separated from the incentre by F_1. Now we draw a line l_2 through p and the incentre. Surely, l_2 cuts through the insphere at two points, one at a distance from p which is greater than $r_d(C) + R_d(C)$. But this means that $r_1(C) > r_d(C) + R_d(C)$.

Now consider the hyperplane F_2 parallel to F_1 through the incentre. Since we have chosen a closest in- and circumcentre pair, there must lie a point $q \notin F_2$ on the insphere on the same side of F_2 as the circumcentre, such that the tangent hyperplane E_1 to the insphere at q also supports C. Hence C lies completely between E_1 and its parallel hyperplane supporting the circumsphere of C on the other side of the centres. But as the distance of E_1 and E_2 is less than $r_d(C) + R_d(C)$ we see that $R_1(C) < r_d(C) + R_d(C)$. □

CHAPTER 3

Radii of regular polytopes

In [**46**] Grünbaum starts the section about regular polytopes as follows: "Regular polytopes, and different kinds of semiregular polytopes, have been a topic of investigation since antiquity, and during the centuries led to many interesting and important notions and results." Hence, computing the radii of regular polytopes has certainly a value of its own. Nevertheless, as known now for more than a century, they often attain the extreme values in geometric inequalities involving different radii. This is especially true for the regular simplices.

While the inner radii of regular simplices are well studied, see Proposition 3.1, very less was previously discovered about their outer radii. In Section 1 of this chapter we will give a lower bound on these radii (Theorem 3.4), and show that this bound is tight whenever d is odd or j is even and $d \neq 2j$ (Theorem 3.14). Together with [**72, 74, 75**], this result implies that the exact value of all radii up to dimension 5 is now known, and thus the lowest dimensional case that still remains unsolved is $R_3(T^6)$ (the only unknown case for 6 dimensional regular simplices). The lowest unsolved outer j-radius with even j is $R_6(T^{12})$.

An important step towards this result is the investigation of quasi isotropic polytopes (Kawashima called them π-polytopes [**55**], but we prefer to call them isotropic as they are in an isotropic position in the sense of [**37**]). Specifically, we will show that the existence of a quasi isotropic j-dimensional polytope with $d+1$ vertices is equivalent to the existence of a projection of the regular simplex such that the lower bound on the radii is attained.

In Section 2 we give some results about outer radii of general simplices and show for certain dimensions d and j that the ratio between the R_j- and r_1-radii of simplices is maximised by the regular simplex.

The final section of Chapter 3 is devoted to the radii of boxes and cross-polytopes. While the inner radii of boxes were computed in [**30**], we could not find a result about their outer radii in the literature. This gap is closed in this

thesis, as well as the results about boxes are transferred to results about cross-polytopes via polarisation. Finally, we show that the radii of cubes and regular cross-polytopes can be obtained almost completely from our results about the outer-radii of regular simplices. This unifies the whole chapter.

1. Regular simplices

The following result about the inradii of simplices is taken from [**4**]:

PROPOSITION 3.1. *For every simplex S*

$$r_j(S) = \max\{r_j^j(S^j) : S^j \text{ is a } j\text{-dimensional face of } S\}$$

holds and T^d has the maximal inner j-radius for all d-simplices of maximal edge-length $\sqrt{2}$, which is

$$r_j(T^d) = \sqrt{\frac{1}{j(j+1)}} \; .$$

In 3-space $r_2(T^3) = \frac{1}{\sqrt{6}}$, but if we project T^3 orthogonal to a pair of orthogonal sides we get a square with diagonal length $\sqrt{2}$, and therefore the inradius of this projection is $\frac{1}{2}$. Hence $r_2(T^3) < \max\{r_2^2(T^3|F) : F \in \mathcal{L}_{2,d}\}$ (recall the remark after Lemma 2.4).

Now we state some previously known results about outer radii of regular simplices, which either follow from Proposition 2.3 or are taken from [**74, 75**]:

PROPOSITION 3.2.   *(i) $R_d(T^d) = \sqrt{\frac{d}{d+1}}$*

$$\text{(ii) } R_1(T^d) = \begin{cases} \sqrt{\frac{1}{d+1}}, & \text{if } d \text{ odd} \\ \sqrt{\frac{d+1}{d(d+2)}}, & \text{if } d \text{ even.} \end{cases}$$

$$\text{(iii) } R_{d-1}(T^d) = \begin{cases} \sqrt{\frac{d-1}{d+1}}, & \text{if } d \text{ odd} \\ \sqrt{\frac{(2d-1)^2}{4d(d+1)}}, & \text{if } d \text{ even.} \end{cases}$$

Proposition 3.2 is not as complete a result as as Proposition 3.1. At the end of this section we will be able to give a result on the outer radii of regular simplices which is much more general than the above Proposition. To do so, we make use of the following definition:

DEFINITION 3.3. *We call any set of orthonormal vectors* $\{s_1, \ldots, s_j\}$, $j \in \{1, \ldots, d\}$ *in* $\mathbb{E}^{d+1}$

  (i) a valid subspace basis *(vsb for short) if* $\sum_{k=1}^{d+1} s_{lk} = 0$ *for all* $l \in \{1, \ldots, j\}$, *and*

  (ii) a good subspace basis *(gsb for short) if it is a vsb and* $\sum_{l=1}^{j} s_{lk}^2 = \frac{j}{d+1}$ *for all* $k \in \{1, \ldots, d+1\}$.

Note that any set of orthonormal vectors $\{s_1, \ldots, s_j\}$ is called a vsb if it spans a j-dimensional subspace of

$$\mathbb{E}_0^{d+1} = \left\{ x \in \mathbb{E}^{d+1} : \sum_{k=1}^{d+1} x_k = 0 \right\},$$

the d-dimensional linear subspace of $\mathbb{E}^{d+1}$ parallel to the hyperplane in which we have embedded T^d.

The projection of T^d onto $\mathbb{E}_0^{d+1}$ can be written as $I^{d+1} - \frac{1}{d+1}\mathbf{1}^{d+1}$, where I^{d+1} denotes the identity matrix in $\mathbb{E}^{(d+1)\times(d+1)}$ and $\mathbf{1}^{d+1}$ the matrix in $\mathbb{E}^{(d+1)\times(d+1)}$ consisting only of 1's. Hence it holds that

$$\sum_{l=1}^{d} s_l \otimes s_l = I^{d+1} - \frac{1}{d+1}\mathbf{1}^{d+1},$$

for every vsb of d elements. This enables us to obtain the important fact that each vsb is a gsb if $j = d$, which we use in Corollary 3.5.

Now we start improving the results on the outer radii of regular simplices by giving a general lower bound, which we will prove to be tight in many cases further on. This theorem will also show the reason why we call a vsb good if it fulfills the condition (ii) in Definition 3.3.

THEOREM 3.4.

$$R_j(T^d) \geq \sqrt{\frac{j}{d+1}}$$

for all $d \geq 2$ *and* $j \in \{1, \ldots, d\}$ *and equality holds iff there exists a gsb* $\{s_1, \ldots, s_j\}$ *in* $\mathbb{E}^{d+1}$.

PROOF. Let P denote the projection onto some subspace spanned by a vsb $\{s_1, \ldots, s_j\}$. It follows that

$$\|Pe_k\|^2 = \langle Pe_k, e_k \rangle = \left\langle \sum_{l=1}^{j} s_{lk}s_l, e_k \right\rangle = \sum_{l=1}^{j} s_{lk}^2.$$

Now assume there exists some $x \in \mathbb{E}^{d+1}$ such that $\|x - Pe_k\|^2 < \frac{j}{d+1}$ for all $k = 1, \ldots, d+1$. Summing over the k's, we get

$$j > \sum_{k=1}^{d+1} \|x - Pe_k\|^2$$

$$= \sum_{k=1}^{d+1} \left(\|x\|^2 - 2\langle x, Pe_k \rangle + \|Pe_k\|^2 \right)$$

$$= (d+1)\|x\|^2 - 2\left\langle x, \sum_{k=1}^{d+1}\sum_{l=1}^{j} s_{lk}s_l \right\rangle + \sum_{k=1}^{d+1}\sum_{l=1}^{j} s_{lk}^2$$

and since $\sum_{k=1}^{d+1} s_{lk} = 0$ and $\sum_{k=1}^{d+1} s_{lk}^2 = 1$

$$= (d+1)\|x\|^2 + j$$

$$\geq j$$

which is a contradiction. This proves the first part of the theorem. To prove the other part, look at the expression above; it is easy to see that equality in $\|x - Pe_k\|^2 \leq \frac{j}{d+1}$ for all k can only be obtained if $x = 0$ and $\sum_{l=1}^{j} s_{lk}^2 = \frac{j}{d+1}$. $\square$

As every vsb of d vectors is already a gsb we obtain the following corollary from Theorem 3.4 and the basis extension property (used on $\mathbb{E}_0^{d+1}$):

COROLLARY 3.5. *For any dimension d and any $j \in \{1, \ldots, d-1\}$ it holds that*

$$R_j(T^d) = \sqrt{\frac{j}{d+1}} \Leftrightarrow R_{d-j}(T^d) = \sqrt{\frac{d-j}{d+1}}.$$

Moreover the corresponding optimal projections take place in orthogonal subspaces.

Corollary 3.5 shows that Proposition 3.2 (ii) and (iii) correspond to each other in the sense that the lower bound of Theorem 3.4 is attained in both cases for

odd dimensions and that the bound is not attained in even dimensions (however, in the even cases the minimal projections are not orthogonal to each other).

The following Proposition is a polar version of John's theorem [**53**]:

PROPOSITION 3.6. *The unit ball* $\mathbb{B}$ *is the ellipsoid of minimal volume containing some body* $C \subset \mathbb{E}^d$ *iff* $C \subset \mathbb{B}$ *and for some* $m \geq d$ *there are unit vectors* $u_1, \ldots, u_m$ *on the boundary of* C*, and positive numbers* $c_1, \ldots, c_m$ *summing to* d *such that*

(i) $\sum_{i=1}^m c_i u_i = 0$ *and*

(ii) $\sum_{i=1}^m c_i u_i \otimes u_i = I^d$.

Of course, if C is a regular polytope we can choose the values of every c_i as $\frac{d}{m}$, where m is the number of vertices of C. However, it is not obvious which other polytopes fulfill this property. Nevertheless, according to [**37**] these polytopes are in an isotropic position, corresponding to the measure μ^* on $\mathbb{S}$ that gives mass $\frac{d}{m}$ to all vertices u_i. This is the source for the following definition:

DEFINITION 3.7. *Let* $C = \operatorname{conv}\{u_1, \ldots, u_m\} \subset \mathbb{B}$ *be a polytope, where all* u_i*'s are situated on* $\mathbb{S}$*. We call* C *quasi isotropic, if all the* c_i*'s in Proposition 3.6 can be taken as* $\frac{d}{m}$*, and* isotropic*, if additionally* $u_{i_1} \neq u_{i_2}$ *for all* $i_1 \neq i_2$.

The following Lemma shows that the quasi isotropic condition is not as strict as it looks like:

LEMMA 3.8. *Suppose the polytope* $C = \operatorname{conv}\{u_1, \ldots, u_m\}$ *fulfills all the conditions of Proposition 3.6 with* $c_i \in \mathbb{Q}$*,* $i = 1, \ldots, m$*. Then* C *is quasi isotropic.*

PROOF. Suppose p is the least common denominator of the c_i's. Hence we can write $c_i = \frac{q_i}{p}$ with $q_i \in \mathbb{N}$ for all i. Now choose every u_i q_i-times and it is easy to see that this set fulfills the quasi isotropic condition. $\qquad\square$

For practical purposes Lemma 3.8 is of minor value as the denominator p can be very big. But the quasi isotropic polytopes are very important as the next Lemma demonstrates:

LEMMA 3.9. *There exists a gsb $s_1, \ldots, s_j$ of $\mathbb{E}^{d+1}$ iff there exists a quasi isotropic polytope $C = \operatorname{conv}\{u_1, \ldots, u_{d+1}\} \subset \mathbb{E}^j$, $j \leq d$. Moreover, if we project T^d onto $\operatorname{span}\{s_1, \ldots, s_j\}$ the projection will be similar to the corresponding C.*

PROOF. If $C = \operatorname{conv}\{u_1, \ldots, u_{d+1}\}$ is a quasi isotropic polytope then

(i) $\|u_k\| = 1$,

(ii) $\sum_{k=1}^{d+1} u_k = 0$, and

(iii) $\sum_{k=1}^{d+1} u_k \otimes u_k = I^j$.

Now let $s_l = \sqrt{\frac{j}{d+1}}\{u_{1,l}, \ldots, u_{d+1,l}\}$, $l = 1, \ldots, j$. This defines a gsb. For showing this it is necessary that the s_l form an orthonormal set, but this is the case because of (iii). $\sum_{k=1}^{d+1} s_{lk}$ has to be 0, but this follows from (ii), and finally we need $\sum_{l=1}^{j} s_{lk}^2 = \frac{j}{d+1}$ for all k, but this is true because of (i). The other direction can be shown using a similar reasoning.

Now, if we project the vertices of T^d onto $\operatorname{span}\{s_1, \ldots, s_j\}$ we get $Pe_k = \sum_{l=1}^{j} s_{lk} s_l = \sum_{l=1}^{j} \sqrt{\frac{j}{d+1}} u_{kl} s_l$. Hence the values $\sqrt{\frac{j}{d+1}} u_{kl}$ are just the coordinates of the vertices of the projection in terms of the basis $s_1, \ldots, s_j$. □

Lemma 3.9 can be used in two ways:

(i) We know that $R_j(T^d) = \sqrt{\frac{j}{d+1}}$ whenever we find a quasi isotropic j-dimensional polytope with $d + 1$ vertices and vice versa (therefore, due to Proposition 3.2 (iii) there cannot be quasi isotropic polytopes with $d + 2$ vertices if d is odd), and

(ii) we know that the radius $R_k(C)$ of any j-dimensional quasi isotropic polytope C with $d + 1$ vertices is $\sqrt{\frac{k}{j}}$ for any $k \leq j$, if the gsb $\{s_1, \ldots, s_j\}$ can be split into two gsb's $\{s_1, \ldots, s_k\}$ and $\{s_{k+1}, \ldots, s_j\}$.

In this section we will concentrate our attention to Part (i) above but come back to (ii) in Section 3.

It is easy to see that all regular m-gons are isotropic in $\mathbb{E}^2$ if their circumradius is 1. Now consider a prism or an anti-prism, with a regular m-gon as the basis and the distance between the bottom and the top m-gon chosen such that the smallest enclosing ellipsoid is a ball. Finally, we scale the whole (anti-) prism to obtain circumradius 1. This polytopes are again isotropic and together with the planar isotropic m-gons they lead us to the following corollary (the cases $j = d-2$ and $j = d - 3$ follow from Corollary 3.5):

COROLLARY 3.10.   *(i) $R_2(T^d) = \sqrt{\frac{2}{d+1}}$, $R_{d-2}(T^d) = \sqrt{\frac{d-2}{d+1}}$ for all $d \geq 2$, and*

(ii) $R_3(T^d) = \sqrt{\frac{3}{d+1}}$, $R_{d-3}(T^d) = \sqrt{\frac{3}{d+1}}$ for all odd $d \geq 3$.

In the following we do not always mention the $d - j$ cases as long as we make no special use of them. The following lemma will turn out to be the last big piece to prove the final theorem of this section. Here we utilise the relation between the simplex radii and the quasi isotropic polytopes to get some additive and multiplicative rules on the involved dimensions:

LEMMA 3.11.   *(i) Suppose $d = d_1 + d_2 + 1$,*

$$R_j(T^{d_1}) = \sqrt{\frac{j}{d_1 + 1}} \ and \ R_j(T^{d_2}) = \sqrt{\frac{j}{d_2 + 1}}.$$

Then

$$R_j(T^d) = \sqrt{\frac{j}{d + 1}}.$$

(ii) Suppose $d + 1 = (d_1 + 1)(d_2 + 1)$,

$$R_{j_1}(T^{d_1}) = \sqrt{\frac{j_1}{d_1 + 1}} \ and \ R_{j_2}(T^{d_2}) = \sqrt{\frac{j_2}{d_2 + 1}}.$$

Then

$$R_j(T^d) = \sqrt{\frac{j}{d + 1}}$$

for all

$$j \in \{k_1, k_2, k_1 k_2, k_1(k_2 + 1), (k_1 + 1)k_2, (k_1 + 1)(k_2 + 1)\},$$

where $k_i \in \{j_i, d_i - j_i, d_i\}$, $i = 1, 2$.

PROOF. Part (i) is quite simple in terms of the polytopes: If C_1 and C_2 are two quasi isotropic polytopes with $d_1 + 1$ and $d_2 + 1$ vertices, respectively, then their convex hull has $d + 1$ (not necessary different) vertices and is again quasi isotropic. For Part (ii) there is a bit more to do. Suppose $\{s_1, \ldots, s_{k_1}\}$ and $\{t_1, \ldots, t_{k_2}\}$ are gsb's in $\mathbb{E}^{d_1+1}$ and $\mathbb{E}^{d_2+1}$, respectively, and consider the following three sets in $\mathbb{E}^{d+1}$:

$$\sqrt{\frac{1}{d_2 + 1}} (\underbrace{s_l^T, \ldots, s_l^T}_{d_2+1})^T, \ l = 1, \ldots, k_1,$$

and

$$\sqrt{\frac{1}{d_1+1}}(\underbrace{t_{l1},\ldots,t_{l1}}_{d_1+1},\ldots,\underbrace{t_{l(d_2+1)},\ldots,t_{l(d_2+1)}}_{d_1+1})^T,\ l=1,\ldots,k_2,$$

and

$$s_{l_1}\otimes t_{l_2},\ l_1=1,\ldots,k_1,\ l_2=1,\ldots,k_2$$

where we take the $\otimes$-matrix as a vector, column by column. Now, it is not diffcult to see that all vectors in the three sets form a vsb of size $k_1+k_2+k_1k_2$ and that each of the three sets forms a gsb. The principle of the according proofs is always the same: if we factor the constant terms in the arising double-sums out, we obtain the desired properties as they are true for the s_{l_1}'s and t_{l_2}'s.   □

Note that the first two groups could also be obtained from Part (i) applying it k_i-times. Also one should recognise that the polytope corresponding to the k_1k_2 gsb is similar to $\mathrm{conv}\{u_{i_1}\otimes v_{i_2},\ i_1=1,\ldots,d_1+1,\ i_2=1,\ldots,d_2+1\}$ if $\mathrm{conv}\{u_1,\ldots,u_{d_1+1}\}$ and $\mathrm{conv}\{v_1,\ldots,v_{d_2+1}\}$ are the polytopes corresponding to the initial gsb's. Finally, the polytopes one gets using Part (ii) stay much more 'regular' compared to the polytopes obtained from Part (i).

EXAMPLE 3.12. *Suppose $d_1=1$ and $d_2=2$ in Lemma 3.11 (ii), so $d=5$. If we forget about the normalising factors, gsb's for d_1 and d_2 could be*

$$\left\{\begin{pmatrix}1\\-1\end{pmatrix}\right\},\left\{\begin{pmatrix}1\\-1\\0\end{pmatrix},\begin{pmatrix}1\\1\\-2\end{pmatrix}\right\},$$

respectively. Using the construction in Lemma 3.11 we get the following three gsb's for $d=5$:

(i) the d_1-gsb by putting the $\begin{pmatrix}1\\-1\end{pmatrix}$ vector $d_2+1=3$ times below each other

$$\left\{\begin{pmatrix}1\\-1\\1\\-1\\1\\-1\end{pmatrix}\right\},$$

(ii) *the d_2-gsb by taking every entry in the original d_2-gsb $d_1 + 1$ times below each other*

$$\left\{ \begin{pmatrix} 1 \\ 1 \\ -1 \\ -1 \\ 0 \\ 0 \end{pmatrix}, \begin{pmatrix} 1 \\ 1 \\ 1 \\ 1 \\ -2 \\ -2 \end{pmatrix} \right\},$$

and

(iii) *the $d_1 d_2$-gsb by multiplying each vector of the d_1-gsb coordinate wise with any vector of the d_2-gsb*

$$\left\{ \begin{pmatrix} 1 \\ -1 \\ -1 \\ 1 \\ 0 \\ 0 \end{pmatrix}, \begin{pmatrix} 1 \\ -1 \\ 1 \\ -1 \\ -2 \\ 2 \end{pmatrix} \right\}.$$

As $R_1(T^1) = \sqrt{\frac{1}{2}}$ and $R_2(T^d) = \sqrt{\frac{2}{d+1}}$ we can say, immediately from Lemma 3.11(ii) that:

COROLLARY 3.13.

$$R_j(T^d) = \sqrt{\frac{j}{d+1}}$$

for all $j \in \{1, \ldots, 5\}$ if d is odd.

But with a bit of work we can get a lot more out of Lemma 3.11(i):

THEOREM 3.14.

$$R_j(T^d) = \sqrt{\frac{j}{d+1}}$$

if

(i) *d is odd, or*

(ii) *j is even and $d \neq 2j$.*

PROOF. We do an inductive proof over j and d. It is known already that (i) and (ii) are true for $j = 1, 2, 3$. So let $j \geq 4$ and suppose $d < 2j$. Then $d - j < j$ and therefore the statement follows inductively by applying Corollary 3.5, because if d is odd we do not depend on j and if d is even then $d - j$ is even if j is, and $2(d - j) = d$ would mean $2j = d$.

Suppose $d > 2j$. If $d - j = 2j$ we can apply Lemma 3.11 (i) with $R_j(T^{j+2})$ and $R_j(T^{d-j-3})$; otherwise we can apply Lemma 3.11 (i) with $R_j(T^j)$ and $R_j(T^{d-j-1})$. $R_j(T^j)$ and $R_j(T^{j+2})$ belong to the $(d < 2j)$-case and we can use the other two by induction if $d - j - 1$ or $d - j - 3$ are good for one of the two cases. But if j is odd we can assume that d is odd and then these two numbers are also odd and we fulfill case (i). On the other hand, if j is even at least one of them is not equal to $2j$ and we obtain case (ii) for at least one of the two pairs.

We are left with the case $d = 2j$, which can only occur in case of even d and therefore this is neither case (i) nor (ii). $\square$

It is easy to see (from the techniques used to prove the above theorem) that, if one could find just a single case where $R_j(T^d)$ attains the general lower bound with $d + 1$ and j both odd, then this would be true for almost all d and j.

The 'only if'-direction in Theorem 3.14 would not be true as one can find gsb's for the special case that $d + 1 = 2j$, with even j for many d:

LEMMA 3.15. *In case of $d = 2j$ and j even*

$$R_j(T^d) = \sqrt{\frac{j}{d+1}}$$

holds if $d + 1 = (d_1 + 1)(d_2 + 1)$ with d_1 a divisor of j and if $\frac{j}{d_1}$ is odd then $\frac{j}{d_1} - 1 \neq \frac{d_1}{2}$.

PROOF. Because d_1 divides j we can make use of Lemma 3.11 (ii) with $j_1 = d_1$ and $j_2 = \frac{j}{d_1}$ or $j_2 = \frac{j}{d_1} - 1$ whichever is even. Now we only have to ensure that $2j_2 \neq d_2$. But from $2\frac{j}{d_1} = d_2$ it follows that $d + 1 = (d_1 + 1)(\frac{2j}{d_1} + 1) = d + \frac{2j}{d_1} + d_1 + 1$ and therefore $j = -\frac{d_1^2}{2}$ which is a contradiction. And from $2\frac{j}{d_1} - 1 = d_2$ it follows that $d + 1 = (d_1 + 1)(\frac{2j}{d_1} - 1) = d + \frac{2j}{d_1} - d_1 - 1$ and therefore $\frac{j}{d_1} = \frac{d_1}{2} + 1$, the case which is excluded by the assumption. $\square$

j,d	1	2	3	4	5	6	7	8	9	10	11	12	13	14	15	16
1	+	-	+	-	+	-	+	-	+	-	+	-	+	-	+	-
2		+	+	+	+	+	+	+	+	+	+	+	+	+	+	+
3			+	-	+	(-)	+	(-)	+	(-)	+	(-)	+	(-)	+	(-)
4				+	+	+	+	+	+	+	+	+	+	+	+	+
5					+	-	+	(-)	+	(-)	+	(-)	+	(-)	+	(-)
6						+	+	+	+	+	+	?	+	+	+	+
7							+	-	+	(-)	+	(-)	+	(-)	+	(-)
8								+	+	+	+	+	+	+	+	?
9									+	-	+	(-)	+	(-)	+	(-)
10										+	+	+	+	+	+	+

TABLE 3.1. The table shows the existence of j-dimensional quasi isotropic polytopes with $d+1$ vertices. The first column states the j value, the first row the value of d. A '+' indicates the existence, a '-' the non-existence. The '(-)' entries show that the nonexistence is not proven but very unlikely, the '?'-s show the open cases for even j. Be careful, in terms of the outer j-radii both '+' and '-', indicate that the radii of the regular simplices are known, and each '(-)' or '?' entry stands for an unsolved case.

Lemma 3.15 includes the case that 3 divides $d+1$ (because j is even) and the case that $d+1 = (d_1 + 1)^2$ with d_1 is not divisible by 4 (because $j = \frac{d_1}{2} + 1$).

On the other hand Lemma 3.15 cannot help in the case $d = 2j$, j even if $d+1$ is a prime, neither does it always help if $d+1$ is not prime. For example, if $d+1 = 5 \cdot 17$ we obtain $j = 42$. Here we would need $j_1 \in \{2, 4\}$, but if $j_1 = 2$ it follows that $j_2 > d_2$, which is a contradiction. Hence $j_1 = 4$, but this is not possible because neither 4 nor 5 divides 42.

2. General simplices

In this section we will present two results about the outer radii of general simplices. We start with a lemma that allows us to give an upper bound in terms of the outer radii of lower dimensional simplices:

LEMMA 3.16. *For every dimension d and every j, such that $d+1$ and $d-j+1$ have a common divisor $k \in \mathbb{N}$, every simplex $S^d = \text{conv}\{x_1, \ldots, x_{d+1}\}$ fits in a j-cylinder of diameter*

$$\min_{\{i_1,\ldots,i_{d+1}\}=\{1,\ldots,d+1\}} \left(\max_{l=0,\ldots,k-1} R_{j'}^{d'}\left(\text{conv}\{x_{i_{1+l(d'+1)}}, \ldots, x_{i_{(d'+1)+l(d'+1)}}\}\right)\right),$$

where $d' = \frac{d+1}{k} - 1$ and $j' = \frac{j}{k}$.

PROOF. Wlog we can assume that

$$\min_{\{i_1,\ldots,i_{d+1}\}=\{1,\ldots,d+1\}} \left(\max_{l=0,\ldots,k-1} R_{j'}^{d'}\left(\text{conv}\{x_{i_{1+l(d'+1)}}, \ldots, x_{i_{(d'+1)+l(d'+1)}}\}\right)\right)$$
$$= R_{j'}^{d'}(\text{conv}\{x_1, \ldots, x_{d'+1}\}) \geq \cdots \geq R_{j'}^{d'}(\text{conv}\{x_{1+(k-1)(d'+1)}, \ldots, x_{d+1}\}).$$

Now for every vertex of S^d the distance to $E = \text{aff}\{E_0, \ldots, E_{k-1}\} \in \mathcal{A}_{d-j,d}$ is at most $R_{j'}^{d'}(\text{conv}\{x_1, \ldots, x_{d'+1}\})$ and it follows $S^d \subset E + R_{j'}^{d'}(\text{conv}\{x_1, \ldots, x_{d'+1}\})\mathbb{B}$, where $E_l \in \mathcal{A}_{d'-j',d'}$ are the affine spaces in the definition of the $R_{j'}^{d'}$-radii of $\text{conv}\{x_{1+l(d'+1)}, \ldots, x_{(d'+1)+l(d'+1)}\}$, $l = 0, \ldots, (k-1)$. $\qquad\square$

Using Lemma 3.16 we can prove the following geometric inequality for the class of simplices:

THEOREM 3.17. *Suppose S^d is a d-simplex. Then for every j, such that*

(i) *$d - j + 1$ divides $d + 1$ or*

(ii) *$j = 1$*

it holds that
$$\frac{R_j(S^d)}{r_1(S^d)} \leq \sqrt{\frac{2j}{d+1}},$$

with equality if $S^d = T^d$.

PROOF.   (i) First, note that if we use the notations of Lemma 3.16 $j' = d'$ and therefore we get

$$R_j(S^d) \leq \max\left\{ R_{d'}(S^{d,d'}) : S^{d,d'} \text{ a } d'\text{-face of } S^d\right\}.$$

But from Proposition 2.3 (i) $\frac{R_{d'}(S^{d,d'})}{r_1(S^{d,d'})}$ is at most $\frac{2d'}{d'+1} = \frac{2j}{d+1}$ and this value is attained by the regular simplex.

(ii) Follows directly from Proposition 2.3 (i) and (iii).

$\qquad\square$

3. Boxes and cross-polytopes

Compared to the general simplices, much more is known about the radii of boxes and general cross-polytopes. We start with a result about the inner-radii of boxes, which is taken from [**30**]. The part about outer radii of cross-polytopes just follows from polarisation, see Proposition 2.2. Afterwards, we will complete the radii of boxes and cross-polytopes by stating the corresponding result about outer radii of boxes. Finally, we unify the whole theory by showing that the radii of hypercubes and regular cross-polytopes could be derived as a corollary of the outer radii of regular simplices.

PROPOSITION 3.18. *Let $0 < a_1 \leq \cdots \leq a_d$. Then*

(i)

$$r_j(B_{a_1,\ldots,a_d}) = \sqrt{\frac{a_1^2 + \cdots + a_{d-k}^2}{j-k}},$$

where k is the smallest of the integers $0, \ldots, j-1$ that satisfies

$$a_{d-k} \leq \sqrt{\frac{a_1^2 + \cdots + a_{d-k-1}^2}{j-k-1}},$$

and

(ii)

$$R_j(X_{a_1,\ldots,a_d}) = \sqrt{\frac{(j-k)\prod_{i=k}^d a_i^2}{\sum_{i=k}^d \prod_{l\neq i} a_l^2}},$$

where k is the smallest of the integers $0, \ldots, j-1$ that satisfies

$$a_k \geq \sqrt{\frac{(j-k-1)\prod_{i=k+1}^d a_i^2}{\sum_{i=k+1}^d \prod_{l\neq i} a_l^2}}.$$

The corresponding result about the outer radii of boxes seems to be very intuitive. It says that one should just project the box through one of its smallest faces. One gets the inner radii of cross-polytopes from polarisation. Before we state the final theorem, we give a technical lemma which will be useful in the proof of the theorem.

LEMMA 3.19. *Let $s_l \in \mathbb{E}^d$, $l = 1, \ldots, j$, $j \le d$, $d \ge 2$ be a set of orthonormal vectors and $a_1, \ldots, a_d \in \mathbb{R}_+$. Then there exists a choice of plus and minus signs in $\sum_{l=1}^{j} (\sum_{k=1}^{d} \pm a_k s_{lk})^2$ such that this is at least $\sum_{k=1}^{d} a_k^2 \sum_{l=1}^{j} s_{lk}^2$.*

PROOF. Essentially we have to show that there is an $\alpha = (\alpha_1, \ldots, \alpha_d)$ with $\alpha_k \in \{-a_k, a_k\}$ such that

$$\Gamma_\alpha := \sum_{1 \le k_1 < k_2 \le d} \alpha_{k_1} \alpha_{k_2} \zeta_{k_1, k_2} \ge 0, \text{ where } \zeta_{k_1, k_2} := \sum_{l=1}^{j} s_{lk_1} s_{lk_2}.$$

This is done by an inductive proof.

First consider the case $d = 2$. Then $\Gamma_\alpha = \alpha_1 \alpha_2 \zeta_{1,2}$. So we choose $\alpha_i = a_i$, $i = 1, 2$ if $\zeta_{1,2} \ge 0$ and if $\zeta_{1,2} < 0$ we choose $\alpha_1 = a_1$ and $\alpha_2 = -a_2$.

Now let $d = 3$. Hence $\Gamma_\alpha = \alpha_1 \alpha_2 \zeta_{1,2} + \alpha_1 \alpha_3 \zeta_{1,3} + \alpha_2 \alpha_3 \zeta_{2,3}$. Now suppose $\Gamma_{(a_1, a_2, -a_3)} < 0$ and $\Gamma_{(-a_1, a_2, -a_3)} < 0$. It follows that

$$0 > \Gamma_{(a_1, a_2, -a_3)} + \Gamma_{(-a_1, a_2, -a_3)} = -2a_2 a_3 \zeta_{2,3}$$

and therefore that $\zeta_{2,3} > 0$. Analogously one can show that $\zeta_{1,2}$ and $\zeta_{1,3}$ are positive; but then we can choose $\alpha = (a_1, a_2, a_3)$.

By knowing that the statement is correct for $d = 2, 3$ we can take an inductive step of 2, that means we assume the statement is proven up to some d and now conclude that it is also true for $d + 2$.

Now suppose the statement would be wrong for $d + 2$, meaning $\Gamma_\alpha < 0$ for all possible choices of $\alpha \in \mathbb{E}^{d+2}$. Hence

$$0 > \Gamma_{\alpha_1, \ldots, \alpha_d, a_{d+1}, a_{d+2}} + \Gamma_{\alpha_1, \ldots, \alpha_d, -a_{d+1}, a_{d+2}} + \Gamma_{\alpha_1, \ldots, \alpha_d, a_{d+1}, -a_{d+2}} + \Gamma_{\alpha_1, \ldots, \alpha_d, -a_{d+1}, -a_{d+2}}$$

$$= 4 \sum_{1 \le k_1 < k_2 \le d} \alpha_{k_1} \alpha_{k_2} \zeta_{k_1, k_2}.$$

However, this is not possible as by the induction hypothesis

$$\sum_{1 \le k_1 < k_2 \le d} \alpha_{k_1} \alpha_{k_2} \zeta_{k_1, k_2} \ge 0$$

for at least one possible choice of α. $\square$

THEOREM 3.20. *Let $0 < a_1 \le \cdots \le a_d$. Then*

(i) $R_j(B_{a_1, \ldots, a_d}) = \sqrt{a_1^2 + \cdots + a_j^2}$, and

(ii) $r_j(X_{a_1,\ldots,a_d}) = \dfrac{\prod_{i=d-j+1}^{d} a_i}{\sqrt{\sum_{i=d-j+1}^{d} \prod_{l \neq i} a_l^2}}.$

PROOF. It suffices to show Part (i), Part (ii) follows then from Proposition 2.2, and as the result is obvious if $d = 1$ we can assume that $d \geq 2$. Any vertex v of $B_{a_1,\ldots,a_d}$ can be written in the form $v = \sum_{k=1}^{d} \pm a_k e_k$ and all possible choices of the plus and minuses in that formular leads to a vertex of $B_{a_1,\ldots,a_d}$. Hence, for every projection $P = \sum_{l=1}^{j} s_l \otimes s_l$ with pairwise orthogonal unit-vectors $s_l \in \mathbb{E}^d$, it holds that $\|Pv\|^2 = \sum_{l=1}^{j} \langle v, s_l \rangle^2 = \sum_{l=1}^{j} (\sum_{k=1}^{d} \pm a_k s_{lk})^2$ and because of Lemma 3.19 there exists a vertex of $B_{a_1,\ldots,a_d}$ such that this is at least $\sum_{k=1}^{d} a_k^2 \sum_{l=1}^{j} s_{lk}^2$. Now extend the set $\{s_1,\ldots,s_j\}$ to an orthonormal basis of $\mathbb{E}^d$. As $\sum_{l=1}^{d} s_l \otimes s_l = I$ it follows that $\sum_{k=1}^{d} s_{lk}^2 = \sum_{l=1}^{d} s_{lk}^2 = 1$, for all $k = 1,\ldots,d$, and therefore that $t_k := \sum_{l=1}^{j} s_{lk}^2 \in [0,1]$. Now, because $\sum_{k=1}^{d} t_k = \sum_{l=1}^{j} \sum_{k=1}^{d} s_{lk}^2$ has to equal j the minimum value of $\sum_{k=1}^{d} t_k a_k^2$ will be achieved for $t_1 = \cdots = t_j = 1$ and $t_{j+1} = \cdots = t_d = 0$. Hence $R_j(B_{a_1,\ldots,a_d}) \geq \sqrt{a_1^2 + \cdots + a_j^2}$. But as the projection of $B_{a_1,\ldots,a_d}$ through its j-face $B_{a_1,\ldots,a_j}$ achieves this value we got the desired result. $\square$

Of course, one can easily get the radii of cubes and regular cross-polytopes from the results about the radii of general boxes and cross-polytopes, but we will state them in an extra corollary as this was the main aim of this chapter:

COROLLARY 3.21. *The following hold:*

(i) $r_j(B^d) = \sqrt{\frac{d}{j}}$, *and*

(ii) $R_j(X^d) = \sqrt{\frac{j}{d}}.$

(iii) $R_j(B^d) = \sqrt{j}$, *and*

(iv) $r_j(X^d) = \sqrt{\frac{1}{j}}.$

PROOF. Part (i) and (ii) follow from Proposition 3.18 by choosing $k = 0$ there, Part (iii) and (iv) from Theorem 3.20. $\square$

One should recognise that we can prove Corollary 3.21 almost without using Proposition 3.18 and 3.20. Except in the case where $2j = d - 1$ and Lemma 3.15 does not hold we can use this lemma and Theorem 3.14 to show (ii) and Theorem 3.14 suffices to show (iii). Parts (i) and (iv) would follow again by duality.

How do we do this in detail? Part (iii) follows from the fact that the cube and all its faces (which are again cubes) are quasi isotropic, that by projecting through a face of a cube all vertices stay on the circumsphere, and that the distance from the centre of the cube to the centre of any of its j-faces is $\sqrt{d-j}$.

To prove Part (ii) we remember the second statement after Lemma 3.9. First, we project T^{2d-1} onto $\sqrt{\frac{1}{2}}X^d$ by using the gsb

$$\sqrt{\frac{1}{2}}\begin{pmatrix} s_1 \\ -s_1 \end{pmatrix}, \ldots, \sqrt{\frac{1}{2}}\begin{pmatrix} s_{d-1} \\ -s_{d-1} \end{pmatrix}, \begin{pmatrix} \mathbf{1}_{d-1} \\ -\mathbf{1}_{d-1} \end{pmatrix},$$

where $s_1, \ldots, s_{d-1}$ is any gsb for T^{d-1}. Now because for every even j, which is not excluded by both the theorem and the lemma, there exists a subset of size j of $s_1, \ldots, s_{d-1}$, wlog $s_1, \ldots, s_j$. But hence the sets

$$\sqrt{\frac{1}{2}}\begin{pmatrix} s_1 \\ -s_1 \end{pmatrix}, \ldots, \sqrt{\frac{1}{2}}\begin{pmatrix} s_j \\ -s_j \end{pmatrix}$$

and

$$\sqrt{\frac{1}{2}}\begin{pmatrix} s_1 \\ -s_1 \end{pmatrix}, \ldots, \sqrt{\frac{1}{2}}\begin{pmatrix} s_j \\ -s_j \end{pmatrix}, \begin{pmatrix} \mathbf{1}_{d-1} \\ -\mathbf{1}_{d-1} \end{pmatrix}$$

are gsb's in $\mathbb{E}^{2d}$ and therefore there exists a projection of X^d onto any j' subspace such that it attains the lower bound $\sqrt{\frac{j'}{d}}$, except the case where $2j'$ or $2j'-1$ does not pass the conditions of Theorem 3.14 or Lemma 3.15.

4. Conclusions and open problems

Surely, the most challenging open question at the end of this chapter is to compute the remaining radii of the regular simplices. As mentioned after Theorem 3.14 there is little hope that in the even d and odd j case the lower bound is attained. Hence here the task is to find a technique to improve the proofs of Steinhagen and Weissbach for even d and $j \in \{1, d-1\}$. But both proofs make very strong use of the property that one has to project on or along a one dimensional space.

In the remaining cases where $d = 2j$ it is absolutely not clear if the lower bound could be achieved or not. As the case where $d+1$ is prime is the most problematic, this should be the case to investigate. Here it seems that there are some relations to coding theory as the question is to find a projection matrix of prime dimension $d+1$ such that 4 divides d.

A different approach would be to investigate which kinds of polytopes do all belong to the class of quasi isotropics. Especially the '(-)' entries of Table 3.1 in the $j = 3$ row would mean that there cannot be 3-dimensional quasi isotropic polytopes with an odd number of vertices.

A minor question, but still quite interesting, is to investigate the combinatorial properties of the quasi isotropic polytopes one obtains from the $\otimes$-matrices in Lemma 3.11 (ii), especially when the starting polytopes are regular or fulfill some minor regularity conditions.

As shown in Theorem 3.17, the ratio of R_j to r_1 of general simplices is maximised by the regular simplex for certain d and j. It seems to be very likely that this statement holds at least for many more pairs (d, j) and possibly in general. But if this conjecture is not true it would also be very interesting to investigate how a non-regular simplex looks like which maximises such a ratio.

The inner and outer j-radii, $j = 1, 2$, of the dodecahedron and the icosahedron cannot be computed in terms of minimal projections of a regular simplex. Despite both being regular and therefore isotropic polytopes (if there circumradius is 1), there does not exist a projection onto j-space, $j = 1, 2$ such that all their vertices are projected onto the j-sphere.

Be careful: One could think, that because the icosahedron contains a pentagonal anti-prism of the same circumradius, and that both can be projected onto the same decagon, this is the optimal projection, because it is optimal for the included anti-prism. But we cannot obtain this result from the anti-prism, because it is *not* quasi isotropic. In fact the pentagonal anti-prism which is quasi isotropic has a slightly bigger height. The anti-prism contained within the icosahedron does not possess the unit ball as its smallest enclosing ellipsoid.

Still, it is possible that the optimal 2-space projection of an icosahedron is along one of its diametrical axes. But its outer j-radii, $j = 1, 2$ are of course bigger than $\sqrt{\frac{j}{3}}$ as the outer j-radii $j = 1, 2$ of a dodecahedron with circumradius 1 are of course bigger than $\sqrt{\frac{j}{3}}$.

As already used in the preceding sections, the outer $(d - 1)$-radii of (anti-) prisms with quasi isotropic basis are the circumradii of the basis, if the (anti-) prisms are again quasi isotropic, means if their height is such that the smallest surrounding ellipsoid is a ball. But even if the height is bigger, the projection

onto the basis will not raise and therefore we know that the circumradius of the basis is the $(d-1)$-radius of the (anti-) prism even in the case of bigger hight than in the isotropic case.

CHAPTER 4

Totally non-spherical bodies

In this chapter we show the existence of bodies of constant breadth with the very special additional property, that each of its 2-dimensional projections in 2-space is different from a disc, although the projections are all of constant breadth (see Proposition 2.5). We designate such bodies as *totally non-spherical*.

If $d = 2$, it is obvious that this is the whole class of constant breadth sets, except the disc itself. The best known 3-dimensional bodies of constant breadth are the Meißner bodies (see [**8**] for a description of the construction) or bodies of revolution of planar sets of constant breadth, if they have a symmetry axis. It is obvious that all the bodies of revolution, if projected along their rotation axis, will generate a disc. But even for the two Meißner bodies, if they are projected orthogonal to an opposite pair of (curved) edges, we obtain a 2-ball, because the projection is again of constant breadth and symmetric.

FIGURE 4.1. A picture of a Meißner body, showing the two types of edges: the ones, which are obtained directly from the intersection of two spheres, and the others, which are rounded of such that the diameter of the whole body equals its width.

Eggleston [**27**] and Weissbach [**74**] described bodies of constant breadth in any dimension which do not have any spherical $(d-1)$-projection (see Figures 4.2 and 4.3). In fact, if d is at least 4, we know from Chapter 3 that

$$\frac{R_{d-1}(T^d)}{r_1(T^d)} > 1$$

and therefore that

$$\frac{R_{d-1}(T_\Gamma^d)}{r_1(T_\Gamma^d)} > 1$$

as for any completion T_Γ^d of T^d

$$R_{d-1}(T_\Gamma^d) \geq R_{d-1}(T^d) \text{ and } r_1(T_\Gamma^d) = r_1(T^d).$$

Hence any completion of an at least 4-dimensional regular simplex does not have a spherical $(d-1)$-projection, and that is what Weissbach showed.

Using Theorem 3.4 in Chapter 3 it is straight forward to improve Weissbach's result, since from $R_j(T^d) \geq \sqrt{\frac{j}{d+1}}$ and $r_1(T^d) = \sqrt{\frac{1}{2}}$ it follows

$$\frac{R_j(T^d)}{r_1(T^d)} \geq \sqrt{\frac{2j}{d+1}}$$

and this is greater 1, if $j > \frac{d+1}{2}$. But this means that any completion of T^d does not have a spherical j-projection for all $j > \frac{d+1}{2}$.
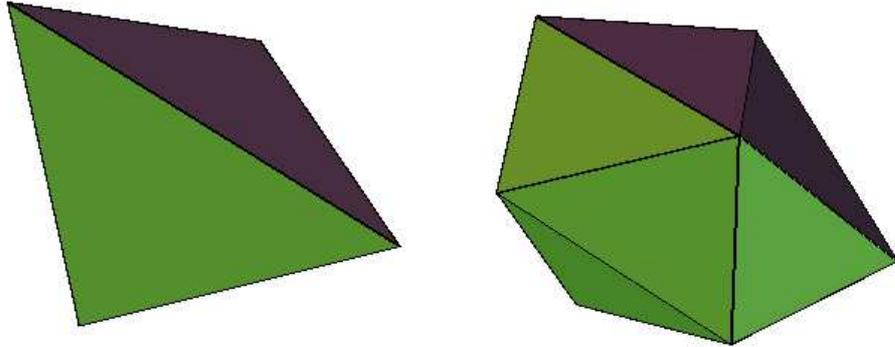
FIGURE 4.2.   A snapshot of a usual tetrahedron and Weissbach's 3-dimensional polytope for which all its completions do not have a spherical projection.
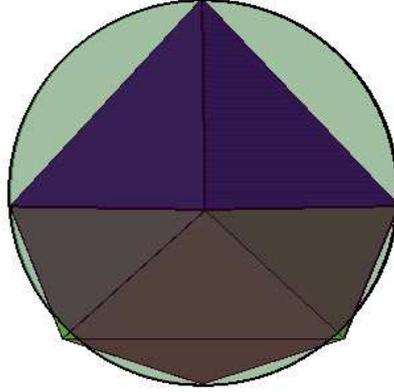
FIGURE 4.3.   A snapshot of Weissbach's 3-dimensional polytope
showing that no cylinder of radius 1 contains it.

So, if $d = 3$, Eggleston's and Weissbach's bodies are totally non-spherical and
the same is true for the 3-dimensional totally isoradial body which is provided in
Chapter 5. But so far nothing was known about totally non-sphericals in higher
dimensions. Our proof of the existence of such bodies in any dimension shows
that the diagram in Figure 2.3 of Chapter 3 is complete. Hence we are able to
state for the first time *all* possible smaller-greater relations between the different
radii.

We will give a construction of non-spherical bodies of any dimension in Section
2; but before, we need to introduce dark clouds, a concept based on [**28**] and [**24**].
We establish the dark clouds in Section 1, and extend them also to spherical dark
clouds, that are dark clouds situated on the sphere.

1. Dark clouds

The idea of dark clouds is to give a packing of balls (clouds) such that no line
(light beam) that is non-parallel to the region where the balls are located, misses
all the balls (meaning that the clouds block all the light). It follows a formal
definition:

DEFINITION 4.1. *Suppose* $\mathbb{L}$ *is a lattice in* $\mathbb{E}^d$*, and* $r\mathbb{B}$ *is a ball of radius* $r > 0$*,
such that* $r\mathbb{B} + \mathbb{L}$ *forms a packing of* $\mathbb{E}^d$*. Let* $\alpha > 0$*,* $a_i \in \mathbb{E}^d$*,* $i = 0, \ldots, n - 1$*. A
dark cloud in* $\mathbb{E}^{d+1}$ *is a packing* $\bigcup_{i=0}^{n-1} (a_i, \alpha i) + r\mathbb{B} + \mathbb{L}$ *such that no line, which*

meets the hyperplane $x_{d+1} = 0$ in a single point, can miss all these translations. The value αn is called the width *of the dark cloud.*
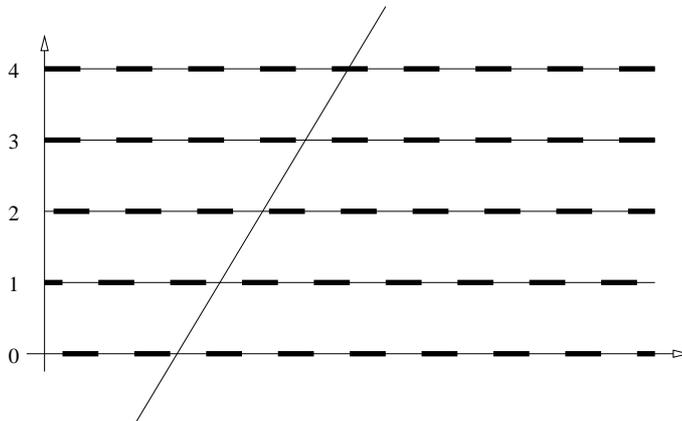
FIGURE 4.4. A sketch of a portion of a dark cloud for $d = 1$ and $n = 5$, and a blocked line through it.

Before studying dark clouds, it is necessary to make sure that dark clouds exist:

LEMMA 4.2. *Dark clouds exist for any $d \in \mathbb{N}$ and any radius $r \leq \frac{1}{2}$.*

PROOF. As every line intersecting $x_{d+1} = 0$ in a single point can be determined by a pair of points $(x, 0), (y, 1) \in \mathbb{E}^{d+1}$, we want to investigate sets of the form

$$K(\lambda, a, i) := \left\{ (x, y) \in \mathbb{E}^{2d} : (i(y - x) + x, i) \in (a, i) + \lambda r \mathbb{B} + \mathbb{L} \right\},$$

where $\lambda \in \{\frac{1}{2}, 1\}$, $a \in \mathbb{E}^d$, $i \in 0, \ldots, n - 1$ for some $n \in \mathbb{N}$, and $\mathbb{L}$ is the unit lattice. Hence $K(\lambda, a, i)$ is the subset of $\mathbb{E}^{2d}$ of all points (x, y) such that the line through $(x, 0)$ and $(y, 1)$ meets the packing $(a, i) + \lambda r \mathbb{B} + \mathbb{L}$. Because $\mathbb{L}$ is the unit lattice we are able to restrict our attention to $x, y \in I^d$. So the density of our sets in $\mathbb{E}^d$ or $\mathbb{E}^{2d}$ are simply their volumes in $\mathbb{E}^d$ or $\mathbb{E}^{2d}$, respectively.

Note that the probability that $(x, y) \in \mathbb{E}^{2d}$ lies in $K(\lambda, a, i)$ for any a is $\lambda^d \rho$, where ρ is the volume of $r\mathbb{B}$. So, if $a_0, \ldots, a_{n-1}$ are chosen at random in $\mathbb{E}^d$, the probability that $(x, y) \notin \bigcup_{i=1}^n K(\lambda, a_i, i)$ is $(1 - \lambda^d \rho)^n$. Consequently, there must exist $a_0, \ldots, a_{n-1} \in \mathbb{E}^d$ such that the density of $\mathbb{E}^{2d} \setminus \bigcup_{i=1}^n K(\lambda, a_i, i)$ is at most $(1 - \lambda^d \rho)^n$.

Now for $(x_0, y_0) \in \mathbb{E}^{2d}$ consider the subset

$$T(x_0, y_0) := \left\{ (x, y) : x \in x_0 + \frac{1}{15n} r\mathbb{B} + \mathbb{L}, y \in y_0 + \frac{1}{15n} r\mathbb{B} + \mathbb{L} \right\}.$$

If $T(x_0, y_0) \cap K(\frac{1}{2}, a_i, i) \neq \emptyset$ then there exist x, y, with $\|x - x_0\| < \frac{r}{15n}$, $\|y - y_0\| < \frac{r}{15n}$, and $(iy - (i-1)x, i) \in (a_i, i) + \frac{1}{2} r\mathbb{B} + \mathbb{L}$, i.e. $\|a_i - iy + (i-1)x\| < \frac{1}{2} r$, mod $\mathbb{L}$. So if $(x', y') \in T(x_0, y_0)$, then $\|x' - x\| < \frac{2r}{15n}$, $\|y' - y\| < \frac{2r}{15n}$, and therefore $\|i(y - y') - (i-1)(x - x')\| < \frac{4}{15} r$. Hence $\|a_i - (iy' - (i-1)x')\| < r$, i.e. $T(x_0, y_0) \subset K(1, a_i, i)$. Now, because the density of $T(x_0, y_0) = \frac{4\rho^2}{225n^2}$, by choosing $\lambda = \frac{1}{2}$ and n large enough, we get $(1 - \frac{1}{2^d}\rho)^n < \frac{4\rho^2}{225n^2}$. Hence, for all $(x_0, y_0) \in \mathbb{E}^{2d}$ there exist a_i, $i = 0, \ldots, (n-1)$, such that $T(x_0, y_0) \cap K(\frac{1}{2}, a_i, i) \neq \emptyset$ for at least one i. But this means that $T(x_0, y_0) \subset K(1, a_i, i)$. In particular $(x_0, y_0) \in K(1, a_i, i)$, so $\bigcup_{i=1}^{n} K(1, a_i, i)$ covers $\mathbb{E}^{2d}$ and that means that the sets $\bigcup_{i=1}^{n} (a_i, i) + r\mathbb{B} + \mathbb{L}$ form a dark cloud. $\square$

But for our purposes we do not only require the existence of dark clouds, we need the balls in the packing to be not too close to each other, such that we can slightly extend them later.

LEMMA 4.3. *Let $\alpha \in (0, 1)$, and $\beta, \gamma > 0$. Then there exists a dark cloud in the region $0 \leq x_{d+1} \leq \alpha$, such that each ball in the cloud has radius $r < \beta$ and any pair of balls is at least $e > \gamma r$ apart.*

PROOF. By Lemma 4.2 there exists a dark cloud with n layers at 1 apart consisting of balls of radius $r < \beta$ in these layers. Now reduce everything by a factor $\frac{\alpha}{n}$. The layers are then in the region $0 \leq x_{d+1} \leq \alpha$ and their distance apart is $\frac{\alpha}{n}$. The balls are now of radius $\frac{\alpha}{n} r$ and in their layers they are $\frac{\alpha}{n}(2 - 2r)$ apart, while the balls in different layers are $\frac{\alpha}{n}(1 - 2r)$ apart. Hence the balls have radius $\frac{\alpha}{n} r < r < \beta$ and their distance apart is at least $\frac{\alpha}{n}(1 - 2r)$. So picking r such that $\frac{1}{r} - 2 > \gamma$ we get the desired result. $\square$

Assume we cut the sphere with two parallel hyperplanes, both having the centre on the same side, such that we obtain two parallel caps on the sphere, one a subset of the other. Now we project the sphere through its centre (so non-orthogonal) onto a hyperplane parallel to the hyperplanes above but outside the

sphere. The projection of the two caps forms an $(d-1)$ dimensional annulus on the hyperplane, see also Figure 4.5.
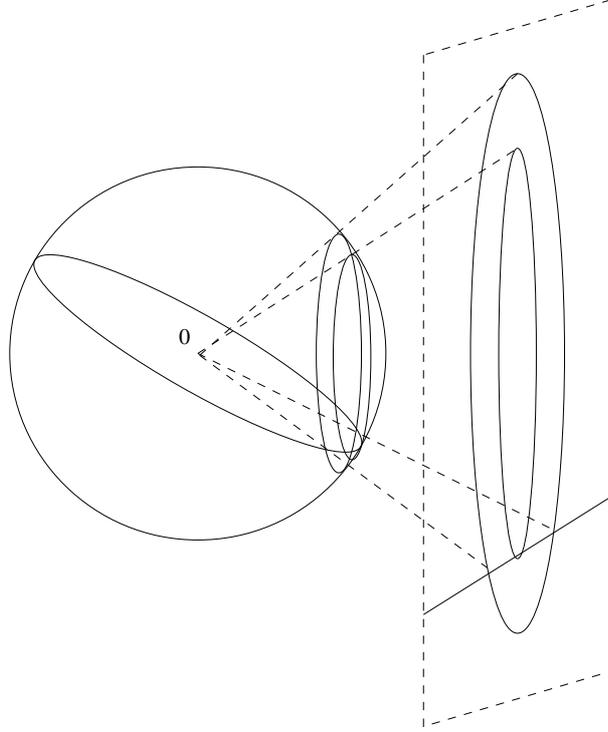
FIGURE 4.5.   Projecting the region between two parallel caps onto an annulus.

Hence the following Lemma prepares the projection of dark clouds onto the sphere:

LEMMA 4.4. *Suppose A is the annulus $1 \leq \|x\| \leq 1 + \epsilon$, $\epsilon > 0$. Then there exists a collection of dark clouds $\mathcal{C}$ such that any line meeting $\mathbb{B}$ cuts at least through one of the balls of $\mathcal{C}$ within A.*

PROOF. Suppose P is a polytope such that $\mathbb{B} \subset P$ and all vertices of $(1+\alpha)P$ are contained in $(1 + \epsilon)\mathbb{B}$ for some α, with $0 < \alpha < \epsilon$. Now we place dark clouds of width α along all the facets of P. Hence every line meeting $\mathbb{B}$ meets also P and because the vertices of $(1 + \alpha)P$ are lying in the annulus each of these lines cuts through one of the dark clouds touching a ball in the cloud within the annulus. $\square$

Now we a are able to introduce the spherical dark clouds:

DEFINITION 4.5. *Any packing of caps on the d-dimensional sphere $\mathbb{S}$ within the region $\alpha - \epsilon \leq x_{d+1} \leq \alpha$, $0 < \alpha < 1$ is called a* spherical dark cloud *of width ϵ, if any great 2-circle on $\mathbb{S}$ which meets the cap $x_{d+1} \geq \alpha$, intersects at least one cap in the packing.*

To show that spherical dark clouds exist we only have to project the annulus in Lemma 4.4 back onto the sphere and transform the projections of balls back into caps on the sphere.

LEMMA 4.6. *Every cap of $\mathbb{S}$ of the form $x_{d+1} \geq \alpha$, $0 < \alpha < 1$ can be blocked by a spherical dark cloud of any width $0 < \epsilon < \alpha$.*

PROOF. If we project the region $\alpha - \epsilon \leq x_{d+1} \leq \alpha$ from 0 onto the hyperplane $x_{d+1} = 2$ it forms an annulus.

Now we apply Lemma 4.4 to obtain a collection of dark clouds which blocks every line meeting the ball surrounded by the annulus. But, because every great 2-circle on $\mathbb{S}$ which meets the cap $x_{d+1} \geq \alpha$ is projected onto such a line on $x_{d+1} = 2$, we obtain by back projection a blocking of great 2-circles on the sphere. So far the projected collection of dark clouds does not necessarily consist of disjoint caps, but because of Lemma 4.3 we can choose the distance of the balls within one cloud to be arbitrary large. So, by replacing the disjoint parts of the projection onto the sphere by equally sized disjoint caps we obtain our spherical dark cloud. $\qquad\square$

2. Existence of totally non-spherical bodies

In the following Lemma we will make use of the existence of spherical dark clouds to describe a set of antipodal caps on the sphere which cannot be missed by any 2-circle on the sphere.

LEMMA 4.7. *For any dimension $d \geq 3$ there exists a finite set of closed caps $\pm C_1, \ldots, \pm C_m$ on $\mathbb{S}$ with disjoint relative interior such that every great 2-circle on $\mathbb{S}$ (and therefore any great j-circle with $2 \leq j \leq d - 1$) meets the relative interior of at least one pair $\pm C_i$.*

PROOF. Every point x on $\mathbb{S}$ has $\|x\| = 1$. Hence every great 2-circle meets the hyperplane $x_i = \frac{1}{\sqrt{d}}$ for some i. Now we block all these hyperplanes as described in Lemma 4.6 in the region $\frac{1}{\sqrt{d}} - \epsilon \leq x_i \leq \frac{1}{\sqrt{d}}$ and handle overlapping caps as we handled them already in the proof of that lemma. But since no great 2-circle can be parallel or approximately parallel to all of these hyperplanes they all hit at least one antipodal pair of the clouds and therefore at least one antipodal pair of caps within the clouds. $\qquad \square$

Although the above proof holds for all $d \geq 3$ we will give a special one for $d \in \{3, 4\}$ as we can avoid using the dark cloud construction in this dimensions and state the collection of caps in an explicit way:

PROOF OF LEMMA 4.7 FOR $d \in \{3, 4\}$. This time we start with the caps $\pm C_i$, $i = 1, \ldots, d$ as follows:

$$C_i := \left\{ x \in \mathbb{S} : x_i \geq \frac{1}{\sqrt{2}} \right\}.$$

If $d = 3$ every great circle must intersect through these caps as, because of Corollary 3.21, the biggest disc which fits into a cube of edge length $\sqrt{2}$ has radius $\frac{\sqrt{3}}{2}$, which is strictly less than 1.

Hence we can assume that $d \geq 4$ and concentrate on great circles which do not entirely lay in a hyperplane of the form $x_i = 0$ (otherwise we can reduce the problem to the $d = 3$ case).

The intersection sets of $\pm C_i \cap \pm C_j$ are only the points with i-th and j-th coordinate $\pm\frac{1}{\sqrt{2}}$ and the rest zero.

Let us now seek a great circle Σ not cutting through the relative interior of the 8 caps. Suppose Σ meets the hyperplane $x_4 = 0$ at the points $\pm(x_1, x_2, x_3, 0)$. So, we have $|x_i| \leq \frac{1}{\sqrt{2}}$, $i = 1, 2, 3$. Now let $\pm y$ be the points on Σ perpendicular to $\pm x$, $|y_i| \leq \frac{1}{\sqrt{2}}$, $i = 1, \ldots, 4$. Now, every point $z \in \Sigma$ is given by $z = x \cos\theta + y \sin\theta$ with $\theta \in [0, 2\pi)$, and we require $|x_i \cos\theta + y_i \sin\theta| \leq \frac{1}{\sqrt{2}}$, $i = 1, \ldots, 4$ for all θ. But as $|x_i \cos\theta + y_i \sin\theta| \leq \sqrt{x_i^2 + y_i^2}$ for all θ it must hold $\sqrt{x_i^2 + y_i^2} \leq \frac{1}{\sqrt{2}}$ and therefore $x_i^2 + y_i^2 \leq \frac{1}{2}$, $i = 1, \ldots, 4$. By adding these inequalities over all i and using $x, y \in \mathbb{S}$ we obtain that $x_i^2 + y_i^2 = \frac{1}{2}$, $i = 1, \ldots, 4$. As $x_4 = 0$ it follows $|y_4| = \frac{1}{\sqrt{2}}$ and therefore that Σ touches $\pm C_4$ in $\pm y$. By symmetry, Σ touches each of $\pm C_i$, $i = 1, \ldots, 4$. But this means that for all $i = 1, 2, 3$ there must also

exist some θ_i such that $x_i \cos \theta_i + y_i \sin \theta_i = \frac{1}{\sqrt{2}}$. Without loss of generality we can assume that $x_i, y_i \geq 0$ for a fixed i. Hence

$$|x_i \cos \theta_i + y_i \sin \theta_i| < \max\{|x_i \cos \theta_i|, |y_i \sin \theta_i|\} \leq \max\{x_i, y_i\} < \frac{1}{\sqrt{2}} \ ,$$

if $\theta \in \left(\frac{\pi}{2}, \pi\right) \cup \left(\frac{3\pi}{2}, 2\pi\right)$. On the other hand if $\theta \in \left[0, \frac{\pi}{2}\right] \cup \left[\pi, \frac{3\pi}{2}\right]$ then $|x_i \cos \theta_i + y_i \sin \theta_i| = |x_i \cos \theta_i| + |y_i \sin \theta_i|$ which is the 1-norm of the point in $\mathbb{E}^2$ with coordinates $x_i \cos \theta_i$ and $y_i \sin \theta_i$. But as the 2-norm of this point is $\frac{1}{\sqrt{2}}$ the only possibilities for θ_i are $\theta \in \left\{\frac{k\pi}{2} : k \in \mathbb{Z}\right\}$ and $x_i, y_i \in \left\{0, \frac{1}{\sqrt{2}}\right\}$ such that $x_i + y_i = \frac{1}{\sqrt{2}}$.

This means that for all $i = 1, 2, 3$, the coordinates x_i, y_i have to be 0 or $\pm\frac{1}{\sqrt{2}}$ with one being 0 and the other one being $\pm\frac{1}{\sqrt{2}}$. But since $x, y \in \mathbb{S}$, there can only be one $i \in \{1, 2, 3\}$ such that $y_i = \pm\frac{1}{\sqrt{2}}$. Hence there are only six different choices for Σ. Nevertheless, since $\cos \frac{\pi}{4} = \sin \frac{\pi}{4} = \frac{1}{\sqrt{2}}$, all possible Σ run through four of the points $\left(\pm\frac{1}{2}, \pm\frac{1}{2}, \pm\frac{1}{2}, \pm\frac{1}{2}\right)$ which are far away from the caps $x_i \geq \frac{1}{\sqrt{2}}$. So by adding caps $\pm C_i =, i = 5, \ldots, 12$ of the form $\sum_{j=1}^4 \pm x_j \geq 2 - \epsilon$, for a sufficiently small ϵ we get the desired set of closed caps. $\qquad\square$

Now we are ready to prove the main result of this chapter. To do so, we take all pairs of antipodal caps and transform them slightly such that the body we obtain remains to be a body of constant breadth of the same diameter as the sphere, but does not have a single circular projection (a similar method was used by Danzer in [**23**]).

THEOREM 4.8. *For all $d \geq 2$ there exists a d-dimensional totally non-spherical body.*

PROOF. All planar convex sets of constant breadth are totally non-spherical. Hence we can assume that $d \geq 3$. As mentioned the basic idea is to replace the pairs of caps C_i and $-C_i$, $i = 1, \ldots, m$ in Lemma 4.7 by asymmetric sets D_i^+ and D_i^- which preserve the constant breadth property for the resulting body. How to do this?

Consider any pair $\pm C_i$, their line of symmetry l_i passing through 0 (the centre of $\mathbb{B}$), and a 2-plane L containing l_i. Let the bounding points of $-C_i \cap L$ are $e^{-i\alpha}$ and $e^{i\alpha}$ (see Figure 4.6).

We construct the point p on l_i lying above 0 relative to $-C_i$, at distance 2 from both $e^{-i\alpha}$ and $e^{i\alpha}$. Hence $p = \left(\sqrt{2 - \sin^2 \alpha} - \cos \alpha\right) e^{i\alpha}$, but it is the same
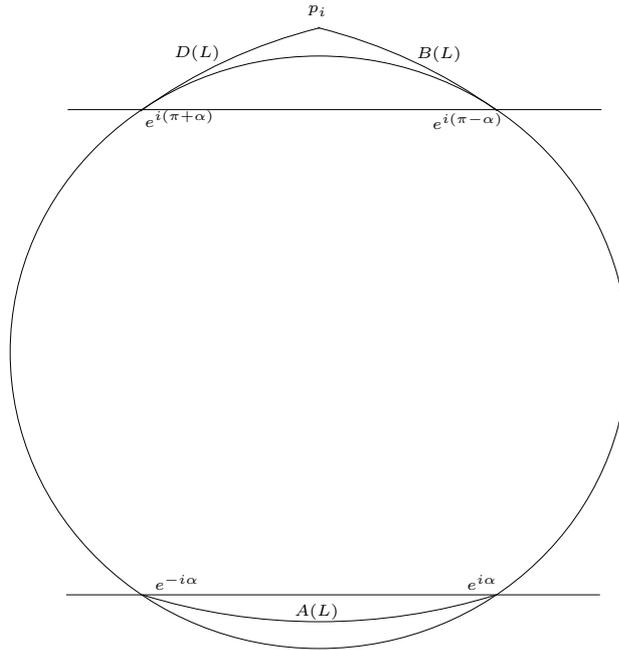
FIGURE 4.6.   A sketch of the replacement of antipodal caps.

for any choice of L through l_i. p lies outside $L \cap \mathbb{B}$ but below the intersection of the tangents to $L \cap \mathbb{B}$ at $e^{i(\pi+\alpha)}$ and $e^{i(\pi-\alpha)}$, respectively. Now consider the three circular arcs of radius 2

  (i) $A(L)$ with centre in p and end points $e^{-i\alpha}$ and $e^{i\alpha}$ within $-C_i \cap L$,

  (ii) $B(L)$ with centre in $e^{-i\alpha}$ and end points $e^{i(\pi-\alpha)}$ and p, and

  (iii) $D(L)$ with centre in $e^{i\alpha}$ and end points $e^{i(\pi+\alpha)}$ and p.

We define D_i^+ as the union over all 2-planes L of the regions bounded by $B(L)$, $D(L)$, and the arc on $\mathbb{S}$ between $e^{i(\pi+\alpha)}$ and $e^{i(\pi-\alpha)}$ and D_i^- as the union over all 2-planes L of the regions bounded by $A(L)$ and the arc on $\mathbb{S}$ between $e^{i\alpha}$ and $e^{-i\alpha}$.

    The resulting body K is again of constant breadth and because of Lemma 4.7 every great 2-circle on $\mathbb{S}$ intersects at least one of the regions $\pm C_i$, $i = 1, \ldots, m$. Hence the orthogonal projection of K onto any 2-plane cannot be a disc. $\square$

    Theorem 4.8 allows us to state as a corollary that:

COROLLARY 4.9. *For all $d \geq 3$ there exists a convex body C such that*

$$r_d(C) \leq \cdots \leq r_2(C) < r_1(C) = R_1(C) < R_2(C) \leq \cdots \leq R_d(C).$$

PROOF. Follows from Theorem 4.8 and that the circumradius of a non-spherical 2-dimensional body of constant breadth is bigger than its half diameter. □

Because of Corollary 4.9 the diagram in Figure 2.3 of Chapter 3 is complete in the sense that for any two radii which are not connected by a directed path there are bodies where the '$<$'-relationship holds in one (totally non-spherical bodies) or the other (ellipsoids with all axis of different length) direction.

3. Conclusions and open problems

In this chapter we successfully proved the existence of non-spherical bodies of constant breadth in any dimensions.

The second proof of Lemma 4.7 in the cases $d \in \{3, 4\}$ showed that the dark cloud construction is avoidable. This would be always possible if one knows a symmetric d-polytope P such that P does not contain a disc of radius 1; such that the intersection of P and $\mathbb{B}$ only contains points p which are not on any $(d-3)$-face of P, and if p is on a $(d-2)$-face then $p \in \mathbb{S}$. To describe such polytopes in general dimension would therefore simplify the matter.

CHAPTER 5

Totally isoradial bodies

In [**51**], Hilbert and Cohn-Vossen considered the following problem: Which properties uniquely characterise the ball in three dimensions? They listed eleven properties, some which are unique for the ball, some not. One of the eleven is the constant breadth property. Already Euler knew that this property does not characterise the disc in 2-space [**29**]. In fact, it does not characterise the ball in any dimension [**56**], the Reuleaux triangle and the Meißner bodies [**60, 59, 78, 8**] are the best known counterexamples in dimension 2 and 3, respectively. However, a body that is not the ball but that has the same s-breadth for every direction $s \in \mathbb{S}$, sounds a bit odd and is surely surprising for anyone who discovers it the first time.

FIGURE 5.1. Since the size of 2-dimensional bodies of constant breadth can be easily measured in any kind of money taking machines, they are a possible alternative to the usual spherical coins as the English 20 and 50 pence show.

A good survey on constant breadth bodies and their properties can be found in [**17**].

A well known extension of the concept of constant breadth is that of constant outer and inner j-measures, $j = 1, \ldots, d-1$ [**10, 17**]; see [**56**] for a definition. It is easy to see that the three classes, bodies of constant breadth, bodies of constant

inner 1-measure, and bodies of constant outer 1-measure, coincide. Firey [**35**] showed that besides the ball, which is contained in all of these classes, non-spherical bodies of constant outer j-measure exist for all $j \in \{1, \ldots, d - 1\}$. However, it is an outstanding open problem if there exists a non-spherical body of constant breadth and constant brightness (constant outer $(d - 1)$-measure), and under the assumption of certain smoothness conditions about the boundary, it is shown in [**10**] that the two properties characterise the ball.

In this light it seems to be quite natural to investigate classes of bodies where the inner or outer j-radii, $1 \leq j \leq d - 1$, are invariant with respect to the direction of the defining flats. This leads us to the much more general class of *isoradial bodies*. Again the classes of bodies where the inner and outer 1-radius are invariant coincide with the constant breadth bodies, and the ball satisfies isoradiality for all r_j and R_j. We call such bodies, that are isoradial for all r_j and R_j, *totally isoradial*. Since any totally isoradial body is a very special body of constant breadth and as the analogue class for inner and outer j-measures only contains the ball, the existence of such a body besides the ball sounds very unlikely. Nevertheless, it will be shown in Section 2 that at least in $\mathbb{E}^3$ there exists a non-spherical totally isoradial body. However, previously we need to state some definitions and basic properties about the isoradials in the first section.

1. Definition and basic properties

As the constant breadth bodies are, like the regular simplices, often attaining extreme relationships between the four basic radii (see Chapter 6), it seems to be important to investigate isoradial bodies as their natural extensions to general dimensions:

DEFINITION 5.1. *Suppose C is a body in $\mathbb{E}^d$ and $j \in \{1, \ldots, d-1\}$. Then we call C*

   (i) outer j-isoradial *(R_j-isoradial for short), if for every $E \in \mathcal{L}_{d-j,d}$ there exists $p \in \mathbb{E}^d$, such that $(p + E) + R_j(C)\mathbb{B} \supset C$,*
  (ii) inner j-isoradial *(r_j-isoradial for short), if for every $F \in \mathcal{L}_{j,d}$ there exists $q \in \mathbb{E}^d$, such that $(q + r_j(C)\mathbb{B}) \cap (q + F) \subset C$,*

(iii) $\mathcal{R}$-isoradial *with* $\mathcal{R} \subseteq \{r_j, R_j : j \in \{1, \ldots, d-1\}\}$, *if C is r_j- and R_j-isoradial for all r_j and $R_j \in \mathcal{R}$,*

(iv) $(\mathcal{R}, \mathcal{S})$-isoradial *with $\mathcal{R}, \mathcal{S} \subseteq \{r_j, R_j, j \in \{1, \ldots, d-1\}\}$, if C is $\mathcal{R}$-isoradial and **not** r_j- or R_j-isoradial for all r_j and $R_j \in \mathcal{S}$,*

(v) totally isoradial, *if C is $\{r_j, R_j, j \in \{1, \ldots, d-1\}\}$-isoradial, and*

(vi) isoradial, *if C is $\mathcal{R}$-isoradial with $\mathcal{R} \neq \emptyset$.*

A body C is R_j-isoradial, if $R_j^k(C|F)$ does not depend on $F \in \mathcal{L}_{k,d}$ for any $k \in \{j, \ldots, d\}$. Every body of constant breadth is $\{r_1, R_1\}$-isoradial, because the two isoradiality classes coincide by Proposition 2.5 (a) with the constant breadth property. Therefore in $\mathbb{E}^2$ the bodies of constant breadth are the only (totally) isoradial bodies. However, in general dimension there are $2d-4$ more possible types of isoradial bodies.

It is obvious that the ball is totally isoradial. This raises the question, whether there exist non-spherical totally isoradial bodies and whether there exist $(\mathcal{R}, \mathcal{S})$-isoradial bodies for every partition $\mathcal{R}, \mathcal{S}$ of $\{r_j, R_j, j \in \{1, \ldots, d-1\}\}$.

LEMMA 5.2. *Let $j \in \{1, \ldots, d-1\}$. Every body C with*

$$R_j(C) = \cdots = R_d(C)$$

is $\{R_j, \ldots, R_{d-1}\}$-isoradial, and every body C with

$$r_d(C) = \cdots = r_j(C)$$

is $\{r_j, \ldots, r_{d-1}\}$-isoradial.

PROOF. From Lemma 2.4 we know that

$$R_j(C) = \min\{R_j(C|F) : F \in \mathcal{L}_{j,d}\}$$

and it is easy to see that in general

$$R_d(C) \geq \max\{R_j(C|F) : F \in \mathcal{L}_{j,d}\}.$$

Isoradiality now follows from $R_j(C) = R_d(C)$.

The same argument holds for the inner radii. $\square$

For example, a right-angled cone fulfills $R_2(C) = R_3(C)$ and therefore it is an R_2-isoradial body (in fact it is $(\{R_2\}, \{r_1, r_2, R_1\})$-isoradial).

The converse of Lemma 5.2 is *not* true, since all 2-dimensional bodies of constant breadth C, that are different from $\mathbb{B}$, neither fulfill $R_1(C) = R_2(C)$ nor $r_1(C) = r_2(C)$.

COROLLARY 5.3. *If for any body C the relation*

$$r_d(C) = \cdots = r_2(C) \le r_1(C) = R_1(C) \le R_2(C) = \cdots = R_d(C)$$

holds then this body is totally isoradial.

PROOF. Follows directly from Lemma 5.2   □

2. A totally isoradial body in 3-space

The knowledge from Proposition 2.5 about constant breadth bodies turns out to be helpful to prove the existence of non-spherical totally isoradial bodies. This proposition allows us to state the following lemma, which will reduce our task of finding non-spherical totally isoradial body in 3-space, to the task of finding a certain R_2-isoradial body:

LEMMA 5.4. *If C is a body such that $r_1(C) < R_{d-1}(C) = R_d(C)$ then there exists a completion C_Γ of C such that*

$$r_d(C_\Gamma) = r_{d-1}(C_\Gamma) < R_1(C_\Gamma) = r_1(C_\Gamma) < R_{d-1}(C_\Gamma) = R_d(C_\Gamma).$$

PROOF. It follows from Proposition 2.5 (c) that there exists a body of constant breadth $C_\Gamma \supseteq C$, such that

$$R_{d-1}(C_\Gamma) \le R_d(C_\Gamma) = R_d(C) = R_{d-1}(C) \le R_{d-1}(C_\Gamma).$$

Thus the relationship holds with equality and every term is bigger than $r_1(C) = r_1(C_\Gamma)$. Hence C_Γ fulfills

$$R_1(C_\Gamma) = r_1(C_\Gamma) < R_{d-1}(C_\Gamma) = R_d(C_\Gamma).$$

Now it follows from Proposition 2.5(d) that

$$r_d(C_\Gamma) + R_d(C_\Gamma) = 2r_1(C_\Gamma),$$

and because C^s is for all $s \in \mathbb{S}$ also a body of the same constant breadth

$$r_{d-1}(C_\Gamma^s) + R_{d-1}(C_\Gamma^s) = 2r_1(C_\Gamma^s)$$

holds. Hence, from

$$R_{d-1}(C_\Gamma^s) = R_{d-1}(C_\Gamma) = R_d(C_\Gamma)$$

for all $s \in \mathbb{S}$, we get $r_{d-1}(C_\Gamma^s) = r_d(C_\Gamma)$ for all $s \in \mathbb{S}$, and therefore $r_{d-1}(C_\Gamma \cap F) \leq r_d(C_\Gamma)$ for all $F \in \mathcal{A}_{d-1,d}$. This implies that

$$r_d(C_\Gamma) = r_{d-1}(C_\Gamma) < R_1(C_\Gamma).$$

$\square$

At this stage we are in the position to state the main result of this chapter:

THEOREM 5.5. *There are non-spherical 3-dimensional totally isoradial bodies.*

PROOF. Because of Lemma 5.4 and Corollary 5.3 we only have to show that there exists a body C such that

$$r_1(C) < R_2(C) = R_3(C) \ .$$

The idea of our construction is to choose a certain set of regions on the unit sphere, such that for any point x of the sphere within the set, the antipodal point on the sphere is not included in this set; thus ensuring that the body formed by the convex hull of the chosen regions has a diameter strictly less than 2. At the same time the choice of the regions will finally be in a way that the body possesses at least three points on every great circle over $\mathbb{S}$, which contain the centre 0 of $\mathbb{B}$ in their convex hull. This guarantees that $R_2(C \cap E) = 1$ for every plane $E \in \mathcal{L}_{2,3}$ and therefore that $R_2(C) = 1$.

The main problem of the construction is the question, how to choose the regions on the sphere, such that both properties above are fulfilled at the same time. Here we use the following idea: First we select a set of planes through the origin, which are in a somewhat general position. These planes will describe the boundaries of the selected regions such that they maintain the first criterion. Then we improve on it by choosing subsets of every area, making sure that the second criterion is also met.

We define the arrangement of planes as follows: Consider an odd number of planes through the origin $E_1, \ldots, E_{2n+1} \in \mathcal{L}_{2,3}$, $n \geq 3$, but fixed, and their intersection with the unit ball, $E_k \cap \mathbb{B} = D_k$, $k = 1 \ldots, 2n+1$ such that they satisfy the following properties:

(i) No three E_k intersect in one line.

(ii) There exists no plane $E \in \mathcal{L}_{2,3}$ different from the E_k, which passes through the intersection $E_{k,l} = E_k \cap E_l$, $k \neq l$ of three different pairs of the planes $E_1, \ldots, E_{2n+1}$.

Every plane E_k, $k = 1, \ldots, 2n+1$ divides $\mathbb{E}^3$ in two halfspaces, which we call E_k^+ and E_k^-. The planes define a structure of cells, arcs and vertices on $\mathbb{S}$, such that for every vertex the antipodal point on the sphere is also a vertex. We label all of these pairs of antipodal vertices by (v_j, w_j), $j \in J = \{1, \ldots, n(2n+1)\}$.

Let $\text{dist}(F, v) = \min_{e \in F} \|e - v\|$ be the usual Euclidean distance measure between any affine space F and a point v and let

$$J^* = \left\{ (j_1, j_2, j_3) \in J^3 : \forall k \in \{1, \ldots, 2n+1\}, \ \exists l \in \{1, 2, 3\}, \ \text{such that } v_{j_l} \notin E_k \right\}$$

be the set of all triples of vertices, where not all vertices lie on one of the linear spaces which define the arrangement. Let

$$s_{(j_1, j_2, j_3), E} = \max_{l \in \{1,2,3\}} \text{dist}(E, v_{j_l})$$

be the maximum distance of one vertex of such a triple to any linear space E and let

$$s = \min_{(j_1, j_2, j_3) \in J^*} \ \min_{E \in \mathcal{L}_{2,3}} s_{(j_1, j_2, j_3), E}$$

be the minimum over all triples in J^* and possible E of the $s_{(j_1, j_2, j_3), E}$. Because of property (ii) and the compactness of $\mathcal{L}_{2,3}$ it follows that $s > 0$. That means every great circle on $\mathbb{S}$ has a distance of at least s to at least one vertex of every triple in J^*.

We colour the cells as follows: For every cell take any point x in the interior of the cell. If x belongs to E_k^+ for an even number of planes E_k, the cell is coloured black, otherwise white. Because of the odd number of planes in the arrangement, every pair of antipodal cells gets different colours and only the boundaries of the cells are coloured both, black and white. The black coloured cells are the pieces we are interested in. We call each one of them as a_i and the collection of a_i's by $\mathcal{A}$. Moreover, we call the white sector antipodal to a_i as b_i, for all i.

Now modify $\mathcal{A}$ as follows (see Figure 5.2). For every i let A_i be a closed area in the interior of a_i. The bounding edges of the A_i are formed by affine planes parallel to the planes which create the boundaries of a_i, such that A_i and a_i are

similar in the way that they have a one-to-one correspondence of bounding edges and vertices. For every vertex v_j (resp. w_j) of a_i, there are two sides of a_i incident on v_j (resp. w_j), say e_{j1} and e_{j2}. Choose the two points on e_{j1} and e_{j2} which are at distance s_{v_j} from v_j (resp. s_{w_j} from w_j), where s_{v_j} and s_{w_j} are at most s and $s_{v_j} \neq s_{w_j}$. Let us call these two points p_{j1} and p_{j2}.
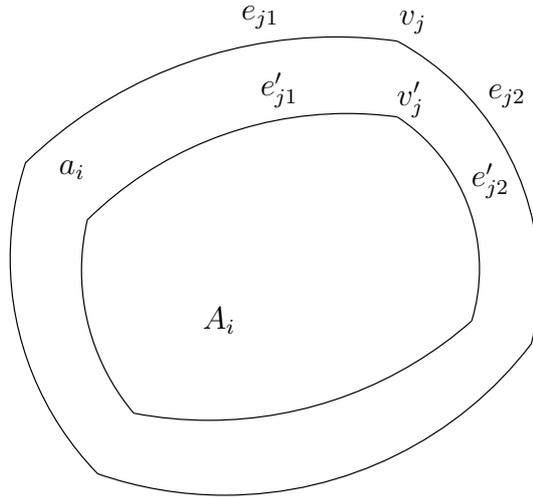
FIGURE 5.2. The regions a_i and A_i.

Join p_{j1} and p_{j2}. Because A_i is similar to a_i, for every vertex v_j (resp. w_j) of a_i there exists a vertex v_j' (resp. w_j') of A_i, with two sides incident on v_j' (resp. w_j'), say $e_{j1}'||e_{j1}$ and $e_{j2}'||e_{j2}$. Join p_{j1} to any point in the interior of e_{j1}', say p_{j1}' and p_{j2} to any point in the interior of e_{j2}', say p_{j2}'. Let the area defined by the ordered points $p_{j1}, p_{j2}, p_{j2}', v_j', p_{j1}'$ ($p_{j1}, p_{j2}, p_{j2}', w_j', p_{j1}'$) be A_{ji} (see Figure 5.3). We will refer to each of these A_{ji} as *tooth*.

Repeat this for every vertex of a_i and for every i. This gives a collection of regions A_i and A_{ji}. We take the convex hull of this collection, name the resulting body C, and reduce the black colouring to only $C \cap \mathbb{S}$.

Now we only have to argue that

(i) C does not contain antipodal points of $\mathbb{S}$ and
(ii) C has three points p_1, p_2, p_3 on every great circle over $\mathbb{S}$, such that the convex hull of the three points contains the centre 0 of $\mathbb{B}$,

as mentioned at the beginning of the construction.

FIGURE 5.3. The distance between p_{j1} and v_j is s_{v_j}. A_{ji} is a tooth like structure. Three more such structures are formed for the other three vertices. Finally, the convex hull of the A_{ji}'s and A_i's forms the desired body C.

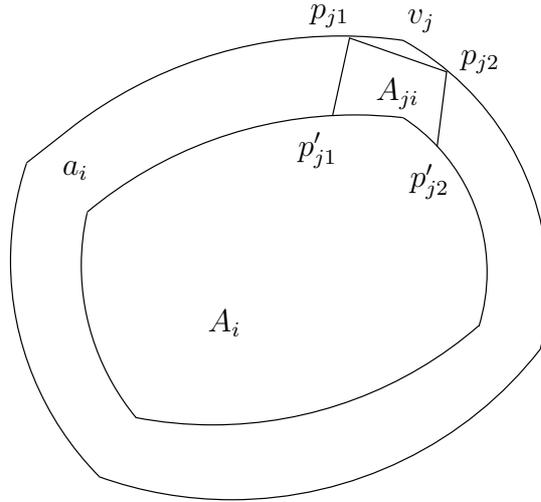In order to prove (i) suppose x is a point in $C \cap \mathbb{S}$. If x is a point in the interior of one of the regions a_i it follows from the colouring that the antipodal point is not in C. Now let x be a point on the boundary of a_i. The only such points are the points p_{j1} and p_{j2} for all j. By construction, for every antipodal vertex pair v_j, w_j the distances of the boundary points to the corresponding vertices s_{v_j} and s_{w_j} are different. Thus the points on the antipodal cell boundary are not antipodal to p_{j1} and p_{j2}. Therefore C does not have any pair of antipodal points.

In order to prove (ii) let $E \in \mathcal{L}_{2,3}$. There are three possible cases (let $k, k' \in \{1, \ldots, 2n+1\}, k \neq k'$):

   (1) $E \neq E_k$ for all k and E does not contain some $E_k \cap E_{k'}$.
   (2) $E \neq E_k$ for all k, but E contains some $E_k \cap E_{k'}$.
   (3) E is one of E_k.

Note that no E can pass through three or more a_i's only through the non-coloured parts. Otherwise E has to cut through the spaces between a vertex of a_i and the tooth close to the vertex. If such vertices are not on the same $E_k, k \in \{1, \ldots, 2n+1\}$, then by definition of s the claim holds. So assume that all such vertices are on a fixed E_k. Now, $E \cap \mathbb{S}$ and $E_k \cap \mathbb{S}$ intersect each other

transversally at a unique pair of antipodal points, and only one of these intersections can permit a cut through the non-coloured parts of the a_i's, which is a contradiction.
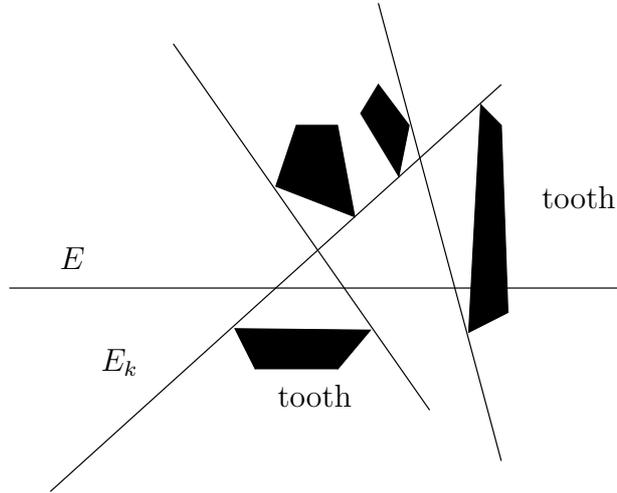
FIGURE 5.4. E intersects E_k only in two antipodal points and thus cannot intersect two of the regions a_{i_1} and a_{i_2} both bounded by E_k only through the non-coloured area.

We divide (1) in three subcases: E is such that it intersects only the non-coloured part of some a_i

(1a) 0 times,

(1b) 1 time, and

(1c) 2 times.

If (1a) happens, $E \cap \mathbb{B}$ contains $(2n+1)$ black sectors on the boundary. Since $(2n+1) \geq 7$, the construction ensures that $E \cap \mathbb{S}$ always includes three points, such that their convex hull contains the centre of $E \cap \mathbb{B}$.

If (1b) or (1c) come true, one or two black sector are lost, respectively. However there are at least three points left, such that their convex hull contains the centre of $E \cap \mathbb{B}$ (see Figure 5.5).

Note the following: If $E \neq E_k, k \in \{1, \ldots, 2n+1\}$ then by the choice of planes in the initial arrangement, neither can E pass through three or more intersections of the E_k's; see property (ii) of the construction, nor can E pass or be close to
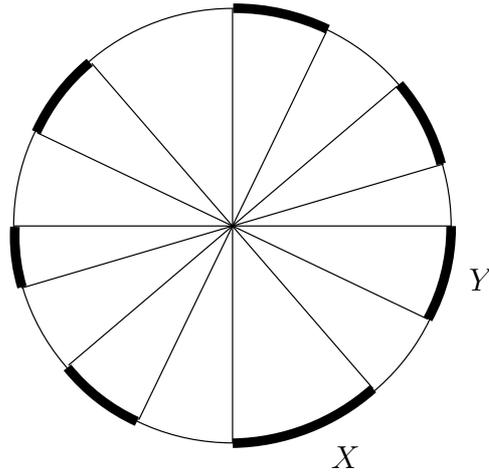
FIGURE 5.5. Case (1a), the coloured parts are the intersection of E with the coloured parts of $\mathbb{B}$. If case (1b) happens, one of the black sectors, say X, will turn white. For case (1c), two black sectors, say X and Y, turn white. This is the worst case with two black sectors lost, still remaining 5 sectors which cannot be situated on the same half sphere.

three or more of them, because of the definition of s. Suppose E passes through two intersections. These two intersections define two pairs of antipodal vertices. Without loss of generality, let us call these two pairs (v_1, w_1) and (v_2, w_2). If both of these pairs lie on some fixed E_k, say E_K, then the only plane passing through both of these pairs is E_K, which is a contradiction because $E \neq E_k$ for all $k \in \{1, \ldots, 2n+1\}$. Therefore, (v_1, w_1, v_2, w_2) generates triples, say for example (v_1, w_1, v_2), not all of which are on the same E_k, thus being members of J^*. Now, by definition of s, E cannot pass through these members of J^* and be closer than s to another intersection. Moreover, E cannot cut through one antipodal vertex pair and maintain a maximum distance of less than s to two more such pairs on the same E_k because of an argument similar to that used for case (1c).

Hence in case of (2), there might exist again three subcases:

(2a) E passes through one intersection and not through the non-coloured part of the interior of any of the a_i,

(2b) E passes through one intersection and additionally through the non-coloured part of the interior of one a_i, and

(2c) E passes through two intersections and not through the non-coloured part of the interior of any of the a_i.

We will show case (2c), since this is the most difficult case. The same argument will easily be applicable to the other two cases.

If (2c) happens, this implies that $E \cap \mathbb{B}$ changes twice from one a_i to another a_i' through the common vertex v_j of a_i and a_i', thus going through a thin white sector between the corresponding teeth. On the antipodal side $E \cap \mathbb{B}$ passes from one b_i to another b_i' through a vertex. Let us consider the vertex v_j common to the regions a_i and $a_{i'}$. Even though, because E passes from a_i to $a_{i'}$ through v_j, it must intersect the tooth close to v_j in a_i, since the sides of a_i incident on v_j and one side of the tooth form a closed curve on $\mathbb{S}$. Similarly the result holds for the tooth close to v_j in $a_{i'}$ (see Figure 5.6).
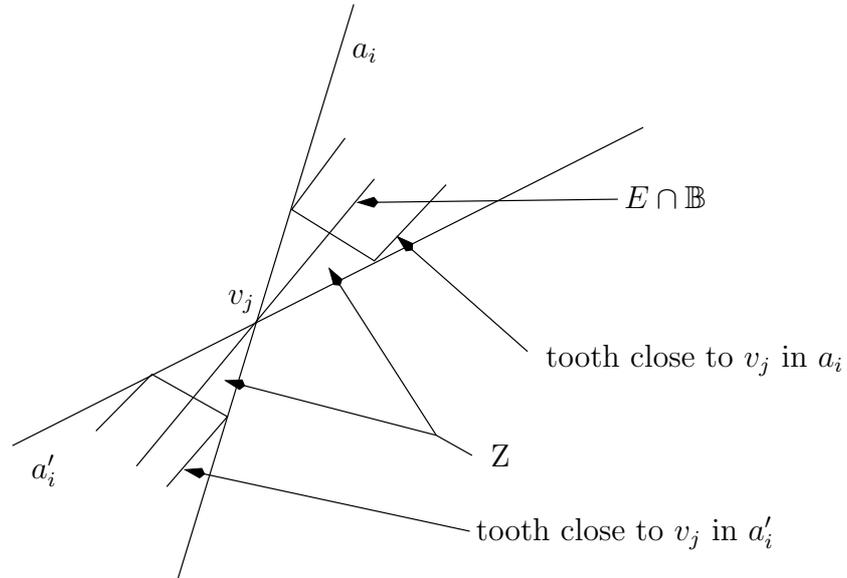
FIGURE 5.6. $E \cap \mathbb{B}$ cuts through a vertex, thus two black sectors come closer but keeping a thin white sector Z between them.

Therefore, in $E \cap \mathbb{B}$ two successive white sectors merge to form one big white sector (thus one black sector which was placed between these two is lost) and two successive black sectors approach each other but do not merge, because a thin white sector Z remains, see Figure 5.7. Since this happens twice ($E \cap \mathbb{B}$ changes twice through a vertex) two black sectors are lost (and thus the two antipodal

white sectors are thinned). In this case $E \cap \mathbb{B}$ has $(2n-1)$ black sectors on its boundary and these sectors cannot all be on the same half space of $E \cap \mathbb{B}$. This is true, because one would need at least $4n-3$ planes E_k to separate them from each other, and since $n \geq 3$ it follows $4n-3 > 2n+1$, which is a contradiction as there exist only $2n+1$ of the E_k's. Hence the convex hull of the black sectors contains the centre of $E \cap \mathbb{B}$ in the interior.
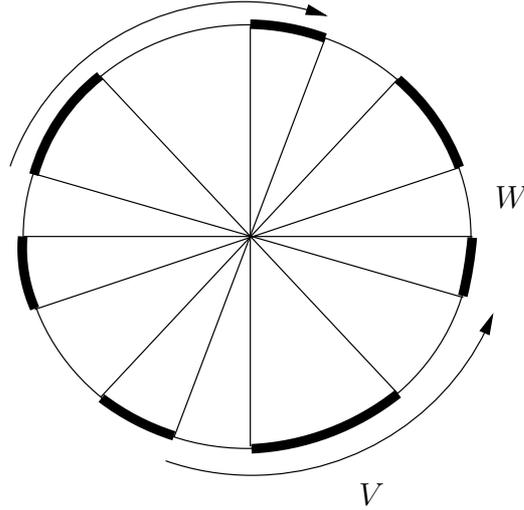
FIGURE 5.7. Case (2): Two white sectors merge to form one big white sector V and two black sectors approach each other but keep a thin white in between. In case of (2c) it can also happen that for example V and W merge, with the result that two black sectors are lost.

In case of (3) $E \cap \mathbb{B}$ contains at least $3n$ points (when for every j one of s_{v_j} and s_{w_j} equals 0) and at most $4n$ points (when for every j both s_{v_j} and $s_{w_j} > 0$). All these points are realised where the teeth touch E. The convex hull of these points contain the centre 0. □

If we reduce the regions A_i to single points the construction of C in Theorem 5.5 still gives a valid C. It is also possible to choose $s(v_j)$ to be 0, thus getting $p_{j1} = p_{j2} = v_j$. Figure 5.8 shows two snapshots of a 2-isoradial body as constructed in Theorem 5.5.
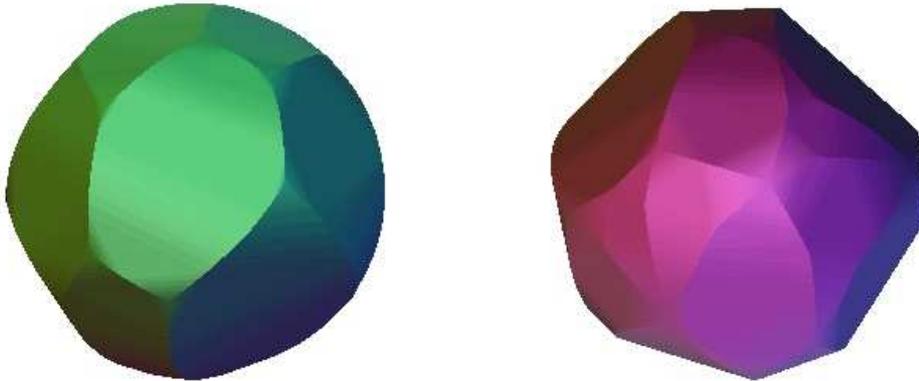
FIGURE 5.8.   Two snapshots of a 2-isoradial body with $r_1 < R_2 = R_3$.

3. Conclusions and open problems

In this chapter we have introduced the class of isoradial bodies as a generalisation of constant breadth and as a radii counterpart of what constant j-measures are for volumes. As the main result we were able to establish the existence of a totally non-spherical body in 3-space, thus solving a question for radii for which the analogue question for j-measures remains open.

Surely, the most obvious open problem at the end of this chapter is to answer the question if there are totally isoradial bodies besides the ball even in higher dimensions. If one uses again Corollary 5.3 then the task is to find a totally non-spherical body with $R_2 = \cdots = R_d$.

But already in 3-space one could ask if there is a totally isoradial body with $R_2 < R_3$, therefore avoiding the use of Corollary 5.3. Nevertheless, it is even possible that R_2-isoradiality in 3-space is equivalent to $R_2 = R_3$. Showing this or maybe even a similar statement in general dimension is also a challenging task.

One could do a step forward on this way if it would be possible to generalise Proposition 2.5 (c) as follows:

OPEN PROBLEM 5.6. *Is it possible to find a completion C_Γ for every convex body C with $r_1(C) \le R_j(C)$ for some $j \in \{2, \ldots, d\}$ such that*

$$R_j(C_\Gamma | F) = R_j(C | F) \text{ for all } F \in \mathcal{L}_{j,d}$$

or at least

$$\min_{F \in \mathcal{L}_{j,d}} R_j(C_\Gamma | F) = \min_{F \in \mathcal{L}_{j,d}} R_j(C | F) ?$$

If the answer to the first Part of Open Problem 5.6 is 'yes' one would get the following corollary, which is marked with a star to indicate that it depends on an unsolved question:

COROLLARY* 5.7. *If C is R_j-isoradial, $j \in \{2, \ldots, d-1\}$ and $r_1(C) = R_j(C)$ then it must hold $r_1(C) = R_j(C) = R_d(C)$.*

PROOF. If Open Problem 5.6 is right, there exists a completion C_Γ of C such that C_Γ is R_j-isoradial and $R_1(C_\Gamma) = R_j(C_\Gamma)$. However, because of Proposition 2.5 (a) it follows $R_1(C_\Gamma | F) = R_j(C_\Gamma | F)$ for all $F \in \mathcal{L}_{j,d}$, and therefore $C_\Gamma | F = \mathbb{B}^j$. Hence

$$R_j(C) = R_j(C_\Gamma) = R_d(C_\Gamma) \ge R_d(C),$$

and therefore $R_j(C) = R_d(C)$. $\square$

After asking for completions within minimal circumscribing j-cylinders and introducing isoradiality as a generalisation of the constant breadth property, there is another quite natural question: Is there a good generalisation of completions (or reductions) to general j-radii?

If one defines a body C to be j-complete if $r_j(D) > r_j(C)$ for all $D \supset C$ then $\mathbb{B}$ is not j-complete, if $j \ne 1$, because $r_j(D) = 1$ if $D = \text{conv}\{\mathbb{B} \cup \{p\}\}$ for all $p \in \mathbb{E}^d$ and $j \ne 1$. Nevertheless, $\mathbb{B}$ is r_2-isoradial, such that this generalisation seems to be not very useful. A 2-complete set in this sense would be an infinite cylinder $\text{span}\{s\} + \mathbb{B}$, $s \in \mathbb{S}$, and unbounded sets are surely something we want to avoid.

Since the ball should be j-complete if we would like to have a chance that there exists a relation between generalised completeness and isoradiality, a better definition should be the following:

DEFINITION 5.8. *A body C is called j-complete if* $\max\{R_j(D|F) : F \in \mathcal{L}_{j,d}\} > \max\{R_j(C|F) : F \in \mathcal{L}_{j,d}\}$ *for all $D \supset C$, and if C is a body, then a body $D \supseteq C$ is called the j-completion of C, if D is j-complete and* $\max\{R_j(D|F) : F \in \mathcal{L}_{j,d}\} = \max\{R_j(C|F) : F \in \mathcal{L}_{j,d}\}$.

It is easy to see that $\mathbb{B}$ is j-complete. But as one could easily add a couple of points from the sphere to the totally isoradial body in Chapter 5 it is not true that an R_2-isoradial or r_2-isoradial is also 2-complete. To show if the other direction holds or not, is another interesting question to proceed on.

CHAPTER 6

Blaschke-Santaló diagrams

In 1916 Blaschke [7] considered a mapping f of 3-dimensional (convex) bodies C onto the plane, defining the two coordinates of $f(C)$ as

$$x = \frac{4\pi F(C)}{M(C)^2}, \, y = \frac{48\pi^2 V(C)}{M(C)^3},$$

where $F(C)$ denotes the surface area, $M(C)$ the mean curvature, and $V(C)$ the volume of C. The set of points obtained for all possible bodies C in $\mathbb{E}^3$ is called the Blaschke diagram, and it is still an open problem to give a complete system of inequalities describing its boundary structure [61, 22].

Similarly, for planar sets, Santaló [63] proposed in 1961 a mapping of triples out of the six quantities, namely area, circumradius, diameter, inradius, perimeter, and width, onto a 2-dimensional diagram (see Section 2 for details). He also provided complete characterisations by inequalities for 6 of the 20 possible mappings, including one pure radii (without area and perimeter) case. Solutions to the three remaining pure radii diagrams are given in [20, 19].

The complete systems of valid inequalities describing the Blaschke-Santaló diagrams are minimal in the sense that removal of any of the inequalities leads to an incomplete description of the diagram. Hence they are the best known way to see which geometric inequalities about radii are really essential and not dominated by others. The disadvantage of these diagrams is that they only involve at most three radii at the same time. Hence one cannot develop inequalities which take all four radii into account.

In the first section of this chapter we state some technical results about the behaviour of radii of Minkowski sums. A survey of the four Blaschke-Santaló diagrams which only consider radii is presented in Section 2. This is followed by the main section of this chapter, in which we extend the concept of Blaschke-Santaló diagrams. Here we analyse the single 3-dimensional diagram one obtains

from considering all four planar radii at the same time. This new diagram has the property that its projections along the coordinate axes are three of the well-known planar diagrams.

Development of this new 3-dimensional diagram is an important step, since it offers a much deeper insight in the whole matter and about the possible radii relations. It enables us to derive essential new valid inequalities, which involve all four radii at once; and six additional planar sets (besides the four, known from the 2-dimensional diagrams), which reveal extreme points of the 3-dimensional diagram are also discovered. At this point we should mention that we use the notions *face* and *extreme point* for these non-convex diagrams in the same way as they have been defined for convex sets in Section 1 of Chapter 2. The only difference is that we allow a face to be non-convex.

In the last section of this chapter we provide an outlook on further possible extensions of the Blaschke-Santaló diagrams, for example, diagrams we obtain by going back to 2-dimensional mappings, but now considering bodies in 3-space, and maybe using also other radii than the standard ones. These extensions will also tie up the concept of Blaschke-Santaló diagrams and our results in the preceding chapters. In particular, the totally isoradial bodies of Chapter 5 will be important in this context.

1. Radii of Minkowski sums

Let $\mathcal{C}^d$ denote the class of all d-dimensional bodies C (note that we do not require the bodies in $\mathcal{C}^d$ to be proper). It is well known that the volume of the Minkowski sum $K + \lambda L$ for two bodies $K, L \in \mathcal{C}^d$ and $\lambda \in \mathbb{R}$ is a polynomial function in λ (from the theory of mixed volumes, see [62] for an overview). Of course, this is also true for $(1 - \lambda)K + \lambda L$.

In this section we study the following questions:

- what can be said about the functions $r_{j,d,K,L}(\lambda) = r_j((1 - \lambda)K + \lambda L)$ and $R_{j,d,K,L}(\lambda) = R_j((1 - \lambda)K + \lambda L)$, $j \in \{1, \dots, d\}$ for arbitrary bodies K, L and

- what do we get if we fix $L = \mathbb{B}$ (in the case of volumes the coefficients of the function $\mathrm{Vol}(K + \lambda L)$ are called the quermassintegrals of K).

LEMMA 6.1. *Suppose* $K, L \in \mathcal{C}^d$ *and* $\lambda \in [0, 1]$. *Then*

a) $r_j((1 - \lambda)K + \lambda L) = (1 - \lambda)r_j(K) + \lambda r_j(L)$ *if*
  (i) $j = 1$ *and* K, L *achieve their diameter along parallel directions, or*
  (ii) $L = \mathbb{B}$.

b) $R_j((1 - \lambda)K + \lambda L) = (1 - \lambda)R_j(K) + \lambda R_j(L)$ *if*
  (i) $j = 1$ *and* K, L *achieve their width along parallel directions, or*
  (ii) $L = \mathbb{B}$.

PROOF. The validity of (a) and (b) under hypothesis (i) is in both cases an easy consequence of the linearity of $\langle \cdot, s \rangle$ and the fact that R_1 and r_1 are the minima and maxima of the s-breadth of a body, respectively.

Hence it remains to show that (a) and (b) hold if $L = \mathbb{B}$.

a) We start with the '$\geq$'-direction. From the definition of the inner j-radii it follows that there exists $F \in \mathcal{A}_{j,d}$ and $q \in F$ such that $(q + r_j(K)\mathbb{B}) \cap F \subseteq K$. Wlog we can assume that $q = 0$ and therefore that $F \in \mathcal{L}_{j,d}$. Hence $r_j(K)\mathbb{B} \cap F \subseteq K$ and, since F is a linear subspace and therefore invariant under scaling, we get that $(1 - \lambda)r_j(K)\mathbb{B} \cap F \subseteq (1 - \lambda)K$. Now we use the monotonicity of the Minkowski sum with respect to set inclusion and obtain

$$(1 - \lambda)K + \lambda\mathbb{B} \supseteq (1 - \lambda)r_j(K)\mathbb{B} \cap F + \lambda\mathbb{B} \supseteq ((1 - \lambda)r_j(K) + \lambda)\,\mathbb{B} \cap F.$$

Hence

$$r_j((1 - \lambda)K + \lambda\mathbb{B}) \geq (1 - \lambda)r_j(K) + \lambda.$$

Now consider the '$\leq$'-direction. Wlog we assume $\lambda \neq 1$ and for reading convenience we set

$$\rho = r_j((1 - \lambda)K + \lambda\mathbb{B}).$$

It follows again from the definition of the inner j-radii that there exists $F \in \mathcal{A}_{j,d}$ and $q \in F$ such that $(q + \rho\mathbb{B}) \cap F \subseteq (1 - \lambda)K + \lambda\mathbb{B}$, and we can assume wlog that $q = 0$ and therefore $F \in \mathcal{L}_{j,d}$. Hence $\rho\mathbb{B} \cap F \subseteq (1 - \lambda)K + \lambda\mathbb{B}$. But from this we get $(\rho - \lambda)\mathbb{B} \cap F \subseteq (1 - \lambda)K$ and therefore

$$\frac{\rho - \lambda}{1 - \lambda}\mathbb{B} \cap F \subset K.$$

So we see

$$\frac{\rho - \lambda}{1 - \lambda} \leq r_1(K),$$

which proves the claim.

b) The proof for the outer radii follows the same scheme. We begin with the '$\leq$'-direction. From the definition of the radii we know that there exists an $E \in \mathcal{L}_{d-j,d}$ such that $E + R_j(K)\mathbb{B} \supseteq K$. This leads immediately to

$$(1-\lambda)(E + R_j(K)\mathbb{B}) = E + (1-\lambda)R_j(K)\mathbb{B} \supseteq (1-\lambda)K,$$

from which we obtain

$$E + ((1-\lambda)R_j(K) + \lambda)\mathbb{B} \supseteq (1-\lambda)K + \lambda\mathbb{B}.$$

Hence

$$R_j((1-\lambda)K + \lambda\mathbb{B}) \leq (1-\lambda)R_j(K) + \lambda.$$

To show the '$\geq$'-direction, we assume wlog that $\lambda \neq 1$, set $\rho = R_j((1-\lambda)K + \lambda\mathbb{B})$ and get from the definition of the radii that $E + \rho\mathbb{B} \supseteq (1-\lambda)K + \lambda\mathbb{B}$. This leads to $E + (\rho - \lambda)\mathbb{B} \supseteq (1-\lambda)K$ and therefore we obtain

$$E + \frac{\rho - \lambda}{1 - \lambda}\mathbb{B} \supseteq K.$$

Hence

$$R_j(K) \leq \frac{\rho - \lambda}{1 - \lambda},$$

which completes the proof.

$\square$

From Lemma 6.1 we obtain the following Corollary:

COROLLARY 6.2. *If L is of constant breadth or if $L = -K$ then*

$$r_j((1-\lambda)K + \lambda L) = (1-\lambda)r_j(K) + \lambda r_j(L)$$

and

$$R_j((1-\lambda)K + \lambda L) = (1-\lambda)R_j(K) + \lambda R_j(L).$$

In both cases condition (i) of Lemma 6.1 holds.

However, in general the radii functions are not linear and not even polynomial. For example, for all polytopes $K, L \in \mathcal{C}^d$ the function $f(\lambda) := r_1^2(K + \lambda L)$ is piecewise quadratic (and contains linear and constant parts). Suppose $K = \text{conv}\{k_1, \ldots, k_n\}$ and $L = \text{conv}\{l_1, \ldots, l_m\}$. Then it is obvious that the vertices

$w(\lambda)_i$ of $K + \lambda L$ can be written as $w(\lambda)_i = k_{i_1} + \lambda l_{i_2}$ and that the diameter of $K + \lambda L$ is achieved between two such vertices. Hence

$$r_1(K + \lambda L) = \frac{1}{2}\|w(\lambda)_i - w(\lambda)_j\|$$

and

$$4r_1^2(K + \lambda L) = \|k_{i_1} - k_{j_1}\|^2 + 2\langle k_{i_1} - k_{j_1}, l_{i_2} - l_{j_2}\rangle\lambda + \|l_{i_2} - l_{j_2}\|^2\lambda^2 \ .$$

The above does also show that f is polynomial only if it is truly quadratic, which means that for all possible λ the diameter of $K + \lambda L$ lies between the same pair of vertices. On the other hand, transitions between the different quadratic pieces of f can only appear if λ is chosen such that the diameter of the polytope $K + \lambda L$ is realised between two different pairs of vertices.

The following example shows that such transitions between quadratic pieces in f can happen, even if K and L are symmetric polytopes. Moreover, since $r_1 = R_2$ for symmetric polytopes we see that the radius function of R_d is not polynomial, either.

EXAMPLE 6.3. *Let $K = \mathrm{conv}\{\binom{-1}{0}, \binom{0}{2}, \binom{1}{0}, \binom{0}{-2}\}$ and $L = \mathrm{conv}\{\binom{-1}{0}, \binom{1}{0}\}$, see Figure 6.1. It follows that $K + \lambda L = \mathrm{conv}\{\binom{-\lambda}{-2}, \binom{\lambda}{-2}, \binom{\lambda}{2}, \binom{-\lambda}{2}, \binom{-1-\lambda}{0}, \binom{1+\lambda}{0}\}$. Hence*

$$r_1^2(K + \lambda L) = \begin{cases} \lambda^2 + 4, & \text{if } \lambda \leq \frac{3}{2} \\ (\lambda + 2)^2, & \text{if } \lambda \geq \frac{3}{2}. \end{cases}$$

It is easy to see that this example can be extended to an example with arbitrary many transitions between the pairs of vertices which achieve diametral distance. See Figure 6.2 for an example with two transitions.

2. The four Blaschke-Santaló diagrams

In this section we present the results of Santaló [63], Hernández Cifre and Segura Gomis [19, 20], who were able to describe the complete boundary structure for the four possible Blaschke-Santaló diagrams which only involves radii. It follows from Proposition 2.1 that in $\mathbb{E}^2$

$$r_2(C) \leq R_1(C) \leq r_1(C) \leq R_2(C)$$
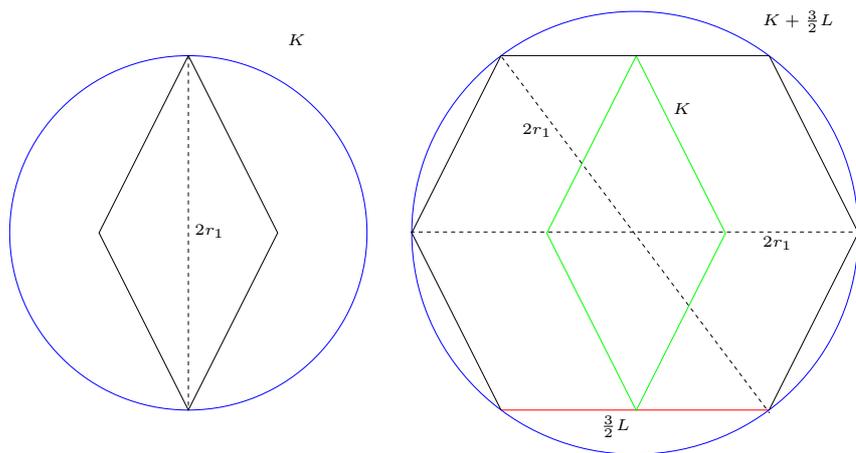
FIGURE 6.1. K and $K + \frac{3}{2}L$ from Example 6.3. As long as $\lambda \leq \frac{3}{2}$ the diameter is achieved between antipodal vertices on the upper and lower line of $K + \lambda L$. However, if $\lambda \geq \frac{3}{2}$ the diameter is attained between the two vertices on the horizontal line in the mid of $K + \lambda L$.

holds for all bodies C. Hence the greatest radius in every radii triple can always be used to normalise the planar sets to unity (for this radius) and therefore the diagrams are subsets of the unit square.

2.1. The (r_2, R_1, r_1)-diagram. The first diagram is the only one which does not involve R_2. Hence r_1 is the greatest radius in this triple and therefore we normalise the planar sets to have diameter 2. For this reason, let $\mathcal{C}^2_{r_1=1}$ denote the class of all 2-dimensional bodies K with $r_1(K) = 1$, and consider the map

$$f_1 : \mathcal{C}^2_{r_1=1} \to [0,1]^2,$$

where

$$f_1(K) = (x,y) = (r_2(K), R_1(K)).$$

f_1 is properly defined, as any $K \in \mathcal{C}^2_{r_1=1}$ is mapped onto the unit square (see Proposition 2.1), and $f_1(\mathcal{C}^2_{r_1=1})$ is a closed set because of Blaschke's convergence theorem [**7**].

Before we describe the boundaries of the Blaschke-Santaló diagram, it is necessary to introduce some notations:

As usual, $\mathbb{B}$ denotes the *disc* and T^2 an *equilateral triangle*. We use the symbol RT for a *Reuleaux triangle* and L for a *line segment*.
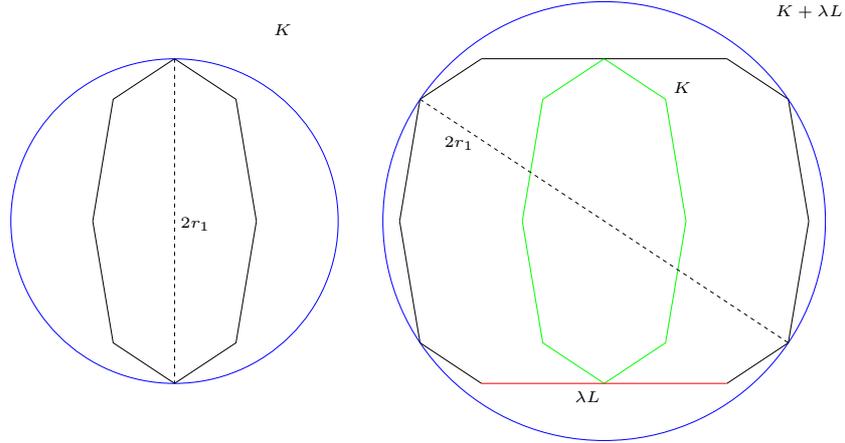
FIGURE 6.2. A sketch of an example with two transitions between the pairs of diametral vertices of $K + \lambda L$. As the left side of the figure shows, the diameter is taken between the upper and the lower vertex if λ is 0. The right part shows that for certain λ the vertices in the northwest and in the southeast corner are diametrical, indicated by the dashed line. Furthermore it is easy to see that if λ is chosen big enough, the distance between the horizontal vertices will exceed the distances between any other possible pairs.

I_γ denotes an *isosceles triangle* where $\gamma \in (0, \pi)$ is the angle between its two equilateral sides (see Figure 6.3). Hence $T^2 = I_{\frac{\pi}{3}}$, and $I_{\frac{\pi}{2}}$ is a right-angled isosceles triangle. Allowing γ to be also 0 or π, we obtain $I_0 = I_\pi = L$.

A *Yamanouti set* Y_ω is defined as the convex hull of T^2 together with the intersection of three circles of radius $\omega \in [2R_1(T^2), 2r_1(T^2)]$ whose centres are the vertices of T^2 (see Figure 6.4). It is easy to see that $Y_{2R_1(T^2)} = T^2$ and $Y_{2r_1(T^2)} = RT$. The Yamanouti sets were first described in 1932 by Yamanouti [**79**].

All sets above are scaled to be of diameter 2, such that they are in $\mathcal{C}^2_{r_1=1}$. Proposition 6.4 below gives the geometric inequalities which describe the boundaries of $f_1(\mathcal{C}^2_{r_1=1})$ and the planar sets which are mapped onto that boundaries. A sketch of the diagram can be found in Figure 6.5.

PROPOSITION 6.4. *The following inequalities are valid for $f_1(\mathcal{C}^2_{r_1=1})$ and the sets associated with each inequality fulfill it with equality:*
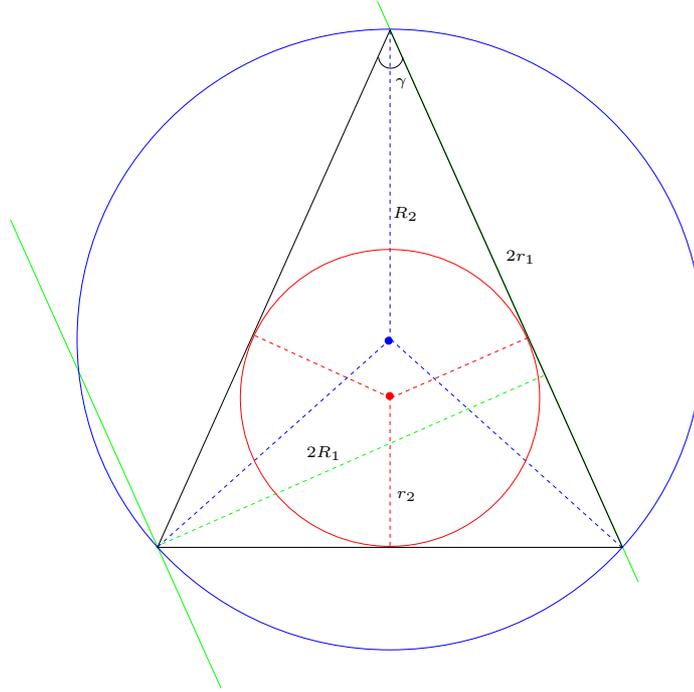
FIGURE 6.3.   An isosceles triangle and its radii in the case of
$\gamma < \frac{\pi}{3}$. The colours indicate the radii: blue for the circumradius
R_2, red for the inradius r_2, and green for the width $2R_1$. We did
not use a special colour for the diameter $2r_1$.

(i) $y \leq 1$, $\{K \in \mathcal{C}^2_{r_1=1} : K$ *is of constant breadth*$\}$,
(ii) $x \leq y$, $\{K \in \mathcal{C}^2_{r_1=1} : K$ *is centrally symmetric*$\}$,
(iii) $y \leq \frac{x}{2} + \sqrt{\frac{1}{3}}$, $\{K \in \mathcal{C}^2_{r_1=1} : K = Y_\omega, \omega \in [2R_1(T^2), 2r_1(T^2)]\}$,
(iv) $4(x-y)^2(2x-y) \leq x^4 y$, $\{K \in \mathcal{C}^2_{r_1=1} : K = I_\gamma, \gamma \leq \frac{\pi}{3}\}$.

A proof of Proposition 6.4, and an argument showing that $f_1(\mathcal{C}^2_{r_1=1})$ is simply
connected, can be found in [**19**].

It is easy to see that the ball $\mathbb{B}$, the Reuleaux triangle RT, the equilateral
triangle T^2, and the line segment L are the four extreme points of the diagram,
each fulfilling two of the inequalities in Proposition 6.4 with equality. Observe
that each of the four inequalities in Proposition 6.4 describes one of the four
boundary pieces connecting the four extreme points in Figure 6.5.

2.2. The (r_2, R_1, R_2)-diagram. As mentioned at the beginning of this sec-
tion the previous diagram was the only one not involving the circumradius. For

FIGURE 6.4.   A Yamanouti set Y_ω with $\omega < 2r_1(T^2)$.

FIGURE 6.5.   The (r_2, R_1, r_1)-diagram.

this reason we call the class of 2-dimensional bodies K with $R_2(K) = 1$ as $\mathcal{C}_1^2$ in short (instead of $\mathcal{C}_{R_2=1}^2$, as it would correspond to the notation in the previous subsection). We also assume (wlog) that all sets in $\mathcal{C}_1^2$ have their circumcentre at the origin 0.

Now consider the map

$$f_2 : \mathcal{C}_1^2 \to [0,1]^2,$$

where

$$f_2(K) = (x, y) = (r_2(K), R_1(K)).$$

Again we know from the total order of the planar radii that f_2 is well defined and from Blaschke's convergence theorem that $f_2(\mathcal{C}_1^2)$ is compact.

To describe the boundary of $f_2(\mathcal{C}_1^2)$ we need the sets defined in Subsection 2.1, this time scaled to have circumradius 1. Additionally, we make use of the piecewise circular equilateral 3-gons $CE_\lambda = (1 - \lambda)T^2 + \lambda\mathbb{B}$, for $\lambda \in [0,1]$ (see Figure 6.6).
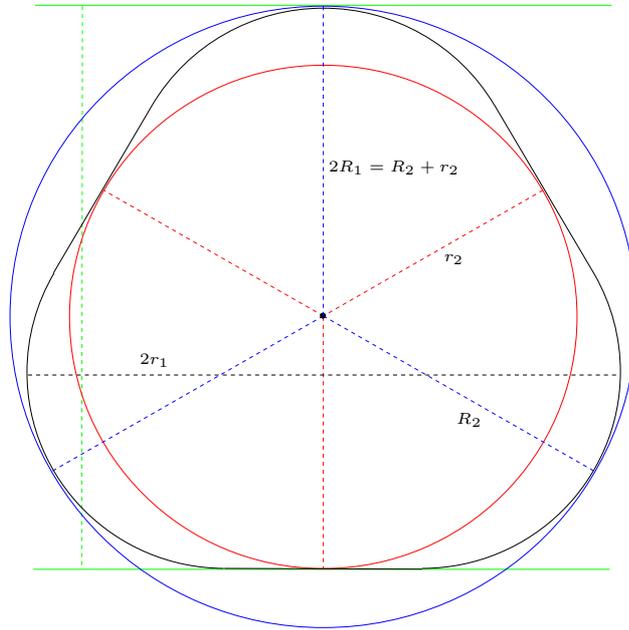
FIGURE 6.6.   The piecewise equilateral 3-gon $CE_{\frac{1}{2}}$.

The results below are taken from [20]. See Figure 6.7 for a sketch of the corresponding diagram.

PROPOSITION 6.5. *The following inequalities are valid for $f_2(\mathcal{C}_1^2)$ and the sets associated with each inequality fulfill it with equality:*

(i) $x \leq y$, $\{K \in \mathcal{C}_1^2 : K \text{ is centrally symmetric}\}$,

(ii) $y \leq \frac{x+1}{2}$, $\{K \in \mathcal{C}_1^2 : K = CE_\lambda, \lambda \in [0,1]\}$,
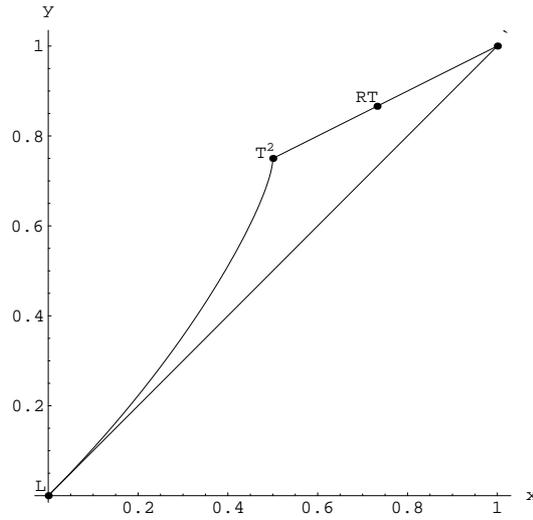
FIGURE 6.7.   The (r_2, R_1, R_2)-diagram.

(iii) $2(2x - y)(y - x) \leq x^3$, $\{K \in \mathcal{C}_1^2 : K = I_\gamma, \gamma \leq \frac{\pi}{3}\}$.

The extreme points of $f_2(\mathcal{C}_1^2)$ are $\mathbb{B}, T^2$, and L; this time RT does not belong to them. It should be mentioned that we introduced the piecewise equilateral 3-gons only to state the original results. Essentially they are not needed because the boundary $y = \frac{x+1}{2}$ is also achieved by the Yamanouti sets and all constant breadth bodies. The first are mapped on the lower part of the $(y = \frac{x+1}{2})$-boundary between T^2 and RT, the second on the upper part between RT and $\mathbb{B}$ (see Figure 6.7).

2.3. The (r_2, r_1, R_2)-diagram. For the third diagram, it is not necessary to change the ground set $\mathcal{C}_1^2$. Define

$$f_3 : \mathcal{C}_1^2 \rightarrow [0, 1]^2,$$

where

$$f_3(K) = (x, z) = (r_2(K), r_1(K)).$$

Obviously, f_3 is again well defined and the image of $\mathcal{C}_1^2$ a closed subset of the unit square (see Figure 6.8).

The results in the following proposition are taken from [**63**]:
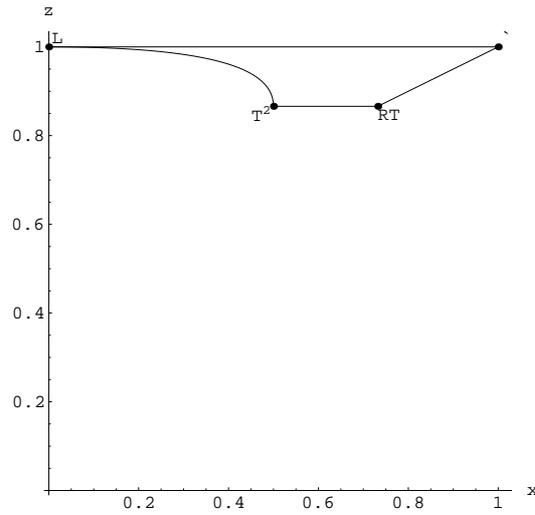
FIGURE 6.8.   The (r_2, r_1, R_2)-diagram.

PROPOSITION 6.6. *The following inequalities are valid for $f_3(\mathcal{C}_1^2)$ and the sets associated with each inequality fulfill it with equality:*

(i) $z \leq 1$, $\{K \in \mathcal{C}_1^2 : K \text{ is centrally symmetric}\}$,
(ii) $z \geq \frac{1+x}{2}$, $\{K \in \mathcal{C}_1^2 : K \text{ is of constant breadth}\}$,
(iii) $z \geq \frac{\sqrt{3}}{2}$, $\{K \in \mathcal{C}_1^2 : K = Y_\omega, \omega \in [2R_1(T^2), 2r_1(T^2)]\}$,
(iv) $(2z^2 - x)^2(1 - z^2) \geq x^2$, $\{K \in \mathcal{C}_1^2 : K = I_\gamma, \gamma \leq \frac{\pi}{3}\}$.

Here the extreme points are again $\mathbb{B}, T^2, RT$, and L, as one can see in Figure 6.8. Note that f_3 is not convex, contrary to the impression evoked by Santaló's original sketch.

2.4. The (R_1, r_1, R_2)-diagram. The last 2-dimensional map we consider is

$$f_4 : \mathcal{C}_1^2 \to [0, 1]^2,$$

where

$$f_4(K) = (y, z) = (R_1(K), r_1(K)).$$

Like the three preceding maps, f_4 is well defined and its image is a closed subset of the unit cube (see Figure 6.9).

The results about the boundaries are again taken from [20]:
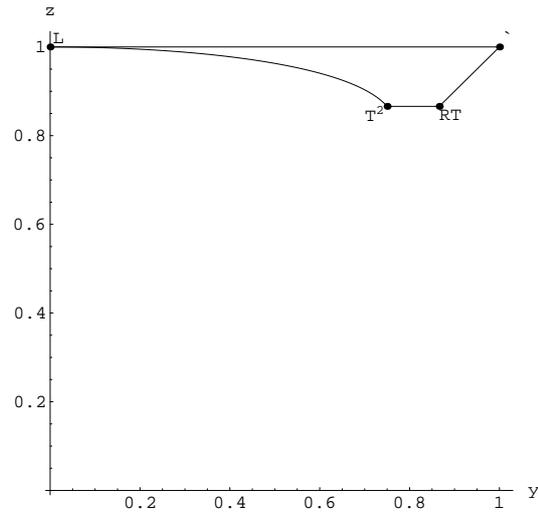
FIGURE 6.9.   The (R_1, r_1, R_2)-diagram.

PROPOSITION 6.7. *The following inequalities are valid for $f_4(\mathcal{C}_1^2)$ and the sets associated with each inequality fulfill it with equality:*

(i) $z \leq 1$, $\{K \in \mathcal{C}_1^2 : K$ is centrally symmetric$\}$,
(ii) $y \leq z$, $\{K \in \mathcal{C}_1^2 : K$ is of constant breadth$\}$,
(iii) $z \geq \frac{\sqrt{3}}{2}$, $\{K \in \mathcal{C}_1^2 : K = Y_\omega, \omega \in [2R_1(T^2), 2r_1(T^2)]\}$,
(iv) $4z^4(1 - z^2) \leq y^2$, $\{K \in \mathcal{C}_1^2 : K = I_\gamma, \gamma \leq \frac{\pi}{3}\}$.

Once more, the extreme points are $\mathbb{B}, T^2, RT$, and L.

3. A single 3-dimensional diagram

The previously described Blaschke-Santaló diagrams are of great value in the analysis of geometric inequalities about the four standard radii. However, as they always omit one of the radii, inequalities involving all four of them cannot be attained. This disadvantage inspired us to define a single 3-dimensional diagram, handling all four radii at once.

Thus, the aim of this section is to describe the 3-dimensional diagram obtained from the map

$$f : \mathcal{C}_1^2 \to [0, 1]^3, \ f(K) = (x, y, z) = (r_2(K), R_1(K), r_1(K)).$$

We know from the arguments in Section 2 that f is well defined and that the image of $\mathcal{C}_1^2$ is compact. As a consequence of Lemma 6.1 we also know that it is star shaped corresponding to the extreme point $f(\mathbb{B}) = (1, 1, 1)$ (therefore without a hole) but it is not convex as its projections along the coordinate axes (the 2-dimensional diagrams in Subsections 2.2 - 2.4) are not convex.

Certainly, well known geometric inequalities like $x \leq z$ are not needed to describe the boundary of the diagram, because they only describe subsets of these sets which fulfill the inequalities $x \leq y$ or $y \leq z$ with equality. So our main purpose is to find inequalities describing 2-dimensional parts of the boundary of the diagram. As $f(\mathcal{C}_1^2)$ is not convex, these boundaries do not have to be faces, and it may even happen that a polynomial inequality induces a 2-dimensional part of the boundary, but the inequality is not valid for $f(\mathcal{C}_1^2)$.

Based on the star shapedness with respect to the upper vertex of the bounding unit cube, $f(\mathcal{C}_1^2)$ behaves on this side, as we will see, almost like a polytope. Due to this fact we start with a collection of planar sets which describe the essential extreme points of the known part of the diagram and compute their convex hull. Then we analyse the combinatorial structure of the computed polytope and prove, facet by facet, what in fact belongs to the real surface structure of $f(\mathcal{C}_1^2)$.

3.1. The essential extreme points. It is not difficult to see that all extreme points $\mathbb{B}, T^2, L$, and RT of the 2-dimensional diagrams from Section 2 are extreme points of $f(\mathcal{C}_1^2)$. Additionally we claim that the six planar sets described below are mapped onto extreme points of the 3-dimensional diagram. Note that we will often call the sets themselves extreme, rather than their images. That they really induce extreme points will be proved in the subsequent subsections.

The first set, which we claim to induce a new extreme point, is the right-angled isosceles triangle $I_{\frac{\pi}{2}}$.

For the second, denote the vertices of $I_{\frac{\pi}{2}}$ by A, B, and C, and, as always, let 0 be the circumcentre. Furthermore, choose two points D and E on the circumcircle of $I_{\frac{\pi}{2}}$, such that the line DE is parallel to AB and separated by AB from C (see Figure 6.10). The set bounded by the lines AC, BC, DE and the circular arcs
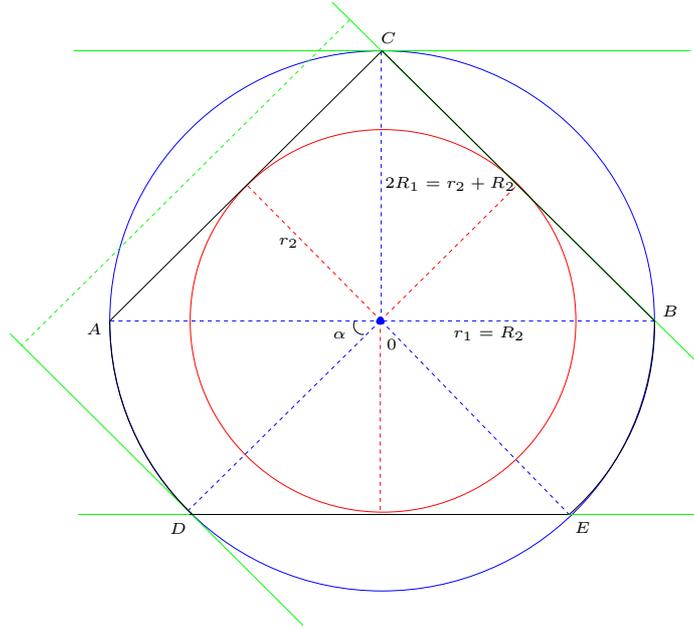
FIGURE 6.10.   The sailing boat $RSB_{\frac{\pi}{4}}$.

AD and BE on the circumcircle is called a *right-angled sailing boat* or RSB_α for short, where $\alpha \in [0, \frac{\pi}{4}]$ denotes the angle between the lines $A0$ and $D0$. It is easy to see that $RSB_0 = I_{\frac{\pi}{2}}$, but one should also note that $RSB_{\frac{\pi}{4}}$ has concentric in- and circumcircles. $RSB_{\frac{\pi}{4}}$ is the second additional set in our list of claimed extreme points.

Now, have a look back at the Reuleaux triangle RT. Name its vertices $A, B,$ and C and its in- and circumcentre is 0 (see Figure 6.11). We draw a line from A (B) to any point A' (B') on the circular arc of radius $2r_1$ around C between A and B, and remove all points below the lines AA' and BB' from RT. The resulting sets are called *sliced Reuleaux triangles*, SR_γ for short, where $\gamma \in [\frac{\pi}{6}, \frac{\pi}{3}]$ is the angle between the lines $A0$ and AA'. Clearly, $SR_{\frac{\pi}{3}} = RT$ and $SR_{\frac{\pi}{6}}$ is a Reuleaux triangle with one flattened side. Finally, as the inradius of RT is $\sqrt{3} - 1$ (see Lemma 6.8 below), the diameter, in- and circumradius of SR_γ are constant for all $\gamma \geq \arcsin(\sqrt{3} - 1)$. We add $SR_{\frac{\pi}{6}}$ and $SR_{\arcsin(\sqrt{3}-1)}$ to our list of candidates for extreme points.
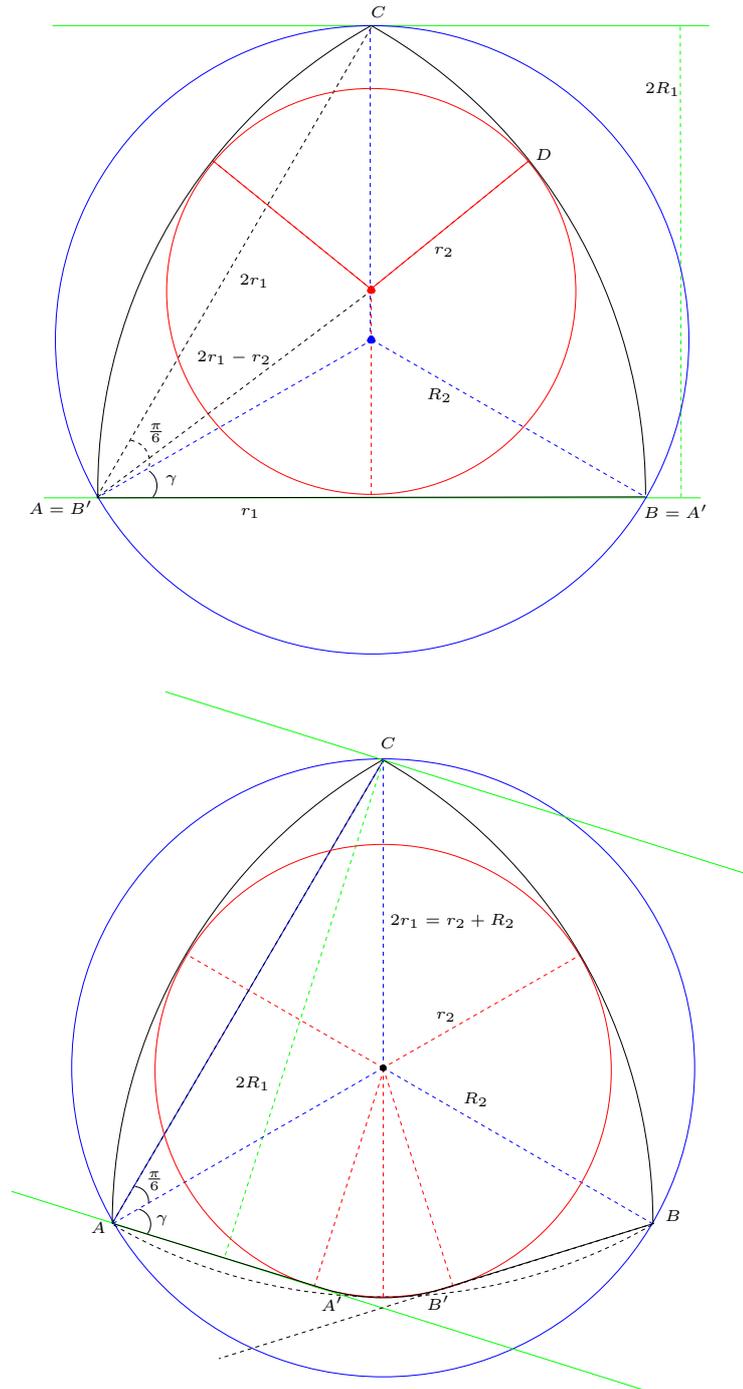
FIGURE 6.11. The sliced Reuleaux triangles $SR_{\frac{\pi}{6}}$ and $SR_{\arcsin(\sqrt{3}-1)}$.

All four radii of $SR_{\arcsin(\sqrt{3}-1)}$ do not change if one draws additional tangents from A and C to the inball between A and C and cuts off everything from $SR_{\arcsin(\sqrt{3}-1)}$ that is separated from the inball by these tangents. We call the resulting set $H_{\sqrt{3}-1}$ and define more generally the sets H_τ, the *hood* sets, $\tau \in [\sqrt{3}-1, 1]$ as follows (see Figure 6.12): We extend the inradius of $H_{\sqrt{3}-1}$ since $r_2(H_\tau) = \tau$ and move at the same time the points C and B along the circumcircle towards $-A$ such that the diameter is constantly $r_2(H_\tau) + R_2(H_\tau)$. Obviously $H_1 = \mathbb{B}$, but most important is the set H_{τ^*}, where τ^* is chosen such that the tangents from B and C to the inball are parallel to $A0$. The set H_{τ^*} is the next to add to our list.

The final group of planar sets, which we like to describe in this subsection, is called *bent trapezoids*, BT_γ for short, where $\gamma \in [0, \frac{\pi}{3}]$. The construction of a bent trapezoid BT_γ is as follows: First draw an isosceles triangle $ACB = I_\gamma$, such that AC and BC are the equilateral sides (see Figure 6.13). Than take a point D on the line through B parallel to AC, such that CAD is again similar to I_γ. Finally, we add the circular arcs from A to B, and from C to D at distance $r_1(I_\gamma)$ from C and A, respectively. Note that $BT_{\frac{\pi}{3}} = SR_{\frac{\pi}{6}}$, that $BT_0 = L$, and $R_1(BT_\gamma) = R_1(I_\gamma)$ for all $\gamma \in [0, \frac{\pi}{3}]$. Finally, as long as γ is chosen such that the line BD does not intersect the interior of the inball of $SR_{\frac{\pi}{6}}$, the inball-diameter ratio is constant for BT_γ (both radii are growing as the circumradius stays equal to 1). The extreme case, when BD is a tangent to the inball, is achieved if $\sin(\gamma) = \frac{3}{4}$ as we will see in the proof of Lemma 6.8 below. We add $BT_{\arcsin(\frac{3}{4})}$ to our collection of predicted extreme points.

Even if only one of the additional planar sets $I_{\frac{\pi}{2}}, RSB_{\frac{\pi}{4}}, SR_{\frac{\pi}{6}}, SR_{\arcsin(\sqrt{3}-1)}$, $BT_{\arcsin(\frac{3}{4})}$, and H_{τ^*} in our list of suspects is indeed an extreme point of $f(\mathcal{C}_1^2)$, it already shows the significance of the 3-dimensional diagram. However, we will soon see that at least five of them are extreme (only for BT_γ this property remains open). But to continue, first of all we need to compute the images of our sets:

LEMMA 6.8. *(i)* $f(L) = (0, 0, 1)$,
(ii) $f(\mathbb{B}) = (1, 1, 1)$,
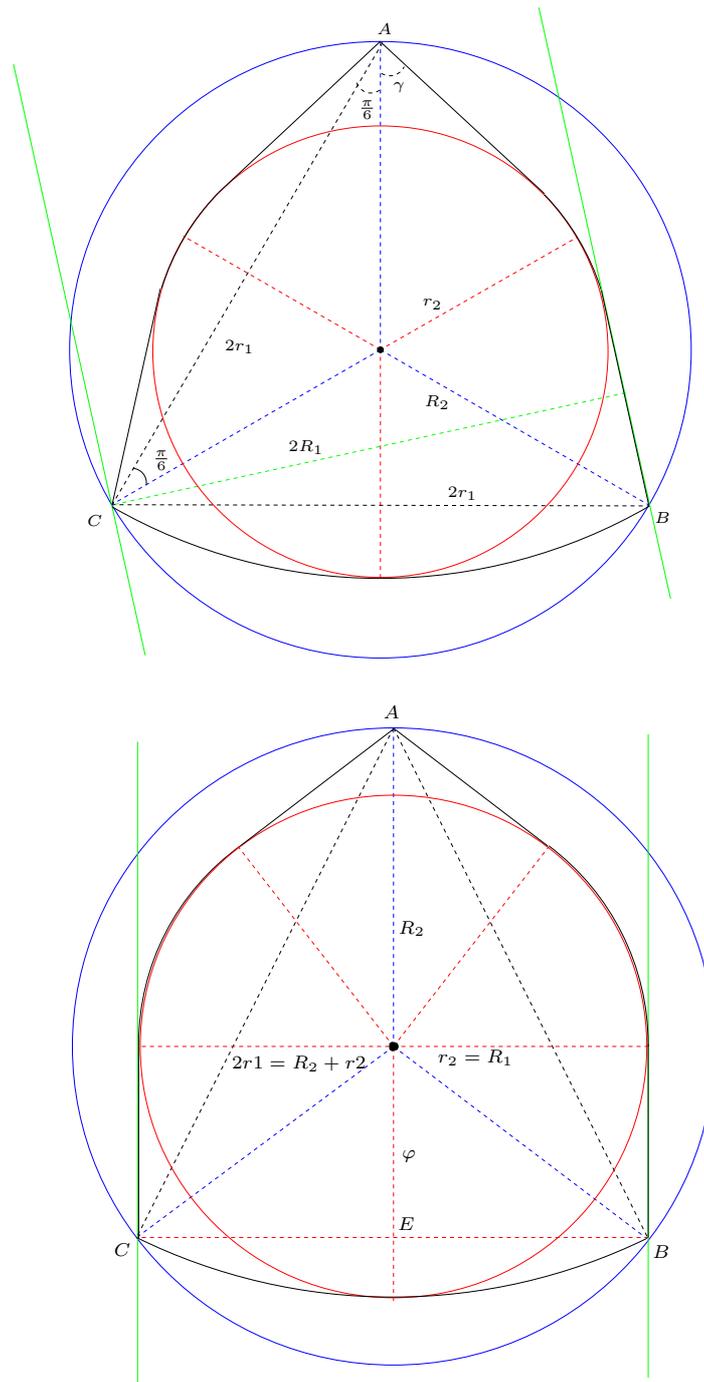
FIGURE 6.12.   The hoods $H_{\sqrt{3}-1}$ and H_{τ^*}.
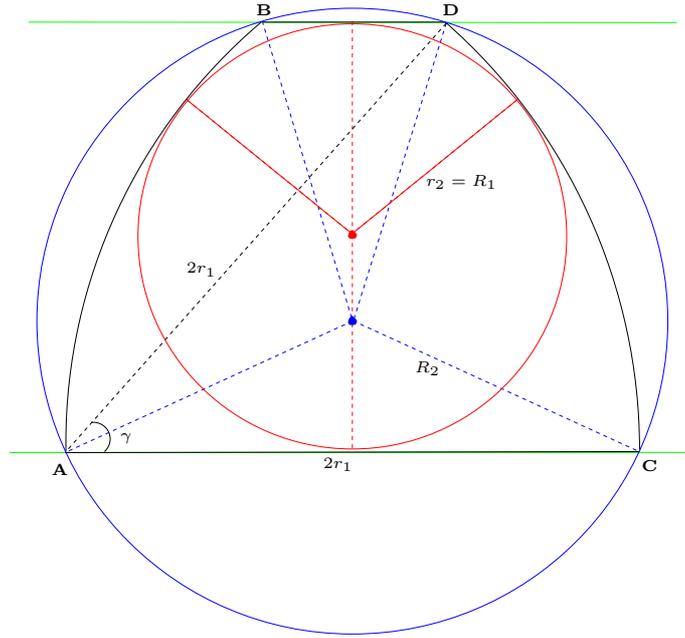
FIGURE 6.13. The bent trapezoid $BT_{\arcsin(\frac{3}{4})}$.

(iii) $f(T^2) = \left(\frac{1}{2}, \frac{3}{4}, \frac{\sqrt{3}}{2}\right)$,

(iv) $f(RT) = \left(\sqrt{3} - 1, \frac{\sqrt{3}}{2}, \frac{\sqrt{3}}{2}\right)$,

(v) $f(SR_{\frac{\pi}{6}}) = \left(\frac{3\sqrt{3}}{8}, \frac{3}{4}, \frac{\sqrt{3}}{2}\right)$,

(vi) $f(SR_{\arcsin(\sqrt{3}-1)}) = \left(\sqrt{3} - 1, \frac{\sqrt{3}}{2}\sin\left(\frac{\pi}{6} + \arcsin\left(\sqrt{3} - 1\right)\right), \frac{\sqrt{3}}{2}\right)$,

(vii) $f(BT_{\arcsin(\frac{3}{4})}) = \left(\frac{3}{4}\cos\left(\frac{1}{2}\arcsin\left(\frac{3}{4}\right)\right), \frac{3}{4}\cos\left(\frac{1}{2}\arcsin\left(\frac{3}{4}\right)\right), \cos\left(\frac{1}{2}\arcsin\left(\frac{3}{4}\right)\right)\right)$,

(viii) $f(I_{\frac{\pi}{2}}) = \left(\sqrt{2} - 1, \frac{1}{2}, 1\right)$,

(ix) $f(RSB_{\frac{\pi}{4}}) = \left(\sqrt{\frac{1}{2}}, \frac{1}{2}\left(1 + \sqrt{\frac{1}{2}}\right), 1\right)$,

(x) $f(H_{\tau^*}) = \left(\tau^*, \tau^*, \frac{\tau^*+1}{2}\right)$, where

$$\tau^* = \frac{1}{2}\sqrt{\zeta + \xi} + \sqrt{-\zeta - \xi + \frac{16}{\sqrt{\zeta + \xi}}} - 1$$

with $\zeta = \frac{1}{3}\left(864 - 96\sqrt{69}\right)^{\frac{1}{3}}$ and $\xi = 2\left(\frac{2}{3}\right)^{\frac{2}{3}}\left(9 + \sqrt{69}\right)^{\frac{1}{3}}$.

PROOF. There is nothing to show for the line and the ball, and the f-values for T^2 are general knowledge. Hence we are left with (iv) to (x).

(iv) Of course, RT has the same diameter and circumradius as T^2, and, since it is of constant breadth, its y and z values are equal. Finally, we get its inradius from Proposition 2.5 (d).

(v) It is easy to see that the values of $SR_{\frac{\pi}{6}}$ differ from the T^2-values only in the x-coordinate. Now, as the incircle of $SR_{\frac{\pi}{6}}$ and the circle of radius $2r_1$ around A have a common tangent at D (see Figure 6.11) we can compute the inradius from the equality $(2r_1 - r_2)^2 = r_1^2 + r_2^2$, which leads to $r_2 = \frac{3}{4}r_1$.

(vi) It was mentioned when we introduced the sliced Reuleaux triangles that the values of $SR_{\arcsin(\sqrt{3}-1)}$ and RT differ only in their y-coordinate. But as

$$\sin\left(\gamma + \frac{\pi}{6}\right) = \frac{R_1(SR_\gamma)}{r_1(SR_\gamma)}$$

(see Figure 6.11), we obtain the desired y-value.

(vii) Since $BT_{\frac{\pi}{3}} = SR_{\frac{\pi}{6}}$ we obtain from (vii)

$$\frac{r_2(BT_{\frac{\pi}{3}})}{r_1(BT_{\frac{\pi}{3}})} = \frac{3}{4}$$

and this ratio stays constant for all BT_γ as long as γ is chosen such that the inball of BT_γ still touches the circular arcs AB and CD. Furthermore, if we choose γ such that BD also touches the inball, obviously $R_1(BT_\gamma) = r_2(BT_\gamma)$ holds. Since

$$\sin(\gamma) = \frac{R_1(BT_\gamma)}{r_1(BT_\gamma)}$$

holds for all bent trapezoids, we obtain that $\sin(\gamma) = \frac{3}{4}$ when the inball touches the circular arcs AB, CD, and the line BD. Hence we only have to compute $r_1(BT_{\arcsin(\frac{3}{4})})$, but this can be derived from the fact that

$$\cos\left(\frac{\gamma}{2}\right) = \frac{r_1(BT_\gamma)}{R_2(BT_\gamma)}$$

for all bent trapezoids, and therefore $r_1(BT_{\arcsin(\frac{3}{4})}) = \cos(\frac{1}{2}\arcsin(\frac{3}{4}))$.

(viii) Now we have to check the $I_{\frac{\pi}{2}}$ values. The y- and z-coordinates are obviously correct and we derive the inradius from the fact that $r_2(I_{\frac{\pi}{2}}) = \tan(\frac{\pi}{8}) = \sqrt{2} - 1$.

(ix) The next to verify are the $RSB_{\frac{\pi}{4}}$ coordinates. By construction, $z = 1$ and it is easy to see that the incircle radius is $\sqrt{\frac{1}{2}}$. Finally, since the distances of each of the lines AC, BC, and DE to their opposite vertices (E, D, and C, respectively) is $R_2 + r_2$, we can easily compute the y-value.

(x) Finally, we have to prove the H_{τ^*} values. It is easy to see that $x = y$ and, because every point on the circular arc around A through B and C is at distance $2z$ from A, that $z = \frac{x+1}{2}$ (see Figure 6.12). So we only need to compute the inradius τ^* of H_{τ^*}. But this can be derived from the two equations: $r_2^2 + \varphi^2 = R_2^2$ and $r_2^2 + (R_2 + \varphi)^2 = 4r_1^2 = (r_2 + R_2)^2$, where φ denotes the distance between the centre of H_{τ^*} and the line from B to C. Since $R_2 = 1$, the two equations can be simplified to $r_2 = \sqrt{1 - \varphi^2}$ and $\varphi^4 + 4\varphi^3 + 8\varphi^2 = 4$. The latter is a polynomial equation of degree 4 which can be solved exactly. That the only positive solution for φ leads to $r_2 = \tau^*$ was checked with two different software packages (Maple [**73**] and Mathematica [**77**]).

$\square$

Note that all sets from Lemma 6.8 have a symmetry axis perpendicular or parallel to one of their diameters, and that they all have concentric in- and circumspheres or orthogonal diameter and width directions (or both).

Another remark we like to make at this point is that one can show

$$r_1(BT_{\arcsin(\frac{3}{4})}) = \frac{1}{4}(1 + \sqrt{7})$$

by using the Pythagorean theorem instead of the trigonometric functions.

Since polytopes are the easiest sets to describe by valid inequalities, we start with an analysis of the convex hull of our candidate set of extreme points. The incidences of vertices and facets in this polytope are used as a starting point in the description of the actual boundary structure of the diagram.

If we take numerical approximations of the values in Lemma 6.8 we can use them as input data for Qhull, a software package that is able to compute an $\mathcal{H}$-representation of a polytope from a $\mathcal{V}$-representation [**36**]. See Appendix A for the in- and output to Qhull and Figure 6.14 for a graph showing the vertex-facet relations Qhull computed.
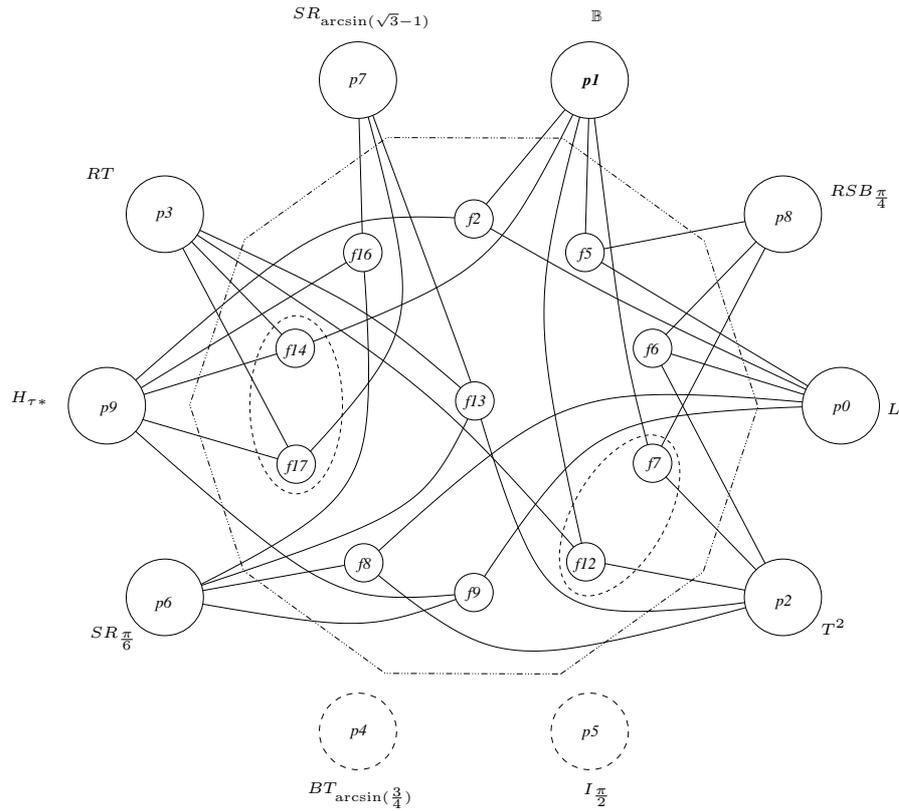
FIGURE 6.14. The vertex-facet incidences Qhull computed for the convex hull of the extreme point list in Lemma 6.8. p0 to p9 are the names Qhull used for the sets in our extreme point list, f2 to f17 denote the eleven facets Qhull distinguishes (the missing values correspond to planes which Qhull found out not to be facets).

The dashed lines in Figure 6.14 indicate that $I_{\frac{\pi}{2}}$ and $BT_{\arcsin(\frac{3}{4})}$ are lying within the convex hull of the other points and that the two facets f14 and f17, and the two facets f7 and f12, respectively, have almost identical normal vectors. In fact $\mathbb{B}$, RT, $H_{\tau*}$, and $SR_{\arcsin(\sqrt{3}-1)}$ are all mapped onto the hyperplane induced by $x + 1 = 2z$, and $\mathbb{B}$, RT, T^2, and $RSB_{\frac{\pi}{4}}$ onto the hyperplane induced by $x + 1 = 2y$. We see that Qhull distinguishes between f14 and f17 or between f7 and f12 just because of imprecisions in the numerical approximations of the coordinates. The reason why we keep $I_{\frac{\pi}{2}}$ and $BT_{\arcsin(\frac{3}{4})}$ in our list of predicted extreme points is based on the non-convexity of $f(\mathcal{C}_1^2)$. We will see that they are important in the following subsections.

The remaining part of this section is organised as follows: we take a look on each facet of the Qhull output to gather information about the real image of $\mathcal{C}_1^2$. In most cases the facets which were computed by Qhull lead to the development of one or two linear or at least polynomial inequalities inducing 2-dimensional parts of the diagram.

3.2. The facet f2 and the $(x \leq y)$-inequality. Qhull computed f2 as the facet containing the images of L, $\mathbb{B}$, and H_{τ^*}. In fact f2 is induced by the valid inequality $x \leq y$ (see Proposition 2.1) and $BT_{\arcsin(\frac{3}{4})}$ is also mapped onto it. Figure 6.15 shows the known parts of this face of $f(\mathcal{C}_1^2)$.
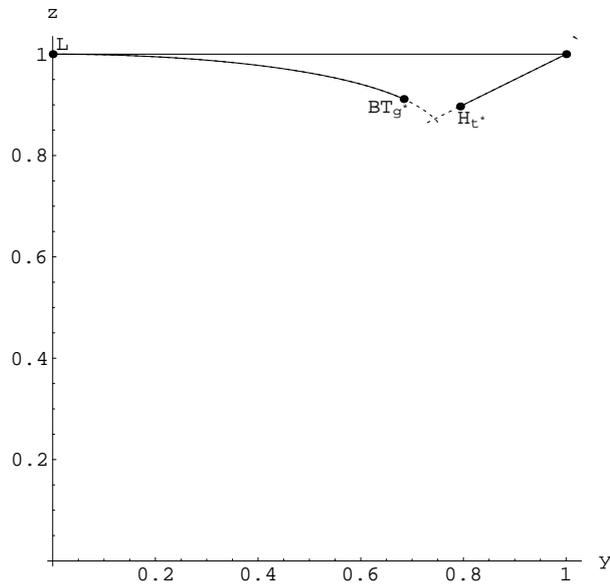
FIGURE 6.15.   The face of $f(\mathcal{C}_1^2)$ induced by the inequality $x \leq y$, projected onto the (y, z)-plane. Here $\gamma^* = \arcsin(\frac{3}{4})$.

We know from Propositions 2.1 and 2.5 that $z \leq 1$ and $z \geq \frac{x+1}{2}$. Hence the two lines through $L, \mathbb{B}$ and $\mathbb{B}, H_{\tau^*}$ are part of the boundary in the $(x = y)$-plane, and the Minkowski sums of $\mathbb{B}$ and L, or $\mathbb{B}$ and H_{τ^*}, respectively, are mapped onto the two boundaries.

We already established the validity of the inequality

(1)
$$y^2 - 4(1 - z^2)z^4 \geq 0$$

for $f(\mathcal{C}_1^2)$ in Proposition 6.7. The proof can be found in [20]. There it was also stated that equality is attained if and only if the planar sets are isosceles triangles; both (if and only if) are *not true*. Only isosceles triangles I_γ with $\gamma \le \frac{\pi}{3}$ fulfill (1) with equality, and (more important) as the inequality does not involve the inradii of the sets, any set $K \in \mathcal{C}_1^2$, with $I_\gamma \subset K \subset BT_\gamma$, $\gamma \le \frac{\pi}{3}$ fulfills (1) with equality (remember that I_γ and BT_γ have same circumradius, width, and diameter). But, as BT_γ is mapped onto the $(x = y)$-plane for $\gamma \le \arcsin(\frac{3}{4})$, the curve induced by the inequality $y^2 - 4(1 - z^2)z^4 \ge 0$ forms the third part of the boundary from L to $BT_{\arcsin(\frac{3}{4})}$ in the $(x = y)$-plane.

The precise boundary between $BT_{\arcsin(\frac{3}{4})}$ and H_{τ^*} remains unknown. Because of the validity of the inducing inequalities, no set in $\mathcal{C}_1^2$ can be mapped below the dashed lines in Figure 6.15. However, one cannot even go beyond $BT_{\arcsin(\frac{3}{4})}$ on the BT_γ-bow as this requires a superset of an isosceles triangle with the same width, diameter, and circumradius; but raising R_1 above $\frac{3}{4}$ means we cannot keep $r_2 = R_1$.

Also it is not possible to go beyond H_{τ^*} on the boundary from $\mathbb{B}$. Suppose there exists a set $K \in \mathcal{C}_1^2$ with $r_2(K) = R_1(K)$ and $r_2(K) + R_2(K) = 2r_1(K)$ that has a smaller inradius than H_{τ^*}. We know from Lemma 2.6 that such a set K must have concentric in- and circumsphere. Now we should have another look at Figure 6.12. Suppose K and H_{τ^*} have the point A as a common point on the circumcircle. Because K has smaller inradius than H_{τ^*} it also has a smaller diameter and hence the other points of K on the circumcircle must lie above the circular arc through B and C. Call them B' and C'. But we also need a pair of antipodal points D and $-D$ on the incircle of K such that the tangents through D and $-D$ also support K. This means there cannot be a point in K separated by such a tangent from 0. But wherever one places D, the tangents through them separate one of the points A, B' or C' from the origin.

Hence the dashed lines in Figure 6.15 cannot represent the boundaries of $f(\mathcal{C}_1^2)$, but the proper part of the boundary is uncertain. The problem seems to be that there is no such 'smooth transition' from H_{τ^*} to $BT_{\arcsin(\frac{3}{4})}$, as between other pairs of vertices that we consider soon.

Nevertheless, the fact that nothing can be beyond H_{τ^*} on the line from $\mathbb{B}$ proves that its image is an extreme point of $f(\mathcal{C}_1^2)$ (as it is an end point of a polytopal edge).

To verify that $BT_{\arcsin(\frac{3}{4})}$ is an extreme point one has to show that the boundary between $BT_{\arcsin(\frac{3}{4})}$ and H_{τ^*} runs above the linear extension of the bow from L to $BT_{\arcsin(\frac{3}{4})}$.

Finally, because of the star shapedness with respect to $\mathbb{B}$ there exist sets in $\mathcal{C}_1^2$ which are mapped to any point between the boundaries of the $(x = y)$-diagram.

3.3. The facet f5 and the $(z \leq 1)$-inequality. f5 is the facet Qhull computed to contain the images of L, $\mathbb{B}$, and $RSB_{\frac{\pi}{4}}$. We can easily see that this facet is induced by the inequality $z \leq 1$ and contains $I_{\frac{\pi}{2}}$. Clearly, the inequality is valid for $f(\mathcal{C}_1^2)$ (we already used its validity in the previous subsection to describe the segment between L and $\mathbb{B}$ in the $(x = y)$-diagram). See Figure 6.16 for a sketch of the image of $\mathcal{C}_1^2$ which is part of the $(z = 1)$-face.
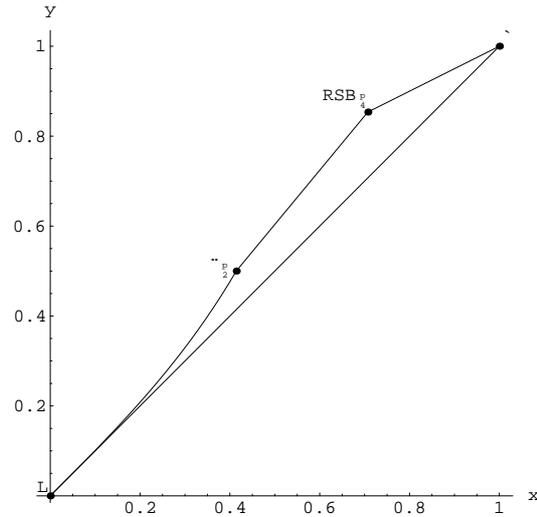
FIGURE 6.16. The face of $f(\mathcal{C}_1^2)$ induced by the inequality $z \leq 1$, projected onto the (x, y)-plane.

We can use once more the Minkowski sums of $\mathbb{B}$ and L, or $\mathbb{B}$ and $RSB_{\frac{\pi}{4}}$ to see that there are sets which are mapped on the segments incident with $\mathbb{B}$. That these segments represent the real boundary of $f(\mathcal{C}_1^2)$ follows immediately from Subsection 3.2 in case of $[f(\mathbb{B}), f(L)]$. The segment between $\mathbb{B}$ and $RSB_{\frac{\pi}{4}}$ is

induced by the valid inequality $y \le \frac{x+1}{2}$ (see Proposition 2.5). Hence we know immediately that this segment is also part of the boundary of the $(z = 1)$-face.

All right-angled sailing boats RSB_α have diameter 2 and if $\alpha \le \frac{\pi}{4}$, also constant (r_2, R_1)-ratio, because the radii are the same as those of a right-angled isosceles triangle with circumradius greater than 1. Hence they are mapped onto the line segment between $I_{\frac{\pi}{2}}$ and $RSB_{\frac{\pi}{4}}$, which is described by $y = \left(\frac{1}{2} + \sqrt{\frac{1}{2}} \right) x$. The bow between L and $I_{\frac{\pi}{2}}$ is a plot of the equality $y = \frac{x}{1-x^2}$. If $\gamma \ge \frac{\pi}{2}$ and $\alpha = \frac{\pi - \gamma}{2}$ the width of an isosceles triangle I_γ is $\tan(\alpha)$ and the inradius is $\tan(\frac{\alpha}{2})$ (see Figure 6.17).
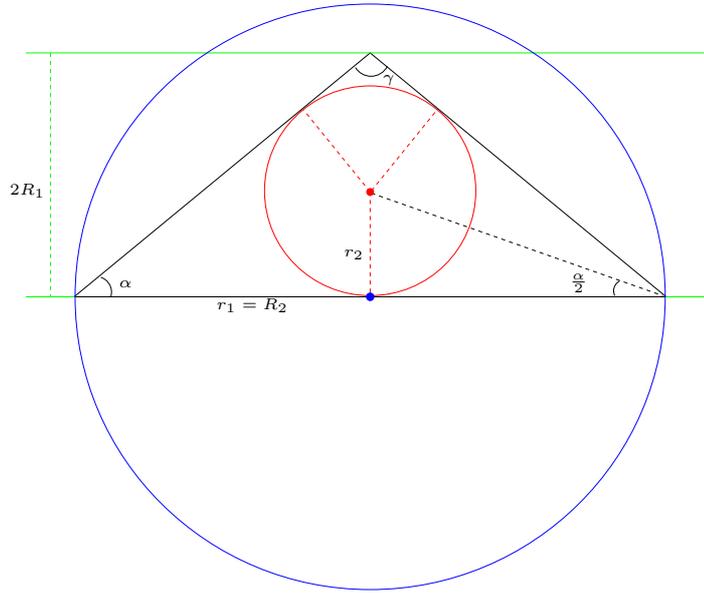
FIGURE 6.17. An isosceles triangle I_γ, with $\gamma \ge \frac{\pi}{2}$.

Hence $y = \frac{1}{2} \tan(2 \arctan(x)) = \frac{x}{1-x^2}$, for all isosceles triangles I_γ with $\gamma \ge \frac{\pi}{2}$ and therefore they are mapped onto the indicated bow. That the I_γ-bow and the RSB_α-line describe the upper boundary of the $(z = 1)$-face, we want to state as a theorem:

THEOREM 6.9. *For any $K \in \mathcal{C}_1^2$ with $r_1(K) = 1$ and $r_2(K) \le \sqrt{\frac{1}{2}}$*

$$R_1(K) \le \begin{cases} \frac{r_2(K)}{1 - r_2(K)^2}, & \text{if } r_2(K) \le \sqrt{2} - 1 \\ \left(\frac{1}{2} + \sqrt{\frac{1}{2}} \right) r_2(K), & \text{if } r_2(K) \ge \sqrt{2} - 1. \end{cases}$$

PROOF. We have already seen that the isosceles triangles I_γ, with $\gamma \in [\frac{\pi}{2}, \pi]$ fulfill the upper part, and the right-angled sailing boats RSB_α, with $\alpha \in [0, \frac{\pi}{4}]$ the lower part of the inequality with equality. Hence it suffices to show the following: For all $K_\omega \in \mathcal{C}_1^2$ with $r_1(K_\omega) = 1$ and $r_2(K_\omega) = \omega$, $\omega \leq \sqrt{\frac{1}{2}}$, it holds that

$$R_1(K_\omega) \leq R_1(I_\gamma), \text{ if } \omega \leq \sqrt{2} - 1$$

or

$$R_1(K_\omega) \leq R_1(RSB_\alpha), \text{ if } \omega \geq \sqrt{2} - 1,$$

where γ or α are chosen such that $r_2(I_\gamma) = \omega$ or $r_2(RSB_\alpha) = \omega$, as the case may be.

We split the proof into two parts. In the first part we will construct a set $K'_{\omega,M} \in \mathcal{C}_1^2$, $r_1(K'_{\omega,M}) = 1$ of maximal width for any fixed position M of the incentre. In the second part we will show that the width of $K'_{\omega,M}$ is maximised if M is situated on the perpendicular bisector of the diametrical chord. From this we finally obtain that argmax $R_1(K'_{\omega,M})$ is I_γ or RSB_α, respectively.

Let $K_{\omega,M} \in \mathcal{C}_1^2$ with $r_1(K_{\omega,M}) = 1$, let A and B be the antipodal points in $K_{\omega,M} \cap \mathbb{S}$ and suppose (wlog) that the centre M of the incircle $M + r_2(K_{\omega,M})\mathbb{B}$ lies in the positive quadrant (see Figures 6.18 and 6.19). Obviously, $K_{\omega,M} \supseteq$ conv$(AB, M + r_2(K)\mathbb{B})$ (therefore $K_{\omega,M}$ contains at least the red bordered area in Figures 6.18 and 6.19). Let $C, D, E,$ and F be those points on the incircle, C, D in the upper halfspace and E, F in the lower, for which the lines AC, BD, AE, and BF are tangents to the incircle. It is well known that there exist at least three supporting lines l_1, l_2, l_3 of $K_{\omega,M}$ which are tangents to the inball if $R_1(K_{\omega,M}) > r_2(K_{\omega,M})$. But since $K_{\omega,M}$ contains conv$\{AB, M + \omega\mathbb{B}\}$, the touching points of the l_i, $i = 1, 2, 3$ must be situated between C and D in the upper halfspace or between E and F in the lower, with at least one on each circular arc.

Case (a): Assume that only one of the supporting lines, say l_1, touches the inball somewhere between E and F. In this case, $2R_1(K_{\omega,M})$ is less than or equal to the maximal distance of any point in $K_{\omega,M}$ to l_1. However, this distance itself is maximised if $l_2 = AC$ and $l_3 = BD$. Hence $R_1(K_{\omega,M}) \leq b_s(K_{\omega,M}) \leq b_s(K'_{\omega,M})$, where b_s denotes the s-breadth in direction of s orthogonally to l_1 and $K'_{\omega,M}$ is
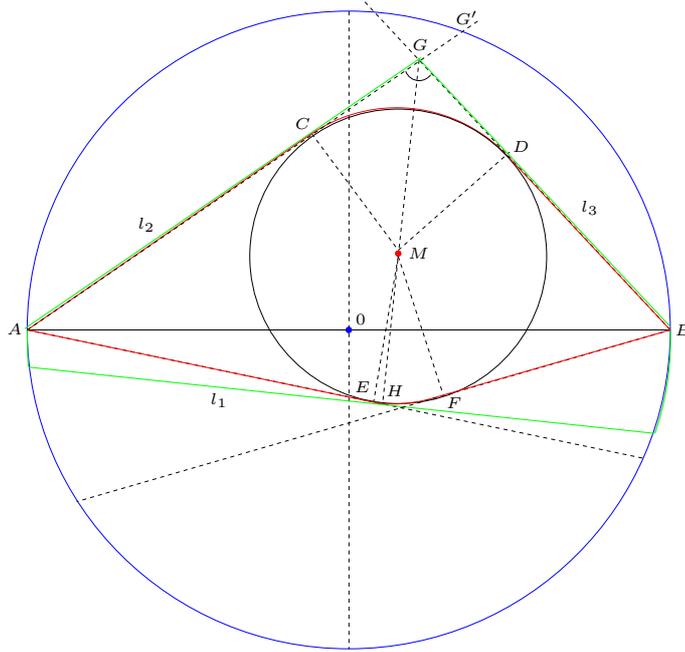
FIGURE 6.18.   The first possible configuration of sets with diam-
eter 2 and given incircle. The red bordered area shows the minimal
set with $r_1 = 1$ and given incircle; the green one the maximal, if
additionally l_1 is fixed as the lower tangent. Here l_2 and l_3 intersect
each other within the circumcircle.

the intersection of the triangle formed by the lines l_1, l_2 and l_3 with $\mathbb{B}$ (indicated
by the green line in Figure 6.18 and 6.19).

Case (b): Now, assume there is only one tangent supporting $K_{\omega,M}$ between
C and D. With the same arguments as above we obtain an upper bound on the
width of $K_{\omega,M}$ by taking E and F as the two other tangent points. But since M
lies in the upper halfspace, it is easy to see that the distance between E and F is
smaller than that between C and D. Hence we cannot achieve an upper bound
as large as in the case where only one tangent touches the inball between E and
F.

Since in the extreme cases (I_γ and RSB_α) the width will be attained in
direction s orthogonally to l_1, it suffices to concentrate on the sets $K'_{\omega,M}$ rather
than on all possible $K_{\omega,M}$. In the remaining part of the proof we want to elaborate
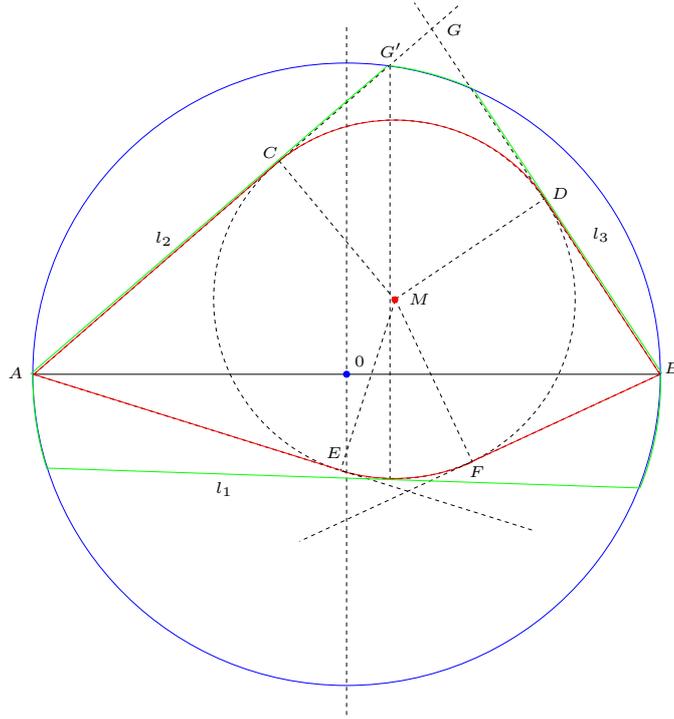
FIGURE 6.19. The second configuration of sets with diameter 2 and given incircle. Here l_2 and l_3 intersect each other outside the circumcircle.

where M should be situated such that the distance of any point in $K'_{\omega,M}$ from l_1 is maximised and that the width of $K'_{\omega,M}$ is indeed attained in this direction (at least in the extreme cases). Note that, if we move M we also have to move the tangent l_1.

Let G be the intersection point of l_2 and l_3 and G' the intersection point of l_2 and $\mathbb{S}$. Obviously, if G belongs to $\mathbb{B}$, then G is the point of $K'_{\omega,M}$ furthest away from l_1 and if not, G' is the furthest (with $G = G'$ if $G \in \mathbb{S}$).

Assume $G \in (\mathbb{E}^2 \setminus \mathbb{B}) \cup \mathbb{S}$. Hence G' is the point furthest away from l_1. Now it is easy to see that if $G' \neq G$ we can increase this distance by moving the inball along l_2 downwards until $G = G'$ and keeping l_1 as a tangent to the inball, parallel to its prior position. Hence we can assume that $G = G'$ in this case.

Now, suppose $G \in \mathbb{B}$. Let H be the point between E and F on the intersection of the incircle and the line GM. Since the circle around G with the distance between G and H as its radius intersects l_1 twice, if it does not touch the inball

at the point H, we see that the distance between G and l_1 is always maximal if l_1 passes through H.

Let therefore l_1 touch the inball at H. We can increase the distance between G and H by moving M such that the angle between l_2 and l_3 at G decreases, reaching its minimum if G either lies on the sphere or l_1 goes through A or B (which is the case if $H = E$ or $H = F$).

In the first case, the distance between G and H does not depend on the position of G on the circumsphere, so we can choose it to be on the perpendicular to AB and therefore we obtain $R_1(K'_{\omega,M}) \leq R_1(RSB_\alpha)$ with α such that $r_2(RSB_\alpha) = \omega$.

In the latter case we are able to move the inball such that G lies on the perpendicular to AB by keeping the angle at G constant and therefore also the distance between G and H. But now it is easy to see that we can increase this distance once more, by moving M upwards, until $l_1 = AB$. Hence we obtain $R_1(K'_{\omega,M}) \leq R_1(I_\gamma)$ where γ is the angle at G.

$\square$

From Theorem 6.9 we obtain the extremity of $RSB_{\frac{\pi}{4}}$ and $I_{\frac{\pi}{2}}$ since both are, like H_{τ^*}, end points of polytopal edges of $f(\mathcal{C}_1^2)$.

Again it follows from the star shapedness of $f(\mathcal{C}_1^2)$ with respect to $\mathbb{B}$ that the $(z = 1)$-face covers the whole region between the boundaries.

3.4. The facet f7/f12 and the $(x + 1 \geq 2y)$-inequality. As mentioned in the description of Figure 6.14 showing the vertex-facet-dependencies in the Qhull results, the facets f7 and f12 are essentially induced by the same inequality $x + 1 \geq 2y$, which we know from Proposition 2.5 to be valid for $f(\mathcal{C}_1^2)$. Figure 6.20 displays the true boundaries of the face.

It was already shown in Subsections 3.2 and 3.3 that the two segments incident with $\mathbb{B}$ are part of the boundary structure of $f(\mathcal{C}_1^2)$; and it was stated as a remark after Proposition 2.3 that Jung's inequality is fulfilled with equality for a set K iff $T^2 \subseteq K \subseteq RT$, as RT is the unique completion of T^2 in $\mathbb{E}^2$. Since the Yamanouti sets are all mapped onto this line, the segment $[T^2, RT]$ is part of the real boundary, too. So we are left with the bow between T^2 and $RSB_{\frac{\pi}{4}}$. In this case we need to describe a new collection of sets which are mapped onto that

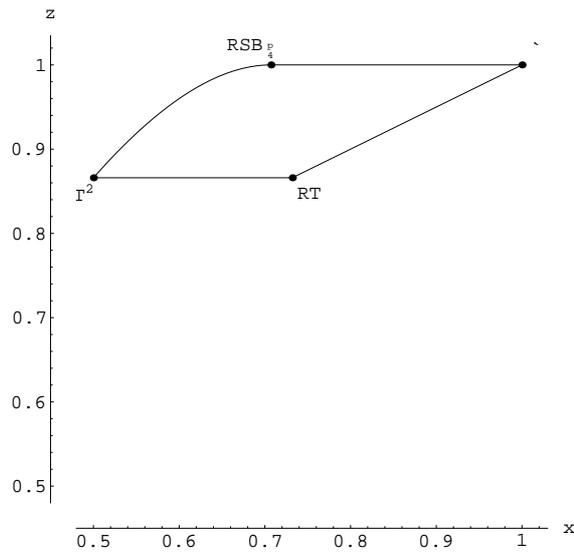FIGURE 6.20.   The face of $f(\mathcal{C}_1^2)$ induced by the inequality $x+1 \geq 2y$, projected onto the (x, z)-plane.

bow. We call them *concentric sailing boats*, or CSB_γ for short, with $\gamma \in \left[\frac{\pi}{3}, \frac{\pi}{2}\right]$, and they are constructed as follows (see Figure 6.21):
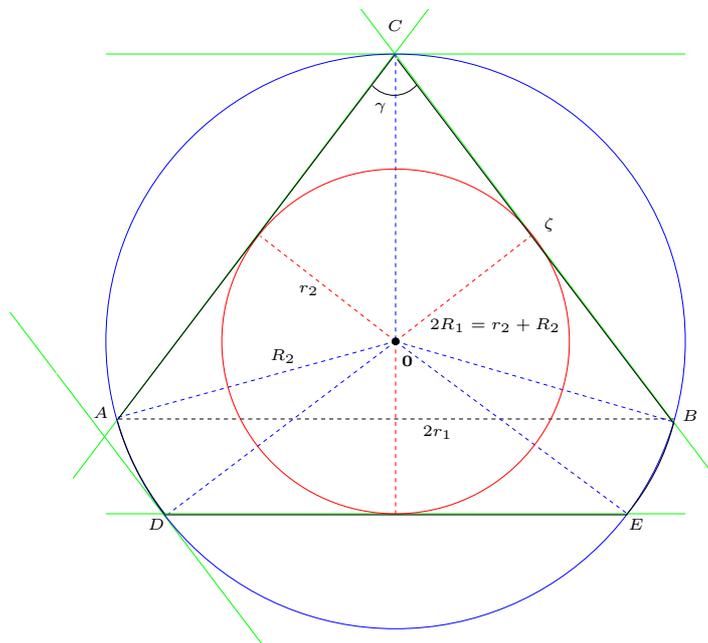
FIGURE 6.21.   A concentric sailing boat CSB_γ with $\gamma \in \left(\frac{\pi}{3}, \frac{\pi}{2}\right)$.

We start with an isosceles triangle I_γ and its circumcircle. Then we draw a circle with centre 0, such that the two equilateral sides of I_γ are tangents to this circle. The construction is completed with an additional tangent l to the circle parallel to the third side of I_γ. Call the points where l intersects the circumcircle as D and E, and the set obtained from extending I_γ along the circumcircle, such that the segment between D and E is the lower boundary of the set, as CSB_γ.

It is obvious that $CSB_{\frac{\pi}{3}} = T^2$ and $CSB_{\frac{\pi}{2}} = RSB_{\frac{\pi}{4}}$, and it is not difficult to see that $r_2(CSB_\gamma) = \sin(\frac{\gamma}{2})R_2(CSB_\gamma)$ and that $r_2(CSB_\gamma) + R_2(CSB_\gamma) = 2R_1(CSB_\gamma)$. For the diameter, $r_1(CSB_\gamma) = \sin(\frac{\gamma}{2})\zeta$ holds, where ζ is the length of one of the equilateral sides of the isosceles triangle we used to construct the sailing boat. Since $\zeta = 2\cos(\frac{\gamma}{2})R_2(CSB_\gamma)$ we can conclude that, if the circumradius is 1 then

$$f(CSB_\gamma) = \left(\sin\left(\frac{\gamma}{2}\right), \frac{\sin\left(\frac{\gamma}{2}\right) + 1}{2}, 2\sin\left(\frac{\gamma}{2}\right)\cos\left(\frac{\gamma}{2}\right) \right).$$

Hence the concentric sailing boats are mapped onto the $(x + 1 = 2y)$-face and here in particular on the bow induced by the equation $z = x\sqrt{1 - x^2}$.

We still need to show that the concentric sailing boats describe the upper-left boundary of the $(x + 1 = 2y)$-face.

THEOREM 6.10. *For any $K \in \mathcal{C}_1^2$ with $r_2(K) + 1 = 2R_1(K)$ and $r_2(K) \leq \sqrt{\frac{1}{2}}$, it holds that*

$$r_1(K) \leq r_2(K)\sqrt{1 - r_2(K)^2}.$$

PROOF. It was shown in Lemma 2.6 that every set $K \in \mathcal{C}_1^2$ which is mapped onto the $(x + 1 = 2y)$-face must have concentric in- and circumsphere. Now suppose K has the same incircle as CSB_γ and C as a common point on the circumsphere. Hence there can neither be a point in K below the line DE nor, because of convexity, above the lines AC or BC within the lower half of the circumcircle, since otherwise K would have a greater incircle than CSB_γ. Hence K cannot contain a line-segment which is longer than the distance of A and B. But this means $r_1(K) \leq r_1(CSB_\gamma)$. $\square$

The convexity of the $(x + 1 = 2y)$-face shows that in fact all concentric sailing boats are extreme points of $f(\mathcal{C}_1^2)$.

That there exist planar sets which are mapped onto every point between the drawn boundaries of the $(x + 1 = 2y)$-face follows once again from the star shapedness of $f(\mathcal{C}_1^2)$.

3.5. The facet f14/f17 and the $(x + 1 \leq 2z)$-inequality. Similarly to the pair f7/f12, the pair f14/f17 is also identified by Qhull as two distinct facets because of the approximate input values. We already stated earlier that the sets $\mathbb{B}, RT, SR_{\arcsin(\sqrt{3}-1)}$, and H_{τ^*} are mapped onto the plane induced by the inequality $x + 1 \leq z$, which is valid for the image of $\mathcal{C}_1^2$ as shown in Proposition 2.5. A plot of the known boundaries of this face is given in Figure 6.22.
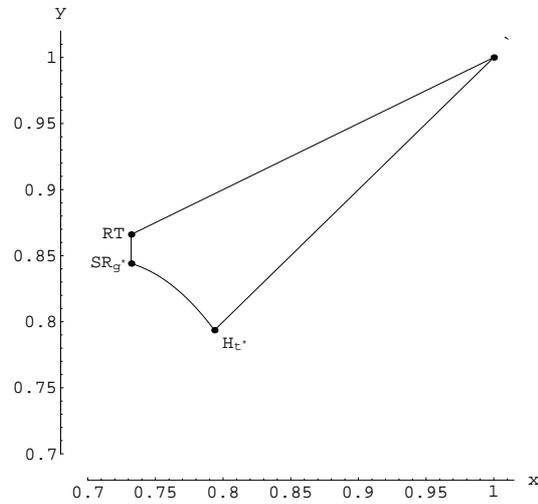
FIGURE 6.22.   The face of $f(\mathcal{C}_1^2)$ induced by the inequality $x + 1 \leq 2z$, projected onto the (x, y)-plane. Here $\gamma^* = \arcsin(\sqrt{3} - 1)$.

The line segments $[\mathbb{B}, H_{\tau*}]$ and $[\mathbb{B}, RT]$ were already treated in Subsection 3.2 and 3.4, respectively, and we know from Proposition 2.3 that every set in $\mathcal{C}_1^2$ has a z-coordinate of at least $\frac{\sqrt{3}}{2}$. As all the sets SR_γ with $\gamma \geq \arcsin(\sqrt{3} - 1)$ differ from RT only in their width, they are of course mapped onto the line segment $[SR_{\arcsin(\sqrt{3}-1)}, RT]$. On the other hand there is no subset of RT in $\mathcal{C}_1^2$ that has the same diameter and inradius as RT and smaller width than $SR_{\arcsin(\sqrt{3}-1)}$, and therefore there cannot be a set in $\mathcal{C}_1^2$ that is mapped beyond $f(SR_{\arcsin(\sqrt{3}-1)})$ on that boundary of the $(x + 1 = 2z)$-face.

Hence the only remaining part of the boundary is the one between $H_{\tau*}$ and $SR_{\arcsin(\sqrt{3}-1)}$, which we will see to be achieved by the general hoods H_τ, $\tau \in [\sqrt{3} - 1, \tau^*]$ (see Figure 6.23 and the definition in Subsection 3.1).

FIGURE 6.23.　A general hood set and its radii.

As in the preceding subsections we first compute an equation involving the two radii r_2 and R_1 which holds for the images of all hood sets. Therefore have a look at Figure 6.23. Let l_1 be the H_τ supporting line through B, l_2 the perpendicular onto l_1 through the centre, and l_3 the line parallel to l_2 through C. We denote by 2ξ the distance between the two lower points B and C, by η the distance from B to l_3, by ζ the distance between l_2 and l_3, and finally by φ the distance between the line BC and the centre. Now it is easy to see that the following equations hold (where we drop the H_τ for better readability):

  (i)　$2r_1 = r_2 + R_2$,

 (ii)　$\eta^2 = 4\xi^2 - 4R_1^2$,

(iii)　$\zeta^2 = R_2^2 - (2R_1 - r_2)^2$,

(iv)　$\xi^2 = R_2^2 - \varphi^2$,

 (v)　$(\varphi + R_2)^2 = 4r_1^2 - \xi^2$, and

(vi) $(\eta + \zeta)^2 = R_2^2 - r_2^2$.

If we use the result in (iv) for ξ and insert it into (v) we get

$$(\varphi + R_2(H_\tau))^2 = 4r_1(H_\tau)^2 - 4(R_2(H_\tau)^2 - \varphi^2),$$

which can be simplified to

$$\varphi = \frac{2r_1^2 - R_2^2}{R_2}.$$

Now we insert both results for ξ and φ into (ii) and obtain

$$\eta^2 = 4\left(R_2^2 - R_1^2 - \left(\frac{2r_1^2 - R_2^2}{R_2}\right)^2\right),$$

which can be reduced to

$$\eta^2 = 16r_1^2 - 16\frac{r_1^4}{R_2^2} - 4R_1^2.$$

But from (i) we know that $4r_1^2 = (r_2 + R_2)^2$ and therefore that

$$\eta^2 = 4(r_2 + R_2)^2 - \frac{(r_2 + R_2)^4}{R_2^2} - 4R_1^2.$$

Using the above formula for η, (iii) for ζ, and that $R_2 = 1$ we finally get the following equation for the relation between the inradius and the width of the hood sets:

$$\left(\left(4(r_2 + 1)^2 - (r_2 + 1)^4 - 4R_1^2\right)^{\frac{1}{2}} + \left(1 - (2R_1 - r_2)^2\right)^{\frac{1}{2}}\right)^2 = 1 - r_2^2.$$

THEOREM 6.11. *For any $K \in \mathcal{C}_1^2$ with $r_2(K) + 1 = 2r_1(K)$ and $r_2(K) \leq \tau^*$,*

$$\left(\left(4(r_2(K) + 1)^2 - (r_2(K) + 1)^4 - 4R_1(K)^2\right)^{\frac{1}{2}}\right.$$

$$\left. + \left(1 - (2R_1(K) - r_2(K))^2\right)^{\frac{1}{2}}\right)^2$$

$$\leq 1 - r_2(K)^2.$$

PROOF. By Lemma 2.6, any $K \in \mathcal{C}_1^2$ with $r_2(K) + 1 = 2r_1(K)$ must have concentric in- and circumcircles. Now assume that $r_2(K) = r_2(H_\tau)$ and that both possess A as a common point on the circumcircle. Hence there can exist no point in K below the circular arc of radius $r_2(K) + R_2(K)$ with centre A. However, H_τ has the same radii like the convex hull of its own incircle and the points A, B, C. Hence K could only have less or equal width if there would be no point on the left of C or on the right of B on its circumcircle, and to have strictly

lower width, even one of B and C could not belong to K. But as we have seen, no point can be situated below B and C on the circumcircle. Thus, K would not have three points on the circumcircle whose convex hull contains the centre, which is a contradiction. Hence $R_1(K) \geq R_1(H_\tau)$, and it is easy to see that the left side of the hood sets equation decreases for constant r_2 and growing R_1, but that the right side remains constant. This proves the theorem. $\qquad\square$

Since $SR_{\arcsin(\sqrt{3}-1)}$ is the lower end point of the left boundary segment we obtain its extremity in $f(\mathcal{C}_1^2)$.

Finally, from the fact that $\mathbb{B}$ is mapped onto this face, it follows immediately that there exist $K \in \mathcal{C}_1^2$ which are mapped on every point within these boundaries.

3.6. The facet f13 and the $\left(z \geq \frac{\sqrt{3}}{2}\right)$-inequality. f13 is the only facet Qhull identified as a non-simplicial facet. The reason is that we have chosen the same approximation for all four extreme points in our list with z-coordinate as $\frac{\sqrt{3}}{2}$, which is the least possible value because of Jung's theorem (see Proposition 2.3 (i)). We also mentioned in the preceding subsections that all sets in $\mathcal{C}_1^2$ which are mapped onto this face must be sandwiched between T^2 and RT. Figure 6.24 shows the face boundary.
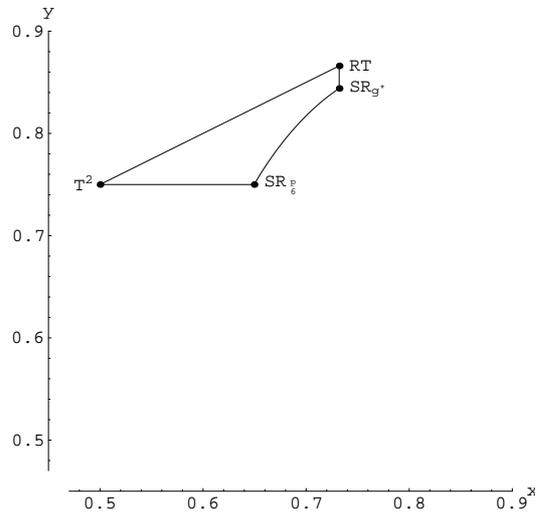

FIGURE 6.24.   The face of $f(\mathcal{C}_1^2)$ induced by the inequality $z \geq \frac{\sqrt{3}}{2}$. Again, $\gamma^* = \arcsin(\sqrt{3}-1)$

We already know from Subsections 3.4 and 3.5 that the two line segments incident with RT are part of the real boundary of $f(\mathcal{C}_1^2)$, and as every set mapped onto this facet is a superset of T^2, no set in $\mathcal{C}_1^2$ can be mapped below the line through T^2 and $SR_{\frac{\pi}{6}}$. But now it is easy to see that it is not possible to extend the inball radius beyond that of $SR_{\frac{\pi}{6}}$ without raising the diameter or at least the width. Hence $SR_{\frac{\pi}{6}}$ is the other end point of the lower boundary and therefore an extreme point of $f(\mathcal{C}_1^2)$. The part of the boundary which is left is the one between $SR_{\frac{\pi}{6}}$ and $SR_{\arcsin(\sqrt{3}-1)}$. For that purpose we consider the general sliced Reuleaux triangles (see Figure 6.25).
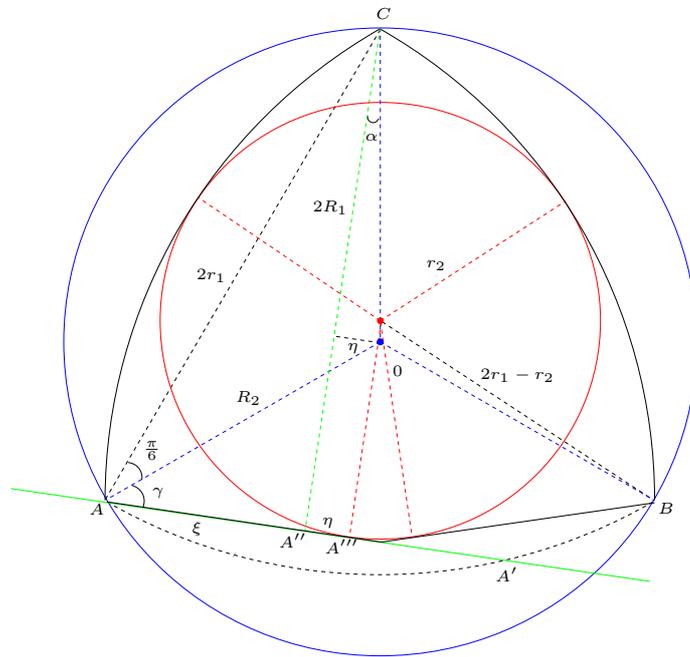
FIGURE 6.25. A general sliced Reuleaux triangle SR_γ, with $\gamma \in \left[\frac{\pi}{6}, \arcsin(\sqrt{3}-1)\right]$.

We use the notations as in the description of the sliced Reuleaux triangles in Subsection 3.1. Additionally, let A'' be the foot point of the perpendicular line from C onto AA', and A''' the point where the incircle touches AA'. Moreover we denote the distance between A and A'' by ξ and the distance between A'' and A''' by η.

It is easy to see that

(2)
$$\xi = 2\cos\left(\gamma + \frac{\pi}{6}\right)r_1$$

and

(3)
$$\eta = \sin(\alpha)R_2 = \sin\left(\gamma - \frac{\pi}{6}\right)R_2$$

where α denotes the angle between the lines CA'' and $C0$. Now, the inradius can be brought in by the equation

$$(\xi + \eta)^2 + r_2^2 = (2r_1 - r_2)^2.$$

If we use formulas (2) and (3) for ξ and η, and that $R_2 = 1$ and therefore $r_1 = \frac{\sqrt{3}}{2}$, we obtain

$$
\begin{aligned}
\xi + \eta &= \sqrt{3}\cos\left(\gamma + \frac{\pi}{6}\right) + \sin\left(\gamma - \frac{\pi}{6}\right) \\
&= \left(\frac{3}{2}\cos(\gamma) - \frac{\sqrt{3}}{2}\sin(\gamma)\right) + \left(\frac{\sqrt{3}}{2}\sin(\gamma) - \frac{1}{2}\cos(\gamma)\right) \\
&= \cos(\gamma).
\end{aligned}
$$

This allows us to state γ as a function of the x-coordinate:

$$\gamma = \arccos(\xi + \eta) = \arccos\left(\sqrt{3 - 2\sqrt{3}x}\right)$$

and finally compute the y-coordinate from $R_1 = r_1 \sin(\gamma + \frac{\pi}{6})$ to obtain

$$y = \frac{\sqrt{3}}{2}\sin\left(\arccos\left(\sqrt{3 - 2\sqrt{3}x}\right) + \frac{\pi}{6}\right).$$

Hence all sliced Reuleaux triangles SR_γ in $\mathcal{C}_1^2$, with $\gamma \in [\frac{\pi}{6}, \arcsin(\sqrt{3} - 1)]$ are mapped onto a bow defined by the above equation.

THEOREM 6.12. *For any $K \in \mathcal{C}_1^2$ with $r_1(K) = \frac{\sqrt{3}}{2}$ and $r_2(K) \geq \frac{3\sqrt{3}}{8}$ it holds that*

$$R_1(K) \geq \frac{\sqrt{3}}{2}\sin\left(\arccos\left(\sqrt{3 - 2\sqrt{3}r_2(K)}\right) + \frac{\pi}{6}\right).$$

PROOF. The sliced Reuleaux triangles define the remaining part of the boundary of the $\left(z = \frac{\sqrt{3}}{2}\right)$-face, because one cannot extend T^2 beyond the circular arcs of radius $\sqrt{3}$ around the lower vertices, and therefore the sliced Reuleaux triangles

are the thinnest sets which contain an inball of a given radius in $\left[\frac{3\sqrt{3}}{8}, \sqrt{3} - 1\right]$. $\square$

From the fact that $SR_{\frac{\pi}{6}}$ is the end point of the lower boundary of the $\left(z = \frac{\sqrt{3}}{2}\right)$-face we have proved our candidate list of extreme points (only the extremity of $BT_{\arcsin(\frac{3}{4})}$ remains open).

Now we draw a vertical line anywhere between the boundaries of the $\left(z = \frac{\sqrt{3}}{2}\right)$-face for any fixed r_2-value between $\frac{1}{2}$ and $\sqrt{3} - 1$. We know from the preceding subsections that there exists a Yamanouti set Y_ω at the upper end of that line (where it hits the segment between T^2 and RT); and the set on the lower end is either the convex hull of T^2 and an incircle of the appropriate size, which touches the lower line of T^2, or it is a sliced Reuleaux triangle. But now it is not difficult to see that, if one moves the incircle from the position it has in the Yamanouti set towards the position it has in the set on the lower end of the vertical line and takes K again as the convex hull of this incircle and T^2, we can reach every point on the line segment by this construction. Hence there exist sets in $\mathcal{C}_1^2$ which are mapped onto p for every point p between the boundaries of the $\left(z = \frac{\sqrt{3}}{2}\right)$-face.

3.7. The facet f8 and the $(y^2 - 4(1 - z^2)z^4 \geq 0)$-inequality. We already used the validity of the inequality

$$y^2 - 4(1 - z^2)z^4 \geq 0$$

in Subsection 3.2 to show that the bow between L and $BT_{\arcsin(\frac{3}{4})}$ is a boundary of the $(x = y)$-face. But because T^2 and $SR_{\frac{\pi}{6}}$ fulfill this inequality with equality as well, we see that the facet f8, which Qhull computed as the convex hull of L, T^2, and $SR_{\frac{\pi}{6}}$ is essentially a 2-dimensional non-linear boundary, induced by the above inequality. It was also mentioned in Subsection 3.2 that a set $K \in \mathcal{C}_1^2$ is mapped onto this boundary iff it is a superset of an isosceles triangle I_γ, with $\gamma \leq \frac{\pi}{3}$, and K differs from I_γ only in its inradius. See Figure 6.26 for a projection of the whole part of the surface of $f(\mathcal{C}_1^2)$ induced by the inequality $y^2 - 4(1 - z^2)z^4 \geq 0$ onto the (x, y)-plane.

It is immediately clear that the left boundary of the figure is described by the isosceles triangles I_γ, $\gamma \leq \frac{\pi}{3}$ themselves, which are mapped onto the bow $2(2x - y)(y - x) = x^3$ (see [20]). The upper bound is induced by the extensions
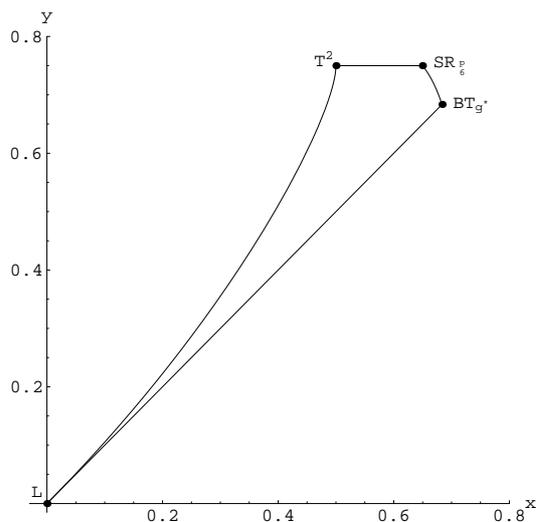
FIGURE 6.26.   The surface of $f(\mathcal{C}_1^2)$, which is induced by the inequality $y^2 - 4(1 - z^2)z^4 \geq 0$; projected onto the (x, y)-plane. Here, we again use $\gamma^* = \arcsin(\frac{3}{4})$.

of T^2, which keep the same width and diameter as T^2, since T^2 is the isosceles triangle with the biggest width.

The boundary on the lower right side of Figure 6.26 is described by the bent trapezoids BT_γ, $\gamma \leq \arcsin(\frac{3}{4})$, because of the validity of $x \leq y$. But as the bent trapezoids leave the line $x = y$ if $\gamma > \arcsin(\frac{3}{4})$ we need to show that they still describe the boundary between $BT_{\arcsin(\frac{3}{4})}$ and $SR_{\frac{\pi}{6}}$.

To do so, we first compute the points where they are mapped in the (x, y)-plane. Since $R_1(BT_\gamma) = \sin(\gamma)r_1(BT_\gamma)$ and $r_1(BT_\gamma) = \cos(\gamma)R_2(BT_\gamma)$ for all bent trapezoids; and because $r_2(BT_\gamma) = \frac{3}{4}r_1(BT_\gamma)$ if $\gamma \geq \arcsin(\frac{3}{4})$, we get that the images of the bent trapezoids BT_γ, with $\gamma \geq \arcsin(\frac{3}{4})$, all fulfill the equation $y = \frac{4}{3}\sin(2\arccos(\frac{4}{3}x))x$.

THEOREM 6.13. *For any $K \in \mathcal{C}_1^2$ for which*

$$R_1(K)^2 - 4r_1(K)^4(1 - r_1(K)^2) = 0$$

and that has inradius $r_2(K) \geq \frac{3\sqrt{3}}{8}$, it holds that

$$R_1(K) \leq \frac{4}{3}\sin\left(2\arccos\left(\frac{4}{3}r_2(K)\right)\right)r_2(K).$$

PROOF. Even if we take the bent trapezoids with $\gamma \geq \arcsin(\frac{3}{4})$, they are mapped onto the boundary as we cannot extend any isosceles triangle I_γ, $\gamma \leq \frac{\pi}{3}$ beyond BT_γ without increasing its width or diameter. $\qquad\square$

Obviously, one can extend every isosceles triangle I_γ, $\gamma \leq \frac{\pi}{3}$ to reach any given inradius between the lower and the upper bounds of the diagram without raising the width or the diameter of the sets. Hence there exists a $K \in \mathcal{C}_1^2$ that is mapped onto (x, y) for all pairs (x, y) within the computed boundaries of this 2-dimensional non-linear part of the boundary.

3.8. The facet f6, the Δ- and the sailing boat inequality. In this subsection we will show that it is very likely that the three extreme points of f6 do not describe a single 2-dimensional boundary; instead, together with $I_{\frac{\pi}{2}}$ they describe two non-linear 2-dimensional parts of the surface of $f(\mathcal{C}_1^2)$. The first of them consists of the three extreme points L, T^2, and $I_{\frac{\pi}{2}}$, with all the isosceles triangles mapped onto the boundaries between them (see Figure 6.27).
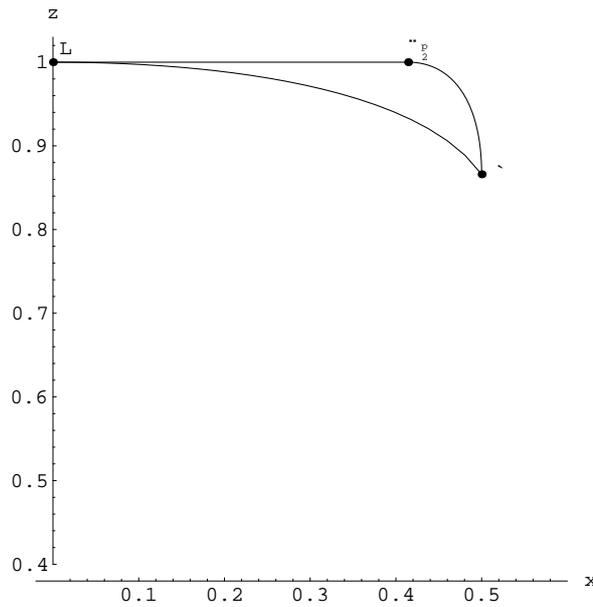

FIGURE 6.27. The non-linear plane, consisting of all triangles in $\mathcal{C}_1^2$, projected onto the (x, z)-plane.

These boundaries are described by the three equations

(i) $(2z^2 - x)^2(1 - z)^2 = x^2$, for $\gamma \leq \frac{\pi}{3}$,

(ii) $(z^2 + x^2 - 2x)^2 = 4(x^2 - 2x^3)$, for $\gamma \in [\frac{\pi}{3}, \frac{\pi}{2}]$, and

(iii) $z = 1$, for $\gamma \geq \frac{\pi}{2}$.

The first equation is taken from [**63**], the third is well known from the preceding subsections. It remains to show the validity of the second equation which holds for the isosceles triangles I_γ with $\gamma \in [\frac{\pi}{3}, \frac{\pi}{2}]$ (see Figure 6.28).
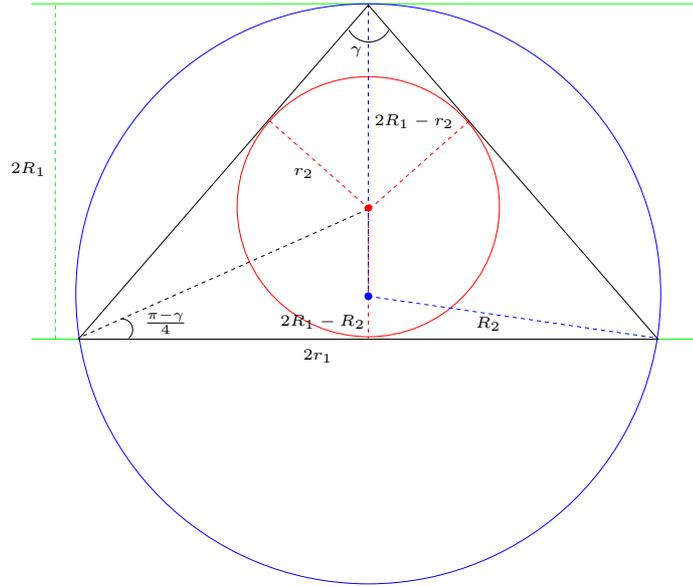
FIGURE 6.28. An isosceles triangle I_γ with $\gamma \in [\frac{\pi}{3}, \frac{\pi}{2}]$.

From $r_1^2 = R_2^2 - (2R_1 - R_2)^2$ we obtain that $z^2 = 4y - 4y^2$, and together with $\cot(\frac{\gamma}{2}) = \frac{2R_1}{r_1}$ this leads to $\cot^2(\frac{\gamma}{2}) = \frac{y}{1-y}$. Hence

$$y = \frac{\cot^2(\frac{\gamma}{2})}{1 + \cot^2(\frac{\gamma}{2})}.$$

But as $\cot^2(\alpha) = \frac{1}{\sin^2(\alpha)} - 1$ for any possible α, and since $\sin(\frac{\gamma}{2}) = \frac{x}{2y-x}$ the above can be simplified to

$$y = 1 - \sin^2\left(\frac{\gamma}{2}\right) = 1 - \frac{x^2}{(2y - x)^2},$$

which is equivalent to the polynomial equation $(2y - x)^2(1 - y) = x^2$. It is easy to verify that the three possible solutions for y in terms of x are 0, $\frac{1}{2}(1 - \sqrt{1 - 2x} + x)$, and $\frac{1}{2}(1 + \sqrt{1 - 2x} + x)$. However, since $\frac{1}{2}(1 + \sqrt{1 - 2x} + x) > \frac{x+1}{2}$ we obtain

$y = \frac{1}{2}(1 - \sqrt{1 - 2x} + x)$ as the only possible solution for the width of the isosceles triangles. Finally we obtain that

$$z^2 = 4y - 4y^2 = 1 - (\sqrt{1 - 2x} + x)^2 = 2x - x^2 + 2x\sqrt{1 - 2x}$$

and therefore the desired equation in (ii).

All triangles $\Delta \in f(\mathcal{C}_1^2)$ are mapped between the boundaries (i)-(iii) in the (x, z)-plane. To see this, suppose Δ is a general triangle with vertices A, B and C, and AB its longest side.

If C is not situated on the circumcircle of the triangle, we immediately have $r_1(\Delta) = R_2(\Delta) = 1$. Hence we can assume that C lies on the circumcircle. Now, we can move C along the circumcircle without affecting the diameter, as long as $|AC| \le |AB|$ and $|BC| \le |AB|$. Obviously, Δ has maximal inradius if C lies on the perpendicular bisector of AB, therefore $\Delta = I_\gamma$, $\gamma \in [\frac{\pi}{3}, \frac{\pi}{2}]$; and the minimal inradius is attained if AC or BC is of diametrical length, therefore $\Delta = I_\gamma$, $\gamma < \frac{\pi}{3}$.

In fact, all triangles are mapped onto a 2-dimensional region of $f(\mathcal{C}_1^2)$, which is induced by the following inequality:

$$\left((2y - x)^2(yz^2 - x^2y - xz^2) - x^2z^2(y - x) + 4x^2y^2(y - x)\right)^2$$
$$\ge 16x^4y^2(y - x)^2(1 - z^2)$$

Moreover, the inequality above (which we call the Δ-inequality) is valid for all the extreme points in our list. But before we discuss the latter fact, we should first prove that all triangles fulfill equality in the Δ-inequality.

LEMMA 6.14. *For every triangle Δ it holds that*

$$\left((2R_1(\Delta) - r_2(\Delta))^2(r_1(\Delta)^2R_1(\Delta) - r_2(\Delta)^2R_1(\Delta) - r_1(\Delta)^2r_2(\Delta))\right.$$
$$\left. - r_2(\Delta)^2r_1(\Delta)^2(R_1(\Delta) - r_2(\Delta)) + 4r_2(\Delta)^2R_1(\Delta)^2(R_1(\Delta) - r_2(\Delta))\right)^2$$
$$= 16r_2(\Delta)^4R_1(\Delta)^2(R_1(\Delta) - r_2(\Delta))^2(R_2(\Delta)^2 - r_1(\Delta)^2)$$

PROOF. We start by identifying the involved values (see Figure 6.29). For reading convenience, we drop the Δ from the radii, therefore writing r_1 instead of $r_1(\Delta)$, and analogously for all other radii.

Of course, the diameter $2r_1$ of any triangle is the length of its longest side a and its width $2R_1$ is the distance of the third vertex from a. Let η be the distance
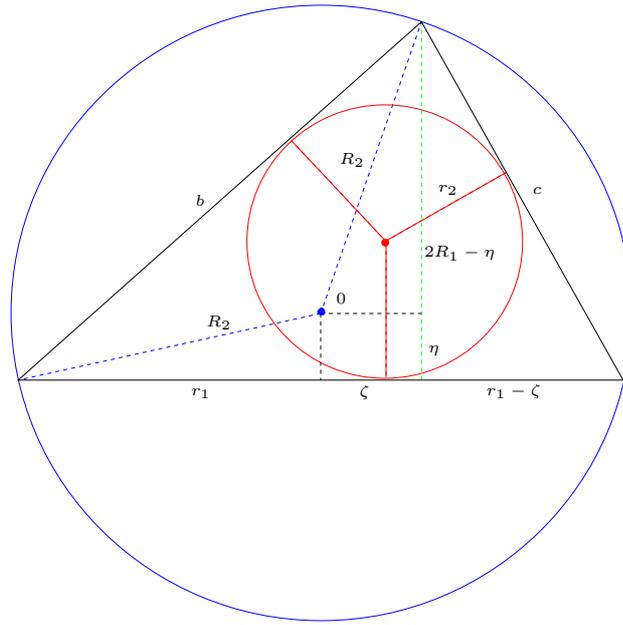
FIGURE 6.29. A general triangle.

of 0 from a and by ζ we indicate the distance between 0 and the perpendicular to a through the third vertex. Moreover we call the other two sides b and c. Now we can state the following equations:

(i) $\eta^2 + r_1^2 = R_2^2$,

(ii) $\zeta^2 + (2R_1 - \eta)^2 = R_2^2$,

(iii) $(r_1 + \zeta)^2 + 4R_1^2 = b^2$,

(iv) $(r_1 - \zeta)^2 + 4R_1^2 = c^2$,

(v) $\frac{1}{2}(2r_1 + b + c)r_2 = 2r_1 R_1$.

(i) to (iv) are just applications of the Pythagorean theorem for the involved right-angled triangles and we get (v) as both sides of the equation are formulas for the area of the triangle. It is easy to see that we can use (i) and (ii) to compute $\eta = \frac{\zeta^2 - r_1^2}{4R_1} + R_1$ and by reinserting η into (i) we get

$$(4) \qquad \left(\frac{\zeta^2 - r_1^2}{4R_1} + R_1\right)^2 + r_1^2 = R_2^2.$$

From (iii) and (iv) we obtain $b^2 - c^2 = 4r_1\zeta$ and (v) can be transformed to $b + c = \frac{4r_1 R_1}{r_2} - 2r_1$. If we divide these two equations, this leads to $b - c = \frac{b^2 - c^2}{b+c} = \frac{2r_2\zeta}{2R_1 - r_2}$

and by adding the equations for $b + c$ and $b - c$ we get

$$b = \frac{2r_1 R_1}{r_2} - r_1 + \frac{r_2 \zeta}{2R_1 - r_2}.$$

Inserting this result for b into (iii), we obtain

$$(r_1 + \zeta)^2 + 4R_1^2 = \left(\frac{2r_1 R_1}{r_2} - r_1 + \frac{r_2}{2R_1 - r_2} \zeta \right)^2$$

which can be simplified, as the linear ζ-terms vanish, to

$$\zeta^2 \left(1 - \frac{r_2^2}{(2R_1 - r_2)^2} \right) = \frac{4r_1^2 R_1^2}{r_2^2} - 4R_1^2 - \frac{4r_1^2 R_1}{r_2}.$$

The last equation can be used to express ζ by

$$(5) \qquad \zeta^2 = \frac{(2R_1 - r_2)^2 (r_1^2 R_1 - r_2^2 R_1 - r_1^2 r_2)}{r_2^2 (R_1 - r_2)}.$$

Finally, one gets the claimed equality by inserting (5) into (4). $\qquad \square$

By filling in the coordinates of the planar sets in our extreme point list, it turns out that the Δ-inequality is valid for all of them. This and the fact that every set K in $\mathcal{C}_1^2$ has an inscribed triangle (maybe degenerated to L) of same circumradius, leads us to the following conjecture:

CONJECTURE 6.15. *The Δ-inequality is valid for $\mathcal{C}_1^2$.*

Now we turn to the second part of the diagram surface which we conjecture to be included in f6: It has the extreme points $T^2, I_{\frac{\pi}{2}}$, and $RSB_{\frac{\pi}{4}}$. The two boundaries between T^2 and $RSB_{\frac{\pi}{4}}$, and between $I_{\frac{\pi}{2}}$ and $RSB_{\frac{\pi}{4}}$ are achieved by the concentric sailing boats CSB_γ, $\gamma \in [\frac{\pi}{3}, \frac{\pi}{2}]$ and the right-angled sailing boats RSB_α, $\alpha \in [0, \frac{\pi}{4}]$, respectively. This motivates us to define a general sailing boat (see Figure 6.30).

To construct such a sailing boat SB, we start with an isosceles triangle I_γ, $\gamma \in [\frac{\pi}{3}, \frac{\pi}{2}]$ with vertices A, B, C, where C is the vertex incident with the two equilateral sides. Afterwards, we extend it along its circumcircle from A to D and from B to E such that DE is parallel to AB and the width of the set is achieved between the line DE and the vertex C.

Of course, the smallest sailing boats (due to set inclusion) are the isosceles triangles themselves and if one chooses D and E at maximal distance one gets a
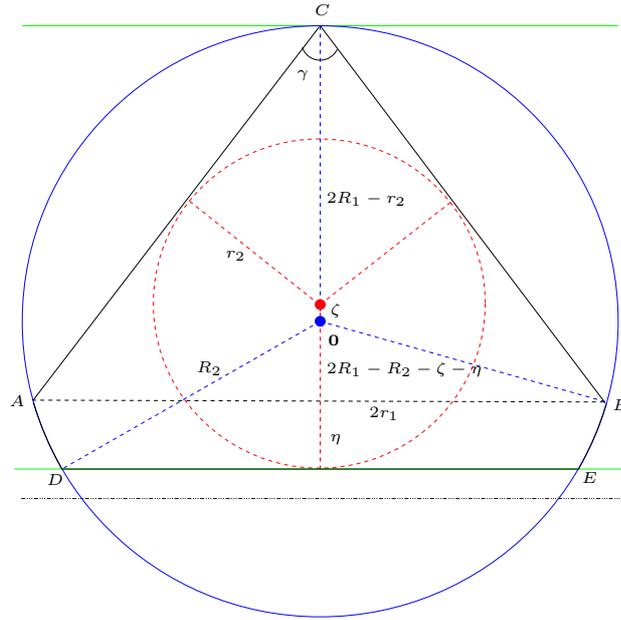
FIGURE 6.30.   A general sailing boat.

concentric sailing boat. Hence all sailing boats are mapped between the bound-
aries indicated by $T^2, I_{\frac{\pi}{2}}$, and $RSB_{\frac{\pi}{4}}$ (see Figure 6.31 for a projection onto the
(x, y)-plane).

LEMMA 6.16. *For all sailing boats SB it holds that*

$$r_2^2(SB)r_1(SB) + 4R_1(SB)r_1(SB)(R_1(SB) - r_2(SB))$$
$$= 4r_2(SB)R_2(SB)\sqrt{R_1(SB)(R_1(SB) - r_2(SB))}$$

PROOF. Let ζ be the distance between the incentre and the circumcentre of
SB and η the distance between the parallel lines AB and DE. Then it is easy
to see that the following equations hold:

(i) $\zeta = r_2 + R_2 - 2R_1$,
(ii) $\sin(\frac{\gamma}{2}) = \frac{r_2}{2R_1 - r_2}$,
(iii) $\tan(\frac{\gamma}{2}) = \frac{r_1}{2R_1 - \eta}$, and
(iv) $r_1^2 + (r_2 - \zeta - \eta)^2 = R_2^2$.
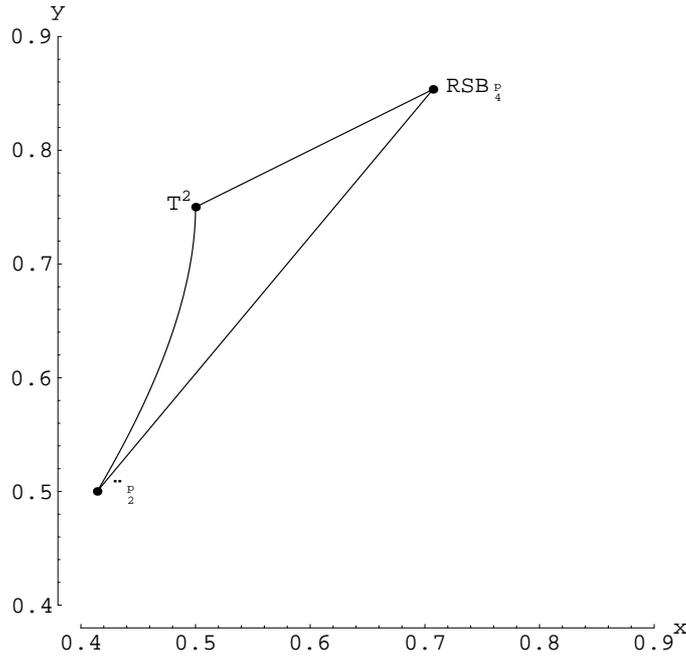
FIGURE 6.31. $\{f(SB) : SB$ a sailing boat$\}$, projected onto the (x, y)-plane.

Since $tan(arcsin(x)) = \frac{x}{\sqrt{1-x^2}}$, we can use (ii) and (iii) to compute

$$
\begin{aligned}
\eta &= 2R_1 - \frac{r_1}{\tan(\arcsin(\frac{r_2}{2R_1-r_2}))} \\
&= 2R_1 - (2R_1 - r_2)\frac{r_1}{r_2}\sqrt{1 - \frac{r_2^2}{(2R_1^2 - r_2)^2}} \\
&= 2\left(R_1 - \frac{r_1}{r_2}\sqrt{R_1(R_1 - r_2)}\right).
\end{aligned}
$$

Now we use the above formula for η and (i) for ζ and insert them both into equation (iv). This leads to

$$
r_1^2 + \left(\frac{r_1}{r_2}\sqrt{R_1(R_1 - r_2)} - R_2\right)^2 = R_2^2
$$

which is equivalent to

$$
r_1^2 + \frac{4R_1 r_1^2}{r_2^2}(R_1 - r_2) = \frac{4r_1 R_2}{r_2}\sqrt{R_1(R_1 - r_2)}
$$

and by multiplying with $\frac{r_2^2}{r_1}$ we obtain the statement of the lemma. $\qquad\square$

As all extreme sailing boats (isosceles triangles, concentric and right-angled sailing boats) describe parts of the boundary of $f(\mathcal{C}_1^2)$, it is likely that the equation in Lemma 6.16 defines a complete 2-dimensional boundary of $f(\mathcal{C}_1^2)$. However, the equation in Lemma 6.16 does not indicate a valid inequality for $f(\mathcal{C}_1^2)$, since the 2-dimensional surface induced by the equation does intersect $f(\mathcal{C}_1^2)$ beyond the boundaries of the sailing boats.

3.9. The facets f9 and f16. f9 probably consists of $BT_{\arcsin(\frac{3}{4})}$, $SR_{\frac{\pi}{6}}$, and H_{τ^*} ($BT_{\arcsin(\frac{3}{4})}$ instead of L as computed by Qhull). This conjecture is motivated by the fact that there is a non-linear boundary of $f(\mathcal{C}_1^2)$ between $BT_{\arcsin(\frac{3}{4})}$ and $SR_{\frac{\pi}{6}}$ (see Subsection 3.7), and that there is an assumed boundary between $BT_{\arcsin(\frac{3}{4})}$ and H_{τ^*} (see Subsection 3.2).

For f16, it is quite possible that a 2-dimensional part of the boundary exists which contains exactly the three extreme points $SR_{\frac{\pi}{6}}$, $SR_{\arcsin(\sqrt{3}-1)}$, and H_{τ^*}, as we know that the sliced Reuleaux triangles and the general hood sets define parts of the boundary of $f(\mathcal{C}_1^2)$.

For both f9 and f16 the problem is mainly to find out about the unknown parts of the boundaries of $f(\mathcal{C}_1^2)$ between H_{τ^*} and $BT_{\arcsin(\frac{3}{4})}$ and between H_{τ^*} and $SR_{\frac{\pi}{6}}$. A possible solution to this could also be an undiscovered eleventh essential extreme point.

Summarising the results about the extreme points in the previous subsections we state the following theorem:

THEOREM 6.17. *The sets $L, \mathbb{B}, T^2, RT, I_{\frac{\pi}{2}}, SR_{\frac{\pi}{6}}, SR_{\arcsin(\sqrt{3}-1)}, RSB_{\frac{\pi}{4}}$, and H_{τ^*} correspond to extreme points of $f(\mathcal{C}_1^2)$.*

Additionally, we can now give a corrected version of the vertex-facet dependency computed by Qhull (see Figure 6.32, and compare it to Figure 6.14). Since not all boundaries are linear, and since therefore $f(\mathcal{C}_1^2)$ is not a polytope, we designate it as the dependency of extreme points and 2-dimensional surface regions.
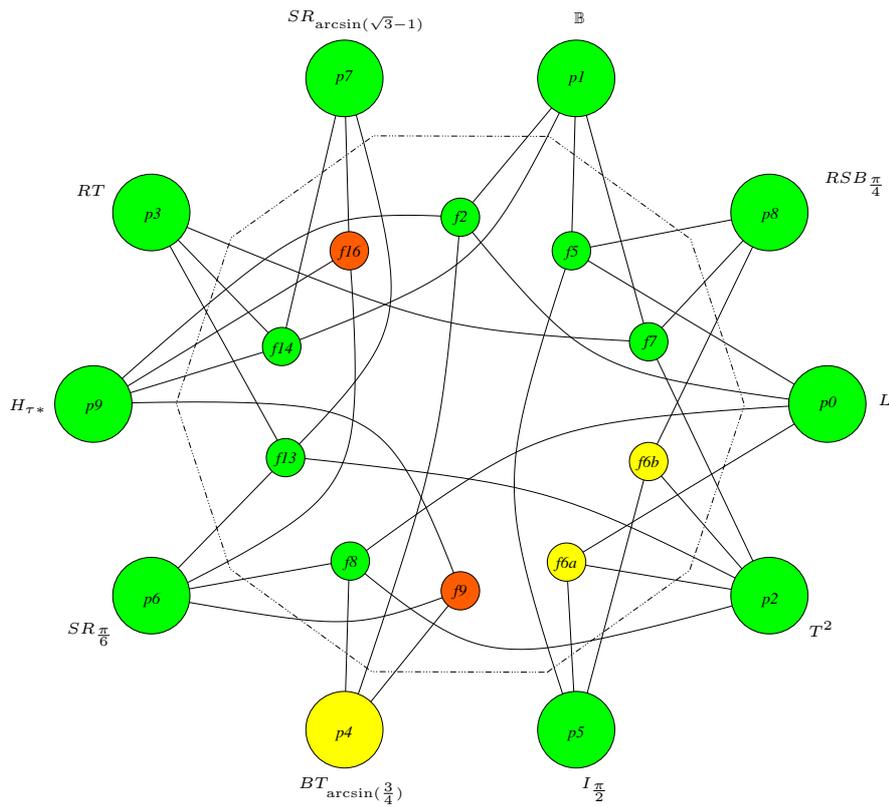
FIGURE 6.32.   The dependencies between extreme points and 2-dimensional surface regions of the 3-dimensional diagram. The green facets and extreme points have been proved in the preceding subsections, the red parts are open. The yellow colour indicates that those facets/extreme points could not be completely verified yet.

4. Possible extensions

The greater part of the new 3-dimensional diagram $f(\mathcal{C}_1^2)$ has been completely described. Nevertheless, the remaining open questions are major challenges for the future.

Besides that, there is a multitude of open questions which arise by extending the concept of Blaschke-Santaló diagrams to convex sets in higher dimensions.

Of course, the first extension that comes into mind is to draw these diagrams for bodies in 3-space. The easiest case to start with are the four possible 2-dimensional diagrams, which we obtain from using only three out of the four

standard radii (the exact analogue in 3-space of the Blaschke-Santaló diagrams in 2-space). It is easy to see that major parts of the boundary of these diagrams can be described again by the standard inequalities from Propositions 2.1, 2.3, and 2.5.

For example, consider the triple (r_3, R_1, R_3) and draw the diagram

$$g : \mathcal{C}_1^3 \to [0,1]^2,$$

where $\mathcal{C}_1^3$ denotes the class of all 3-dimensional bodies K with $R_2(K) = 1$ and

$$g(K) = (x, y) = (r_3(K), R_1(K)).$$

By Proposition 2.1 we know that $y \geq x$ and from Proposition 2.5 we obtain $y \leq \frac{x+1}{2}$ (see Figure 6.33).

FIGURE 6.33.   The known boundaries of the (r_3, R_1, R_3)-diagram for 3-dimensional bodies. The dashed line is an upper bound; the real boundary of the diagram lies below this line.

In the 2-dimensional case Steinhagen's inequality (see Proposition 2.3 (ii)) only induces a single point on the boundary of the diagram, the image of T^2. However, if one considers 3-dimensional bodies, the regular simplex is not reduced (see the remarks after Proposition 2.5) and therefore the inequality $y \leq \sqrt{3}x$ induces a whole line segment of the boundary of $g(\mathcal{C}_1^3)$. The intersection of the inequalities $y \leq \frac{x+1}{2}$ and $y \leq \sqrt{3}x$ is formed by $g(TB)$, which is obtained from

intersecting T^3 with a ball of radius $2R_1(T^3) - r_2(T^3)$ and scaling it to attain circumradius 1.

Hence the only unknown part in this diagram is the part between 0 (the image of all lower dimensional sets) and $\left(\frac{1}{3}, \sqrt{\frac{1}{3}}\right)$ (indicated by a dashed line in Figure 6.33). Since in the analogue Blaschke-Santaló diagram the boundary between 0 and T^2 is reached by the mappings of isosceles triangles, it is very likely that some kind of simplices which generalise the isosceles triangles (e.g, an isosceles pyramid over T^2 or a simplex which consists of four isosceles triangles) form the remaining part of the boundary.

It is easy to see that the three other 2-dimensional diagrams, involving only standard radii, would also be completely known if it would be possible to close the gap in the boundary between T^3 and the lower dimensional sets. Note that in the two diagrams involving r_1 and R_2 we get the image of T^2 as an additional extreme point on the z-axis (see Figure 6.34).
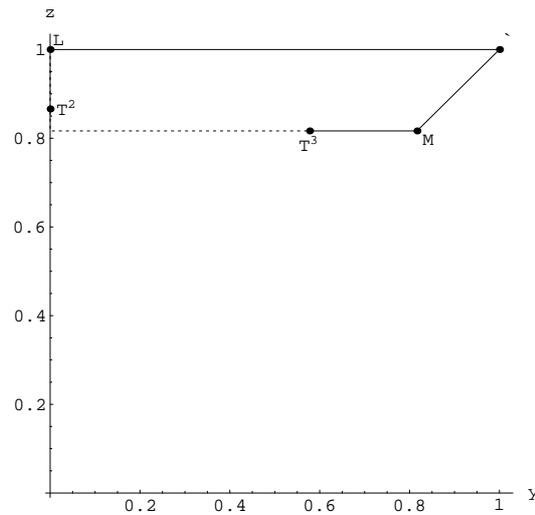

FIGURE 6.34. The known boundaries of the (R_1, r_1, R_3)-diagram for 3-dimensional bodies. The dashed line is a lower bound; the real boundary of the diagram lies above this line. The point M indicates the image of the Meißner bodies, the point T^2 the image of the lower 2-dimensional regular simplex, which is the lowest possible point on the z-axis.

Moreover, as the major part of the boundaries of these diagrams for convex sets of any fixed dimension are described by the inequalities of Propositions 2.1, 2.3, and 2.5, it should be possible to answer the question for complete systems of inequalities in any dimension, as well. This will be subject of further work.

However, there are two more possible generalisations of such diagrams for 3-dimensional bodies: One is the analogue diagram of $f(\mathcal{C}_1^2)$ for $\mathcal{C}_1^3$, obtained by taking all four standard radii into account. Of course this task is even harder than its 2-dimensional counterpart, but it is not very difficult to see that at least the standard inequalities again induce faces of the boundary.

For example, the intersection B_4 of four balls of equal radii placed at the vertices of a regular simplex is not of constant breadth, but B_4 has the same inradius, width, and circumradius as any of the two Meißner bodies M. Hence both, B_4 and M, fulfill the valid inequality $2R_1 \leq r_2 + R_2$ with equality and, since this holds for all bodies of constant breadth, the inequality induces a 2-dimensional boundary face of the 3-dimensional diagram.

The last possible extension we like to introduce are diagrams which take non-standard radii into account. This task is quite difficult as a general order of the radii like that of the standard ones does not exist, as shown in the diagram in Figure 2.3 of Chapter 2. In 3-space we only know that for every body C

$$r_3(C) \leq \{R_1(C), r_2(C)\} \leq \{R_2(C), r_1(C)\} \leq R_3(C),$$

where within the curly brackets everything ('<', '=', and '>') is possible.

Nevertheless, we can describe some parts of such diagrams with our knowledge from the preceding chapters. Figure 6.35 shows the 2-dimensional diagram one gets from the radii (R_2, r_1, R_3).

Since both R_2 and r_1 are less than or equal to R_3, we can scale the bodies such that their circumradius is 1 and consider the map into the (x, y)-plane, where x indicates the outer 2-radius R_2 and y the half diameter r_1. Important parts of the boundary have not been discovered so far (the horizontal and vertical dotted lines in Figure 6.35 indicate only weak lower bounds for the boundaries). However, it follows from the results of Chapter 4 and 5 that there exist points below the $x = y$ line (induced by the totally non-spherical bodies, indicated by TN in Figure 6.35) and, more significantly, there exist points on the boundary
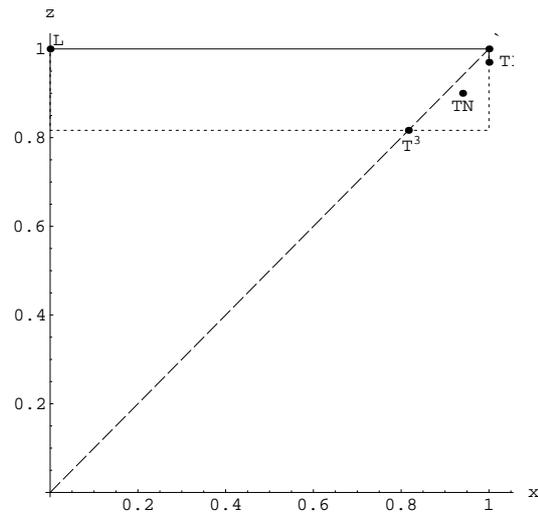
FIGURE 6.35.   The (R_2, r_1, R_3)-diagram for 3-dimensional bodies.

$x = 1$ with $y \neq 1$ (induced by the special totally isoradial bodies we constructed in Chapter 5, indicated by TI in Figure 6.35).

Since geometric inequalities involving the non-standard radii are almost unknown, approaching these diagrams is a challenging task for future work. A possible first step could be to concentrate on subsets of $\mathcal{C}_1^d$, like simplices or bodies of constant breadth and their generalisations.

Qhull results for the 3-dimensional Blaschke-Santaló diagram

The Qhull input can be read as follows: The first line states the dimension, the second the number of vertices. Thereafter each line represents the coordinates of a point in the $\mathcal{V}$-presentation of the polytope given by Lemma 6.8.

3		
10		
0	0	1
1	1	1
0.5	0.75	0.866025
0.732051	0.866025	0.866025
0.649519	0.75	0.866025
0.732050	0.844028	0.866025
0.683578	0.683578	0.911438
0.414214	0.5	1
0.707107	0.853553	1
0.793580	0.793580	0.896790

TABLE A.1.   The approximative coordinates of the extreme points in our list, used as Qhull input.

One should notice for the output of Qhull that the input points are named as p0 to p9, but only the irredundant remain listed. f2 to f17 denote the eleven computed facets (the six missing numbers were internally used by Qhull for hyperplanes spanned by three vertices, which later turned out as non-facetinducing). For each vertex a list ('neighbours') is given, which presents the facets containing this vertex. The information in the output for each facet describes the type of

- p9 (v3):   0.79   0.79   0.9
  neighbours: f2 f9 f14 f16 f17
- p1 (v1):   1   1   1
  neighbours: f2 f5 f7 f12 f14
- p0 (v0):   0   0   1
  neighbours: f2 f5 f6 f8 f9
- p8 (v5):   0.71   0.85   1
  neighbours: f5 f6 f7
- p2 (v2):   0.5   0.75   0.87
  neighbours: f6 f7 f8 f12 f13
- p6 (v6):   0.65   0.75   0.87
  neighbours: f8 f9 f13 f16
- p3 (v7):   0.73   0.87   0.87
  neighbours: f12 f13 f14 f17
- p7 (v8):   0.73   0.84   0.87
  neighbours: f16 f17 f13

TABLE A.2.   The Qhull output, Part 1: The vertices and the containing facets.

the facet ('flags'), a normal vector ('normal'), a list of the vertices contained, the neighbouring facets, and if the facet is not simplicial, a list of its edges ('ridges').

- f2
    - flags: bottom simplicial
    - normal: 0.7071 -0.7071 -0
    - vertices: p9 (v3) p1 (v1) p0 (v0)
    - neighbouring facets: f5 f9 f14
- f5
    - flags: top simplicial
    - normal: -0 0 1
    - vertices: p8 (v5) p1 (v1) p0 (v0)
    - neighbouring facets: f2 f6 f7
- f6
    - flags: bottom simplicial
    - normal: -0.6317 0.5233 0.572
    - vertices: p8 (v5) p2 (v2) p0 (v0)
    - neighbouring facets: f8 f5 f7
- f7
    - flags: top simplicial
    - normal: -0.4472 0.8944 5.698e-06
    - vertices: p8 (v5) p2 (v2) p1 (v1)
    - neighbouring facets: f12 f5 f6
- f8
    - flags: top simplicial
    - normal: -0 -0.1758 -0.9844
    - vertices: p6 (v6) p2 (v2) p0 (v0)
    - neighbouring facets: f6 f9 f13
- f9
    - flags: bottom simplicial
    - normal: 0.3093 -0.4203 -0.8531
    - vertices: p6 (v6) p9 (v3) p0 (v0)
    - neighbouring facets: f2 f8 f16
- f12
    - flags: bottom simplicial
    - normal: -0.4472 0.8944 -7.192e-06
    - vertices: p3 (v7) p2 (v2) p1 (v1)
    - neighbouring facets: f7 f14 f13

TABLE A.3.   The Qhull output, Part 2: The first seven facets.

- f14
    - flags: top simplicial
    - normal: 0.4472 -3.338e-06 -0.8944
    - vertices: p3 (v7) p9 (v3) p1 (v1)
    - neighbouring facets: f2 f12 f17
- f16
    - flags: top simplicial tested
    - normal: 0.2712 -0.238 -0.9326
    - vertices: p7 (v8) p6 (v6) p9 (v3)
    - neighbouring facets: f9 f17 f13
- f17
    - flags: bottom simplicial tested
    - normal: 0.4472 -2.033e-05 -0.8944
    - vertices: p7 (v8) p3 (v7) p9 (v3)
    - neighbouring facets: f14 f16 f13
- f13
    - flags: bottom tested coplanar
    - merges: 1
    - normal: -0 -0 -1
    - vertices: p7 (v8) p3 (v7) p6 (v6) p2 (v2)
    - neighbouring facets: f8 f12 f16 f17
    - ridges:
        - r4   tested
            vertices: p3 (v7) p2 (v2)
            between f13 and f12
        - r3   tested
            vertices: p6 (v6) p2 (v2)
            between f8 and f13
        - r1   tested
            vertices: p7 (v8) p6 (v6)
            between f16 and f13
        - r2   tested
            vertices: p7 (v8) p3 (v7)
            between f13 and f17

TABLE A.4.   The Qhull output, Part 3: The remaining facets.

Bibliography

[1] P.K. Agarwal, B. Aronov, and M Sharir. Line transversals of balls and smallest enclosing cylinders in three dimensions. *Discrete Comput. Geom.*, 21:373–388, 1999.

[2] R. Alexander. The width and diameter of a simplex. *Geom. Dedicata*, 6:87–94, 1977.

[3] P.W. Awyong. An inequality relating the circumradius and diameter of two-dimensional lattice-point-free convex bodies. *Amer. Math. Monthly*, 106:252–255, 1999.

[4] K. Ball. Ellipsoids of maximal volume in convex bodies. *Geom. Dedicata*, 41:241–250, 1992.

[5] U. Betke and M. Henk. A generalization of Steinhagen's theorem. *Abh. Math. Semin. Univ. Hamb.*, 63:165–176, 1993.

[6] U. Betke, M. Henk, and L. Tsintsifa. Inradii of simplices. *Discrete Comput. Geom.*, 17:365–375, 1997.

[7] W. Blaschke. Eine Frage über konvexe Körper. *Jahresber. Deutsch. Math.-Verein.*, 25:121–125, 1916.

[8] J. Böhm and E. Quaisser. *Schönheit und Harmonie geometrischer Formen*. Akademie Verlag, 1991.

[9] H.F. Bohnenblust. Convex regions and projections in Minkowski spaces. *Ann. of Math.*, 39:301–308, 1938.

[10] T. Bonnesen and W. Fenchel. *Theorie der konvexen Körper*. Springer, Berlin, 1934.

[11] O. Bottema, R.Ž. Djordjević, R.R. Janić, D.S. Mitrinović, and P.M. Vasić. *Geometric Inequalities*. Wolter-Noordhoff, 1968.

[12] R. Brandenberg, A. Dattasharma, and P. Gritzmann. Isoradial bodies. in preparation.

[13] R. Brandenberg and D. Larman. Dark clouds on spheres and totally non-spherical bodies of constant breadth. submitted.

[14] A. Brieden, P. Gritzmann, R. Kannan, V. Klee, L. Lovász, and M. Simonovits. Deterministic and randomized polynomial-time approximation of radii. preprint, 2000.

[15] H. Bückner. Über Flächen von fester Breite. *Jber. Deutsch. Math. Ver.*, 45:96–139, 1936.

[16] Y.D. Burago and V.A. Zalgaller. *Geometric Inequalities*. Springer, 1988.

[17] G.D. Chakerian and H. Groemer. Convex bodies of constant width. In P. Gruber and J. Wills, editors, *Convexity and its applications*, pages 49–96. Birkhäuser, 1983.

[18] T.M. Chan. Approximating the diameter, width, smallest enclosing cylinder, and minimum-width annulus. In *Proceedings of the 16th ACM Symposium on Computational Geometry*, volume 8, pages 300–309, 2000.

[19] M.A. Hernández Cifre. Is there a planar convex set with given width, diameter, and inradius? *Amer. Math. Monthly*, 107:893–900, 2000.

[20] M.A. Hernández Cifre and S. Segura Gomis. The missing boundaries of the Santalo diagrams for the cases (d, ω, R) and (ω, R, r). *Discrete Comput. Geom.*, 23:381–388, 2000.

[21] M.A. Hernández Cifre, G. Salinas, and S. Segura Gomis. Complete systems of inequalities. *J. Ineq. Pure Appl. Math*, 2(Article 10), 2001. Online Journal; http://jipam.vu.edu.au/.

[22] H.T. Croft, K.J. Falconer, and R.K. Guy. *Unsolved Problems in Geometry*, volume II of *Problem Books in Mathematics*. Springer, 1991.

[23] L. Danzer. Über die maximale Dicke der ebenen Schnitte eines konvexen Körpers. *Arch. Math.*, 8:314–316, 1957.

[24] L. Danzer. Packungs- und Überdeckungsprobleme. Manuscript, 1976.

[25] B.V. Dekster. Reduced strictly convex plane figure is of constant width. *J. Geom.*, 26:77–81, 1986.

[26] H.G. Eggleston. On the projection of a plane set of finite linear measure. *Acta Math.*, 99:53–90, 1958.

[27] H.G. Eggleston. Minimal universal covers in E^n. *Israel J. Math.*, 16:149–155, 1963.

[28] P. Erdős and C.A. Rogers. Covering space with convex bodies. *Acta Arith.*, 7:281–285, 1962.

[29] L. Euler. De curvis triangularibus. *Acta Acad. Sci. Imp. Petropolitanae*, II:3–30, 1778.

[30] H. Everett, I. Stojmenovic, P. Valtr, and S. Whitesides. The largest k-ball in a d-dimensional box. *Comp. Geom.*, 11:59–67, 1998.

[31] U. Faigle, W. Kern, and M. Streng. Note on the computational complexity of j-radii of polytopes. *Math. Prog.*, 73A:1–5, 1996.

[32] K.J. Falconer. Singularities of sets of constant width. *Geom. Dedicata*, 11:187–193, 1981.

[33] P. Filliman. The largest projections of regular polytopes. *Israel J. Math.*, 64:207–228, 1988.

[34] P. Filliman. The extreme projections of the regular simplex. *Trans. Amer. Math. Soc.*, 317:611–628, 1990.

[35] W.J. Firey. Convex bodies of constant outer p-measure. *Mathematika*, 17:21–27, 1970.

[36] The Geometry Center, Univerity of Minnesota, 207 Church Street, Mineapolis, MN 55455, USA, http://www.geom.umn.edu/software/qhull/. *Qhull*, 3.1 edition, 2001.

[37] A.A. Giannopoulos and V.D. Milman. Extremal problems and isotropic positions of convex bodies. *Isr. J Math.*, 117:29–60, 2000.

[38] A.A. Giannopoulos and V.D. Milman. Euclidean structure in finite dimensional normed spaces. In *Handbook of the Geometry of Banach Spaces*, volume 1, pages 707–779. Elsevier, 2001.

[39] P. Gritzmann and V. Klee. Inner and outer j-radii of convex bodies in finite-dimensional normed spaces. *Discrete Comput. Geom.*, 7:255–280, 1992.

[40] P. Gritzmann and V. Klee. Computational complexity of inner and outer j-radii of polytopes in finite-dimensional normed spaces. *Math. Program.*, 59:163–213, 1993.

[41] P. Gritzmann and M. Lassak. Estimates for the minimal width of polytopes inscribed in convex bodies. *Discr. Comp. Geom.*, 4:627–635, 1989.

[42] H. Groemer. Extremal convex sets. *Monatsh. Math.*, 96:29–39, 1983.

[43] H. Groemer. Stability of geometric inequalities. In P. Gruber and J. Wills, editors, *Handbook of Convex Geometry*, pages 125–150. North-Holland, 1993.

[44] P.M. Gruber and J.M. Wills, editors. *Handbook of Convex Geometry*, volume A. North–Holland, 1993.

[45] P.M. Gruber and J.M. Wills, editors. *Handbook of Convex Geometry*, volume B. North–Holland, 1993.

[46] B. Grünbaum. *Convex Polytopes*, volume XVI of *Pure and Applied Mathematics*. Wiley, 1967.

[47] H. Hadwiger. *Altes und Neues über konvexe Körper*, volume III of *Elemente der Mathematik vom höheren Standpunkt aus*. Birkhäuser, 1955.

[48] M. Henk. *Ungleichungen für sukzessive Minima und verallgemeinerte In- und Umkugelradien*. Dissertation, Universität-GH Siegen, 1991.

[49] M. Henk. A generalization of Jung's theorem. *Geom. Dedicata*, 42:235–240, 1992.

[50] M. Henk and G.A. Tsintsifas. Some inequalities for planar convex figures. *El. Math.*, 49:120–125, 1994.

[51] D. Hilbert and S. Cohn-Vossen. *Anschauliche Geometrie*. Springer - Verlag, Berlin, 1932. Translation: Geometry and the Imagination, Chelsea Publ., New York, 1952.

[52] M.E. Houle and G.T. Toussaint. Computing the width of a set. *IEEE Trans. Pattern Anal. Math. Intell.*, 10(5):761–765, 1988.

[53] F. John. Extremum problems with inequalities as subsidiary conditions. In *Courant Anniversary Volume*, pages 187–204. Interscience, 1948.

[54] H.W.E. Jung. Über die kleinste Kugel die eine räumliche Figur einschließt. *J. Reine Angew. Math.*, 123:241–257, 1901.

[55] T. Kawashima. Polytopes which are orthogonal projections of regular simplexes. *Geom. Dedicata*, 38:73–85, 1991.

[56] V. Klee. Is a body spherical if its HA-measurements are constant? *Amer. Math. Monthly*, 76:539–542, 1969.

[57] K. Leichtweiss. Zwei Extremalprobleme der Minkowski-Geometrie. *Math. Zeitschr.*, 62:37–49, 1955.

[58] G.Y. Perel'man. K radii of a convex body. *Sib. Mat. Z.*, 28:185–186, 1987.

[59] H. Rademacher and O. Toeplitz. *The Enjoyment of Math*. Princeton University Press, 1957.

[60] F. Reuleaux. *Theoretische Kinematik, Grundzüge einer Theorie des Maschinenwesens.* Vieweg, 1875.

[61] J.R. Sangwine-Yager. The missing boundary of the Blaschke diagram. *Am. Math. Mon.*, 96:233–237, 1989.

[62] J.R. Sangwine-Yager. Mixed volumes. In P.M. Gruber, editor, *Handbook of convex geometry*, volume A, chapter 1.2, pages 43–71. North-Holland, 1993.

[63] L.A. Santaló. Sobre los sistemas completos de desigualdades entre tres elementos de una figura convexa plana. *Math. Notae*, 17:82–104, 1961.

[64] R. Schneider. *Convex bodies: The Brunn-Minkowski theory*, volume 44 of *Encyclopedia of mathematics and its applications*. Cambridge Univerity Press, 1993.

[65] E. Schulte and S. Vrećica. Preassigning the shape for bodies of constant width. *Monatsh. Math.*, 96:157–164, 1983.

[66] P.R. Scott. Two inequalities for convex sets in the plane. *Bull. Austral. Math. Soc.*, 19:131–133, 1978.

[67] P.R. Scott. A family of inequalities for convex sets. *Bull. Austral. Math. Soc.*, 20:237–245, 1979.

[68] P.R. Scott. Sets of constant width and inequalities. *Q. J. Math. Oxf. II. Ser.*, 32:345–348, 1981.

[69] P.R. Scott. An extension of Blaschke's theorem in the plane. *El. Math.*, 46:102–106, 1991.

[70] P.R. Scott and P.W. Awyong. Inequalities for convex sets. *J. Ineq. Pure Appl. Math.*, 1(Article 6), 2000. Online Journal; http://jipam.vu.edu.au/.

[71] D.O. Shklarsky, N.N. Chentzov, and I.M. Yaglom. Geometric inequalities and problems on maxima and minima. *Nauka*, 1970.

[72] P. Steinhagen. Über die grösste Kugel in einer konvexen Punktmenge. *Abh. Math. Sem. Univ. Hamburg*, 1:15–26, 1921.

[73] Waterloo Maple Inc., 57 Erb Street West, Waterloo Ontario, N2L6C2, Canada, http://www.maplesoft.com. *Maple*, 7.00 edition, 2001.

[74] B. Weissbach. Über die senkrechten Projektionen regulärer Simplexe. *Beitr. Algebra Geom.*, 15:35–41, 1983.

[75] B. Weissbach. Über Umkugeln von Projektionen regulärer Simplexe. *Beitr. Algebra Geom.*, 16:127–137, 1983.

[76] B. Weissbach. Schranken für die Dicke der Simplexe. *Beitr. Algebra Geom.*, 26:5–11, 1987.

[77] Wolfram Research Inc., 100 Trade Center Drive, Champaign, IL 61820, USA, http://www.wolfram.com. *Mathematica*, 4.1 edition, 2000.

[78] I.M. Yaglom and V.G. Boltyanskiĭ. *Convex figures*, volume 4 of *Library of the mathematical circle*. Holt, Rinehart and Winston, 1961.

[79] M. Yamanouti. Notes on closed convex figures. *Proc. Physico-Math Soc. Japan Ser. (3)*, 14:605–609, 1932.